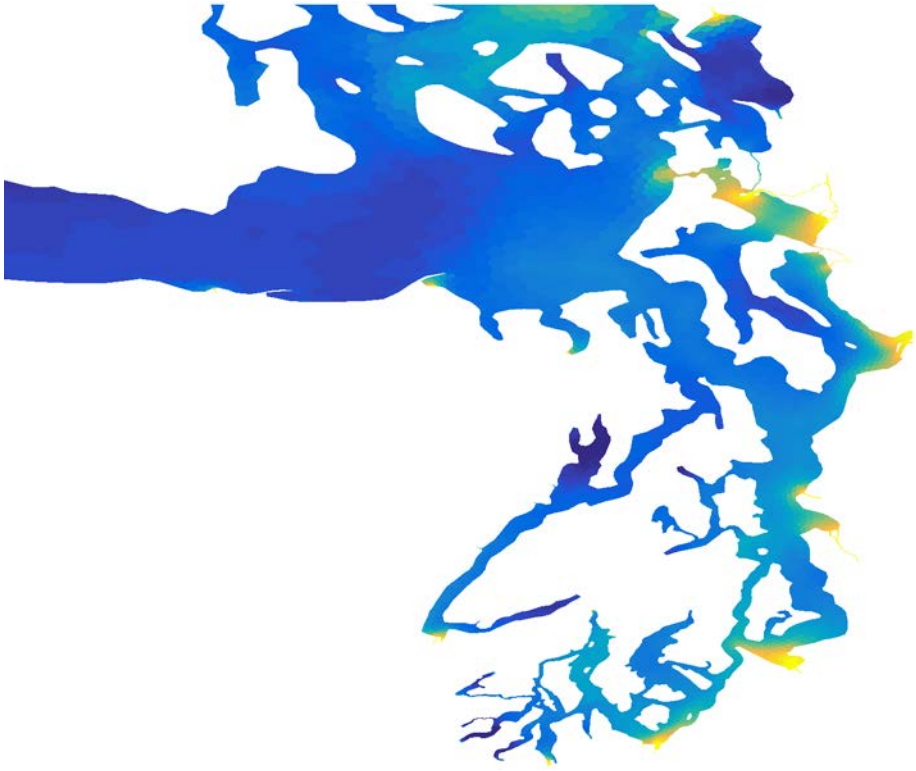

Salish Sea Model

Ocean Acidification Module and the Response to Regional Anthropogenic Nutrient Sources

DEPARTMENT OF ECOLOGY
State of Washington

June 2017

Publication No. 17-03-009

Publication and contact information

This report is available on the Department of Ecology's website at
https://fortress.wa.gov/ecy/publications/SummaryPages/1703009.html

The Activity Tracker Code for this study is 15-053 (Ocean Acidification Module)

For more information contact:

Publications Coordinator
Environmental Assessment Program
P.O. Box 47600, Olympia, WA 98504-7600
Phone: (360) 407-6764

Washington State Department of Ecology - www.ecy.wa.gov

o	Headquarters, Olympia	(360) 407-6000
o	Northwest Regional Office, Bellevue	(425) 649-7000
o	Southwest Regional Office, Olympia	(360) 407-6300
o	Central Regional Office, Union Gap	(509) 575-2490
o	Eastern Regional Office, Spokane	(509) 329-3400

Cover image: Number of days during 2008 when the saturation state for aragonite in the surface layer is predicted to be less than 1, ranging from about 170 days (*dark blue*) to 365 days (*bright yellow*)

Salish Sea Model

Ocean Acidification Module and the Response to Regional Anthropogenic Nutrient Sources

by

Greg Pelletier[1], Laura Bianucci[2], Wen Long[2], Tarang Khangaonkar[2], Teizeen Mohamedali[1], Anise Ahmed[1], and Cristiana Figueroa-Kaminsky[1]

[1]Environmental Assessment Program
Washington State Department of Ecology
Olympia, Washington 98504-7710

[2]Coastal Science Division
Pacific Northwest National Laboratory
Seattle, Washington 98109

This page is purposely left blank

Table of Contents

List of Figures and Tables

Page

Figures

Tables

Abstract

Several monitoring programs indicate the presence of lower pH and related changes in carbonate system variables in the Salish Sea[1] as compared to the shallow North Pacific waters offshore. Pacific Ocean waters are influenced by increasing global atmospheric partial pressure of carbon dioxide (pCO_2) which has been identified as a dominant contributor to lower pH and related carbonate chemistry changes. However, local biological processes may also significantly contribute to the local values of pH and carbonate system variables. Thus, regional human nutrient contributions may exacerbate changes to the local carbonate system chemistry.

Of specific interest are changes to the aragonite saturation state (Ω_{arag}), a form of calcium carbonate used by many shell-building organisms. If the Ω_{arag} is low or under-saturated, calcifying organisms may not be able to build shells, which could result in a cascade of impacts to the food web.

The present project examines how regional freshwater/land-derived sources of nutrients generally impact acidification in the Salish Sea. Regional human contributions of nutrients and carbon originate within the Puget Sound and Salish Sea watersheds from point and nonpoint sources.

The purpose of this project is to:

- Expand the existing Salish Sea Model, developed by the Pacific Northwest National Laboratories (PNNL) for the Washington State Department of Ecology and U.S. EPA, to evaluate pH, Ω_{arag}, and related carbonate system variables.
- Quantify the influences of regional nutrient sources on the carbonate system variables.

This expands the capabilities of the Salish Sea Model by adding total dissolved inorganic carbon (DIC) and alkalinity as state variables, including source and sink terms related to air-sea exchange, respiration, photosynthesis, nutrient gains and losses, sediment fluxes, and boundary conditions. Boundary conditions account for both Pacific Ocean upwelled water and regional human nutrient contributions and air emissions around the Salish Sea. This effort also identifies geographical areas and seasons experiencing greater influence from regional sources of nutrients to Salish Sea waters.

Results from this effort indicate that increased dissolved inorganic nitrogen (DIN), phytoplankton biomass, and non-algal organic carbon caused by regional anthropogenic nutrient sources can constitute significant contributors to acidification in the Salish Sea. Predicted impacts due to regional anthropogenic nutrient sources include changes in pH and DIC in both bottom and surface waters that are comparable in magnitude to published estimates of the changes caused by increasing global atmospheric pCO_2.

[1] The Salish Sea includes the Strait of Juan de Fuca, the Strait of Georgia, Puget Sound, and all of their connecting channels and adjoining waters, such as Haro Strait, Rosario Strait, Bellingham Bay, Hood Canal, and the waters around and between the San Juan Islands in the state of Washington and the Gulf Islands in British Columbia, Canada.

The Ω_{arag} decreased, on average, due to regional anthropogenic nutrient sources. The impact is predicted to be greatest at the bottom of the water column. Regional anthropogenic nutrient sources account for up to about 43% of the total anthropogenic depletion of Ω_{arag} at the bottom, and up to about 15% of the total anthropogenic depletion of Ω_{arag} at the surface. Regional anthropogenic nutrient loadings increased pH and Ω_{arag} in some areas, particularly in several South Puget Sound shallow inlets and bays.

The Ω_{arag} in certain regions appears to be more sensitive to anthropogenic nutrient loadings. Specifically, portions of the main basin, South Sound, Port Susan, Skagit Bay, and Whidbey Basin all present higher sensitivity of Ω_{arag} in response to anthropogenic nutrient loadings. Hood Canal appears to be generally decoupled from the rest of the Salish Sea in terms of the magnitude of anthropogenic, land-derived nutrient influence. This is likely due in part to circulation and the lower level of development in the Hood Canal region.

Acknowledgements

This project received funding from grants to the Washington State Department of Ecology from the United States Environmental Protection Agency (EPA), National Estuarine Program, under EPA grant agreements PC-00J20101 and PC00J89901, Catalog of Domestic Assistance Number 66.123, Puget Sound Action Agenda: Technical Investigations and Implementation Assistance Program. The content of this document does not necessarily reflect the views and policies of EPA, nor does mention of trade names or commercial products constitute an endorsement or a recommendation for their use.

The authors of this report thank the following people for their contributions to this study:

- Mindy Roberts (Washington Environmental Council) and Brandon Sackmann (Integral Consulting, Inc.) for leading the project while they were employed at the Department of Ecology. Mindy contributed to the introductory and discussion sections of this report. Brandon created Matlab scripts that were used to process model input and output data.
- The PNNL Institutional Computing (PIC) program at Pacific Northwest National Laboratory (PNNL) for providing access to the High Performance Computing facility.
- The following scientists who reviewed this report:
  - Brian Rappoli (Ocean and Coastal Acidification and Coral Reef Protection Program, U.S. Environmental Protection Agency)
  - Simone Alin (Pacific Marine Environmental Laboratory, National Oceanic and Atmospheric Administration)
  - Samantha Siedlecki (Joint Institute for the Study of the Atmosphere and Ocean, University of Washington)
  - Stephanie Jaeger (Department of Natural Resources and Parks, Water and Land Resources Division, King County)
  - Christopher Krembs and Tom Gries (Department of Ecology)

We also thank the following entities and people for providing monitoring data and tools that we used in this report to compare to model predictions:

- University of Washington (UW) – UW PRISM cruise data collected and processed in collaboration with National Oceanic and Atmospheric Administration (NOAA). Data were received from Simone Alin (NOAA) and Jan Newton (UW). Parker MacCready provided Matlab scripts that were used to process meteorological data.
- King County – data were downloaded online or provided by Stephanie Jaeger and Kim Stark.
- Padilla Bay National Estuarine Research Reserve System – data downloaded online, with assistance from Nicole Burnett and Jude Apple.
- Ecology's Marine Monitoring Unit – data received from Mya Keyzers and Julia Bos.

Introduction

Background

This computer modeling project was identified as a Key Early Action of the Washington State Blue Ribbon Panel on Ocean Acidification (Washington State Blue Ribbon Panel on Ocean Acidification, 2012). The panel was appointed by Governor Christine Gregoire to identify the causes and consequences of ocean acidification. A fundamental question was how much of the low pH is caused by nutrients reaching the Salish Sea from point source discharges, increased inputs of nitrogen and carbon from rivers, and atmospheric emissions of nitrogen and carbon, by increasing the production and respiration of organic matter. Decision-makers must understand the relative contributions of these regional human sources compared with the influences of global atmospheric partial pressure of carbon dioxide (pCO_2) increases that have decreased the pH of the Pacific Ocean.

The Washington State Ocean Acidification Blue Ribbon Panel report (2012) and Scientific Summary (Feely et al., 2012) provide important context. Long et al. (2014) Section 1.0 describes the historical and scientific background regarding acidification. We summarize key topics but refer to previously published documents for details.

Study area and surroundings

Long et al. (2014) Section 1.0 describes the study area, climate, Pacific Ocean influences, and regional watershed influences on the Salish Sea. Figure 1 presents the land areas discharging to the Salish Sea that are part of this project.

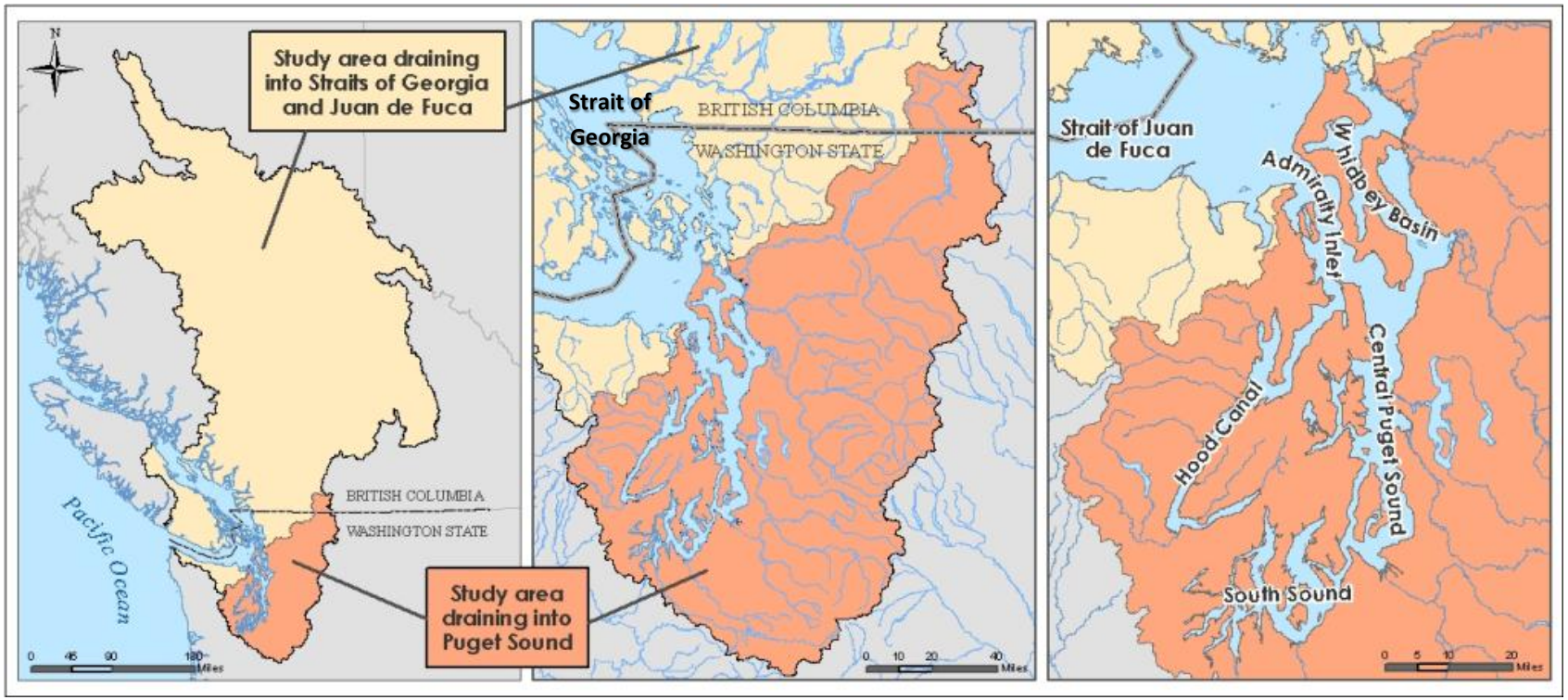

Figure 1. Salish Sea (Puget Sound, Strait of Georgia, Strait of Juan de Fuca) with land areas discharging to marine waters within the model domain.

Source: Long et al., 2014; Mohamedali et al., 2011.

History of study area

The study area and human uses are outlined in Sackmann (2009). The Washington State Blue Ribbon Panel on Ocean Acidification (2012) describes when and how ocean acidification concerns were first identified as well as the state of knowledge at that time. Washington Sea Grant (2014) and its partners updated key scientific findings since 2012.

Parameters of interest

Long et al. (2014) Section 1.0 describes the parameters of interest in acidification modeling, including the simulation of dissolved inorganic carbon (DIC) and total alkalinity (TA) as state variables. Washington State has established water quality criteria for pH, which can affect marine life. In addition, low aragonite saturation state (Ω_{arag}) can interfere with the metabolic processes of calcifying organisms (Washington State Blue Ribbon Panel on Ocean Acidification, 2012). While Washington does not have water quality criteria for Ω_{arag}, the parameter has received strong interest as it is likely to affect calcium carbonate shell-building organisms (e.g., Waldbusser et al., 2014; Bednaršek et al., 2014).

A critical step during the lifecycle of certain bivalve species is the initial biomineralization in the larval stage. (Waldbusser et al., 2015) Recent investigations have demonstrated that decreased larvae survival rates result when the water chemistry remains below certain thresholds (including Omega<1, but often greater than this threshold), yet the biomineralization mechanism itself is not entirely understood (Thomsen et al., 2015).

Results of previous studies

Previous investigations are summarized in Washington State Blue Ribbon Panel on Ocean Acidification (2012), Long et al. (2014), and Sea Grant (2014). Several studies add to the understanding of the region. Murray et al. (2015) reported pH, alkalinity, and DIC from the San Juan Islands. The authors attribute 22% of the carbon to increases in global atmospheric pCO_2 since preindustrial conditions. Wootton and Pfister (2012) identified a declining trend in pH near Tatoosh Island, in the Strait of Juan de Fuca, greater than the trend in Hawaii (Doney et al., 2009).

Previous research has quantified the role of global anthropogenic sources due to increased atmospheric pCO_2 (Feely et al., 2010; Feely et al., 2016), but no previous effort has isolated the impacts to the Salish Sea from regional human contributions relative to impacts from the Pacific Ocean and global atmospheric pCO_2. A separate modeling effort at the University of Washington will focus on short-term forecasts of acidic conditions (MacCready et al., 2013; https://faculty.washington.edu/pmacc/LO/LiveOcean.html).

Regulatory criteria or standards

Washington State has established water quality criteria for marine pH under Washington Administrative Code (WAC) 173-201A-210. Table 1 and Figure 2 summarize the aquatic life pH criteria for marine water and the use designations by location in the Salish Sea.

Table 1. Washington State aquatic life pH criteria for marine water.

Use Category	pH Units
Extraordinary quality	pH must be within the range of 7.0 to 8.5 with a human-caused variation within the above range of less than 0.2 units.
Excellent quality	pH must be within the range of 7.0 to 8.5 with a human-caused variation within the above range of less than 0.5 units.
Good quality	Same as Excellent quality
Fair quality	pH must be within the range of 6.5 to 9.0 with a human-caused variation within the above range of less than 0.5 units.

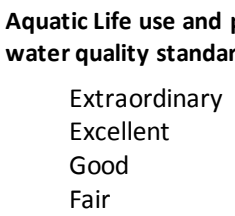

Figure 2. Washington State aquatic life use designations for the Salish Sea.

Washington State has not established water quality criteria for aragonite saturation. In 2012, the Washington State Department of Ecology (Ecology), on behalf of Governor Christine Gregoire, requested that the U.S. Environmental Protection Agency (EPA) lead the development of any change in water quality criteria related to acidification. Several individual research efforts are evaluating impacts on different biota at different aragonite saturation states (e.g., Chan et al., 2016; Busch et al., 2014); however, no consensus exists regarding what level of saturation state might protect biota.

Saturation states below 1.0 chemically favor dissolution or non-formation of aragonite-based shells, but other biotic impacts have been documented at higher saturation states. For example, Waldbusser et al. (2014) summarizes impacts to native Olympia oysters at a saturation state of 1.4 (Hettinger et al., 2012) and commercial non-native species at 1.5 to 2.0 (Barton et al., 2012). In addition, sensitivity to low saturation states of aragonite may vary by region as well as by species (e.g., Mackas and Galbraith, 2012; Bednaršek, 2012).

Project Description

Project goal

One of the key science questions that the Blue Ribbon Panel posed was: *How important are local drivers to the ocean acidification signal?* Previous research has begun to address the importance of global sources in the Pacific Ocean off the Washington coast (Feely et al., 2016) and in Puget Sound (Feely et al., 2010). This project aims to begin to quantitatively address the importance of the regional nutrient sources in the Salish Sea. Thus, the project goal is to quantitatively evaluate the relative impacts of regional human contributions in the Salish Sea based on best available information. The present report also recommends appropriate next steps.

Project objectives

The project objectives include the following:

- Expand the existing Salish Sea circulation and biogeochemical model (Khangaonkar et al. (2012a,b) to include acidification parameters. Specifically, we added state variables for DIC and total alkalinity (TA) to the Salish Sea Model. The original model development plan, described in Sackmann (2009), Yang et al. (2010), and Khangaonkar et al. (2012a), is currently being updated to include the sediment diagenesis capabilities following the approach and project plan described in Roberts et al. (2015a).
- Calibrate the model to the available information on pH and related parameters in the Salish Sea. The model version used for this work includes the Sediment Diagenesis Module. To calibrate the model, we built on previous calibration work performed using 2006 data as described in Khangaonkar et al. (2012a,b). We also consulted data available from other time periods with more abundant acidification-related data. The carbonate system module was calibrated using 2008 data. We followed the modeling approach outlined in the project plan (Roberts et al., 2015b).

- Evaluate the likely relative impacts of the Pacific Ocean and regional anthropogenic nutrient loading sources (e.g., freshwater point sources and nonpoint sources) on acidification, which may vary by time of year, by basin, or vertically within the water column.
- Recommend next steps and identify potential management actions consistent with the level of certainty of the predictions.

Information needed and sources

Long et al. (2014) Section 4.0 details information needs for boundary conditions and model comparison data as well as data availability. These include:

- Water column monitoring data from Ecology's marine ambient monitoring program.
- Supplemental data from the National Oceanic and Atmospheric Administration (NOAA), Ocean Survey Vessel (OSV) Bold, and the University of Washington (UW).
- River and wastewater treatment plant inputs of nutrients.
- Atmospheric partial pressure of carbon dioxide (pCO_2).
- Rate parameters for model kinetics processes.

Section 4.7 of Long et al. (2014) identifies primary information gaps, which are areas where some data may exist, but additional data would be useful, as follows:

- Vertical mixing
- Sediment fluxes
- Biological processes (e.g., phytoplankton abundance and community structure)
- Marine water alkalinity, pCO_2, or total DIC
- Process studies for rate parameters

These data could improve the model calibration as improved information becomes available.

Long et al. (2014) Section 3.0 and Khangaonkar (2012a,b) describe the FVCOM-ICM model of the Salish Sea. Appendix A of Long et al. (2014) describes the model theory that was implemented to expand the capabilities of the Salish Sea Model.

Study boundaries and model grid

Figure 3 presents maps of monitoring stations and the domain and grid of the Salish Sea Model. See Section 3.1, Long et al. (2014), and Sackmann (2009) for a description of the study area. Figure 1 presents the watershed boundary. The marine water model domain (Figure 3b) includes portions of the U.S. and Canada.

The unstructured model grid consists of 9,013 nodes and 13,941 elements to solve the governing equations (Khangaonkar et al., 2012a). A sigma-stretched coordinate system was used in the vertical plane with ten terrain-following sigma layers distributed with higher layer density near the surface (Figure 4). The thicknesses of the surface and bottom layers are presented in Figure

5. The thickness of the surface layer ranges from about 0.16 meters in the shallow nearshore areas to 7.6 meters in the deepest areas, with average thickness of about 1.9 meters across the model domain. The thickness of the bottom layer ranges from about 0.75 meters in the shallow nearshore areas to 35 meters in the deepest areas, with average thickness of about 8.6 meters across the model domain. The number of model grid layers within the euphotic zone depth of approximately 20 meters varies from all 10 layers in the nearshore areas to the top 2 layers in the deepest areas.

Ecology collected 148 samples of CO_2 system variables from six stations representing a spectrum of ocean and inland influences (Figure 6) monthly from June 2014 to May 2015 (Keyzers, 2014; Pelletier et al., 2017 *in review*).

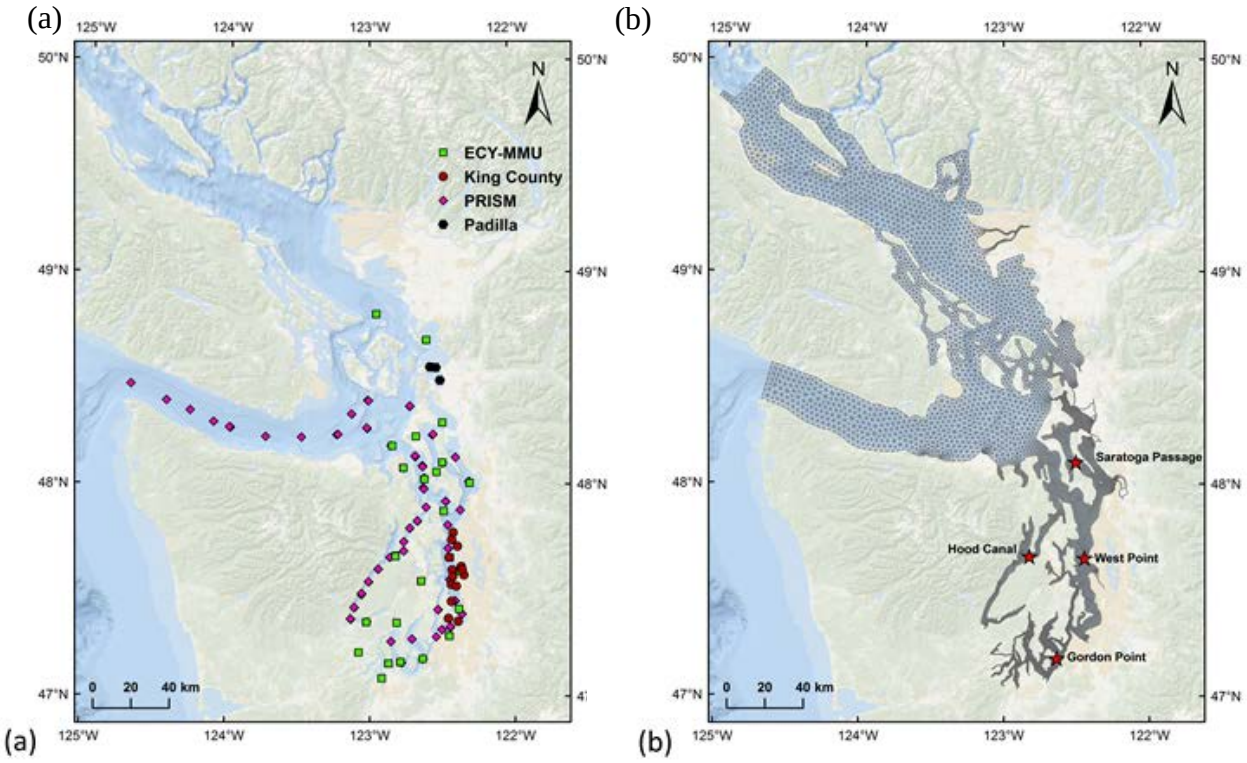

Figure 3. Locations of sampling stations, and model domain and grid.

(a) Location of observations from Puget Sound Regional Synthesis Model cruises (*PRISM, pink diamonds*), Department of Ecology's Marine Monitoring Unit (*ECY-MMU, green squares*), King County's Marine and Sediment Assessment Group (*brown circles*), and Padilla Bay NOAA National Estuarine Research Reserve System (*black hexagons*).

(b) Salish Sea Model (SSM) domain and grid. *Stars indicate the four stations used for analysis: Gordon Point, West Point, Hood Canal, and Saratoga Passage.*

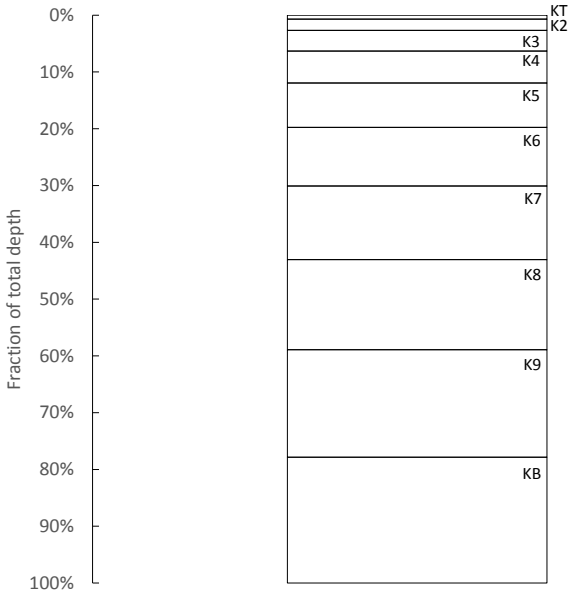

Figure 4. Grid layer relative thickness from top (KT) to bottom (KB) of water column.

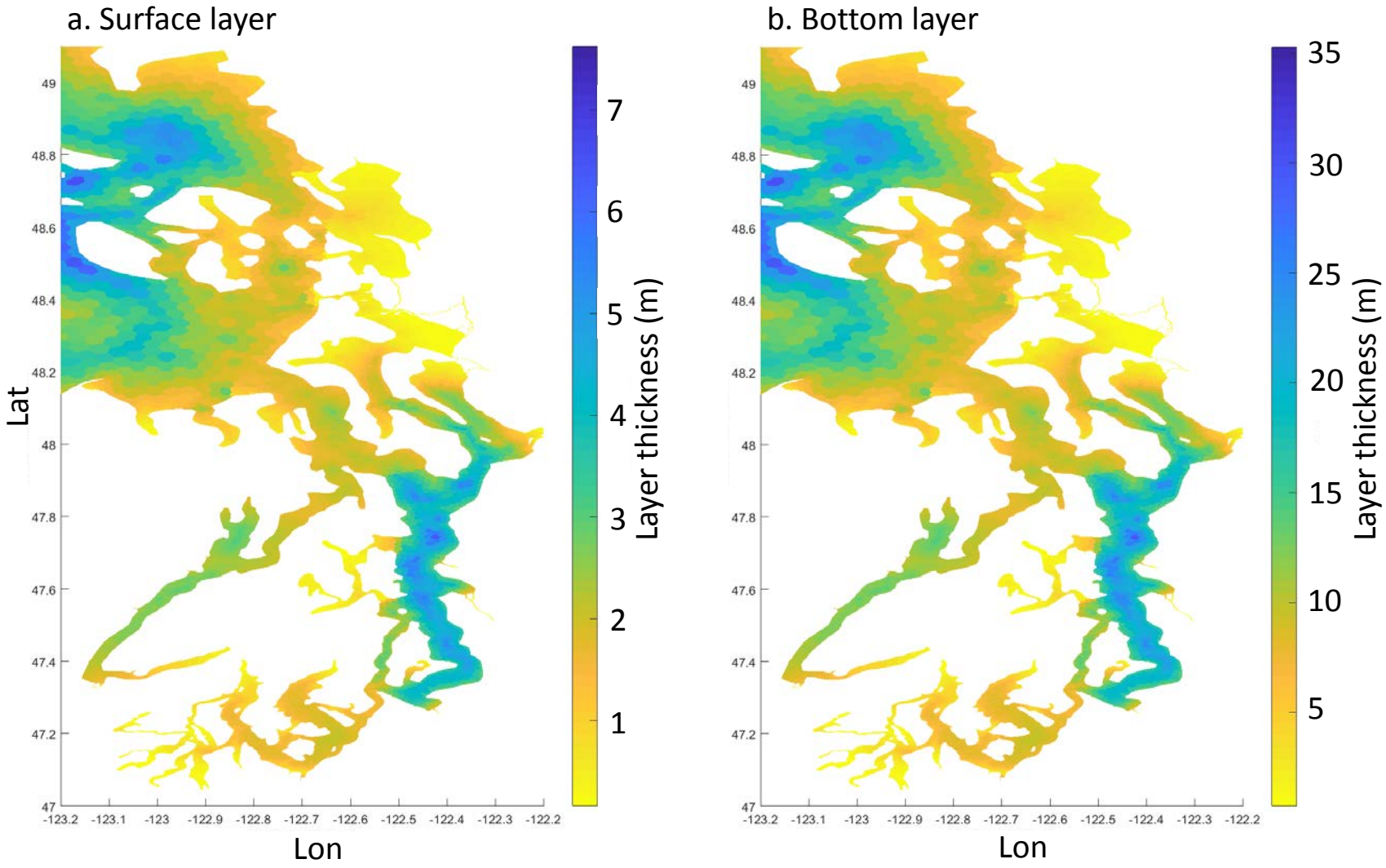

Figure 5. Thickness of the surface layer and bottom layer of the model grid.

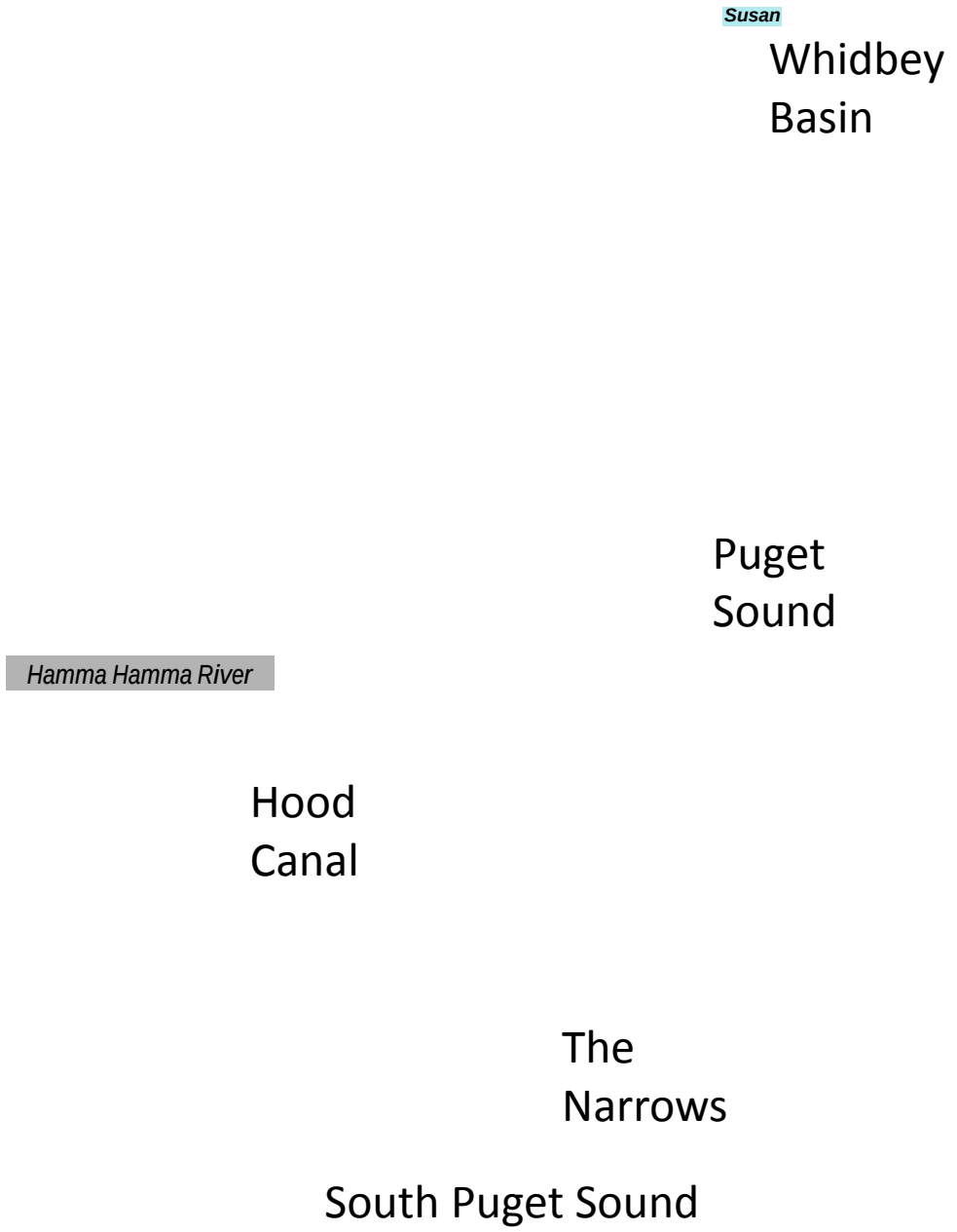

Figure 6. Locations of Ecology's sampling stations for carbonate system variables during 2014-15.

Methods

While our current focus is on Puget Sound, the model extends to the Straits of Juan de Fuca and Georgia (Figure 3b); therefore, we refer to the model as the Salish Sea Model (SSM). This project builds on related work on dissolved oxygen (Sackmann, 2009; Khangaonkar et al., 2012a,b; Roberts et al., 2015), and a previously published model approach document (Long et al., 2014). Bianucci et al. (2017) describe setup and calibration of the Ocean Acidification Module of the SSM.

The hydrodynamic component of the SSM is an application of the unstructured grid Finite-Volume Community Ocean Model (FVCOM; Chen et al., 2003). The unstructured grid framework allows for the representation of complex shoreline geometry, waterways, and islands in the Salish Sea. The biogeochemical component is an adaptation of the Integrated Compartment Model (CE-QUAL-ICM; Cerco and Cole, 1993; Cerco and Cole, 1994) for operation on an FVCOM framework, which we refer to as FVCOM-ICM when coupled with the FVCOM hydrodynamic model (Kim and Khangaonkar, 2010).

Crucial improvements from the original CE-QUAL-ICM are the addition of a two-layer sediment module (Di Toro, 2001) and the inclusion of carbonate system variables (TA, DIC) in the water column. In total, FVCOM-ICM currently tracks 16 state variables in the water column: diatoms, dinoflagellates, dissolved oxygen (DO), nitrate (NO_3), ammonium (NH_4), phosphate (PO_4), labile and refractory dissolved organic carbon (LDOC, RDOC), labile and refractory particulate organic carbon (LPOC, RPOC), labile and refractory dissolved organic nitrogen (LDON, RDON), labile and refractory particulate organic nitrogen (LPON, RPON), total alkalinity (TA), and dissolved inorganic carbon (DIC).

A schematic diagram represents the processes included in the model (Figure 7). FVCOM-ICM is run non-concurrently and uses hydrodynamic fields previously computed by FVCOM using the same model grid. The SSM has been described in detail (Khangaonkar et al., 2012a,b; Khangaonkar et al., 2011; Yang et al., 2010), so here we describe the improvements to the previously published version of the model to address the carbonate system. A separate report addresses improvements related to sediment diagenesis (Pelletier et al., 2017).

To represent the carbonate system in the water column, TA and DIC were included in the model. In contrast to other state variables, which have units of grams per cubic meter (i.e., g/m^3, which is equivalent to mg/L), TA and DIC are modeled in terms of millimole per cubic meter (umol/kg). In the case of TA, it increases due to processes that produce NH_4 or consume NO_3, while consumption of NH_4 and production of NO_3 decrease TA. Therefore, TA in the model increases due to new primary production, remineralization of LDON and RDON, water column denitrification, and sediment fluxes of NH_4; it decreases due to regenerated primary production, water column nitrification, and sediment fluxes of NO_3 (see Appendix A.1).

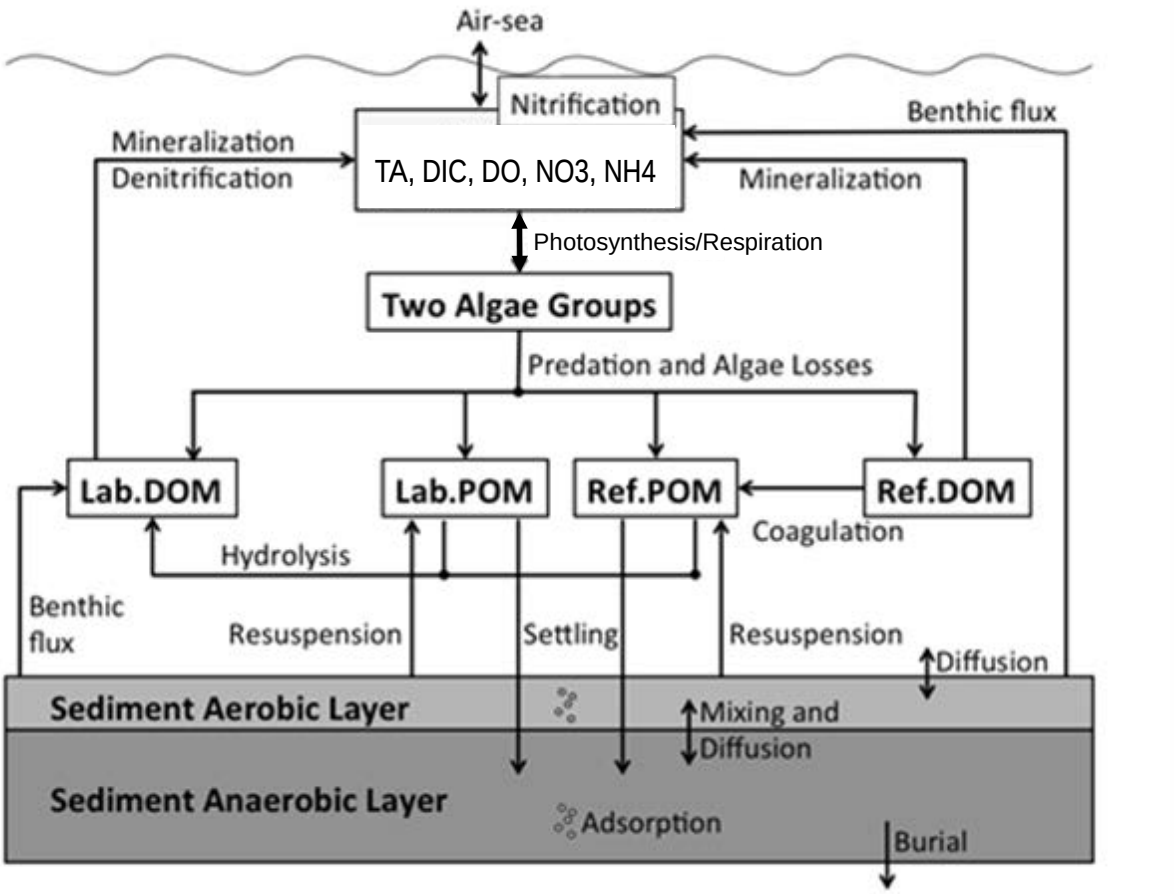

Figure 7. Biogeochemical process diagram for the Salish Sea Model.

The processes that consume DIC are primary production and water column nitrification. Production of DIC occurs through remineralization of LDOC and RDOC, water column denitrification, phytoplankton losses by predation, basal metabolism and photorespiration, and sediment fluxes (see Appendix A.2). The model also includes air-sea exchange of CO_2, which can either increase or decrease DIC depending on whether the surface partial pressure of CO_2 (pCO_2) is lower or higher than the atmospheric pCO_2 (the latter is an input to the model). Therefore, we also introduced the calculation of the seawater pCO_2 and carbonate system constants such as the solubility of CO_2 (K0) using the same equations and approach as in the CO2SYS software by Lewis and Wallace (1998). The user needs to provide input to the model the choice of K1, K2, and KSO4 dissociation constants for carbonic acid and bisulfate ion and the desired formulation of the borate-to-salinity ratio to be used.

In our current setup, we used the formulations by Lueker et al. (2000) for K1 and K2, the KSO4 of Dickson (1990), and the borate-to-salinity ratio of Uppstrom), as used in other recent observational studies (e.g., Takahashi et al., 2014; Fassbender et al., 2016). Furthermore, the gas transfer velocity currently used for both air-sea exchange of CO_2 and DO is from Wanninkhof (2014), but the user is allowed to choose among several options (e.g., Ho et al., 2006; Nightingale et al., 2000; Wanninkhof, 1992).

We developed and applied the SSM in three phases:

1. Model setup and testing
2. Calibration to existing information
3. Application to scenarios

Model Setup and Testing

The model was set up to represent year 2008 based on the DIC and TA observations available to us at the time of developing the pH module. The year 2008 had DIC and TA data from two University of Washington (UW) Puget Sound Regional Synthesis Model (PRISM) cruises in two different months (February and August), covering all of Puget Sound and the Strait of Juan de Fuca (Feely et al., 2010; Reum et al., 2014; Figure 3a).

Previous to our 2008 simulation, the model had been calibrated to year 2006 (all except carbonate system variables), and all model parameters remained unchanged for the 2008 simulation (Pelletier et al., 2017; see Khangaonkar et al., 2012a for information on the 2006 calibration before adding the carbonate-system and sediment modules, and see Table A1 for a subset of model parameters in the current FVCOM-ICM). The model was run for two years, both representing 2008 conditions. We refer to the first year as a "spin-up" time needed for the simulated variables to eliminate the effect of initial conditions; the second year is a stable simulation that can be compared against observations.

The initial and boundary conditions for variables other than TA and DIC have been described elsewhere (Khangaonkar et al., 2012a,b), so here we focus on the setup of the new carbonate variables and sediment component. The sediment module, described in more detail in Pelletier et al. (2017), was initialized by assuming the sediment is at steady state with the initial depositional fluxes of particulate organic matter (POM) to the sediment layer (based on initial settling fluxes). Initial conditions for DIC for the start of the model spin-up year were taken as the mean of the observations for all the available PRISM cruises (2008 to 2014), while initial conditions for TA for the start of the model spin-up year were calculated as a function of initial salinity (S), following the regression:

$$TA = 646.7 + 47.7 * S \qquad \text{Eqn 1}$$

Where TA is in μmol/kg and S in psu (Fassbender et al., 2016). Fassbender et al. (2016) reported a residual of 1 ± 17 μmol/kg, with most of the samples for the regression having salinity greater than 27 psu.

The open boundary conditions at the Juan de Fuca and Johnstone Straits were also calculated as regressions of S, temperature (T), and dissolved oxygen (DO) (Ianson et al. in prep):

$$DIC = -17.51 * T - 0.95 * DO + 2440.62; \qquad \text{Eqn 2}$$

$$TA = 470.13 + 52.85 * S \quad \text{if } S < 33.85 \text{ and} \qquad \text{Eqn 3}$$

$$TA = -4932.6 + 212.44 * S \quad \text{if } 33.85 \leq S \leq 34.65 \qquad \text{Eqn 4}$$

Where DIC, TA, and DO are given in μmol/kg, T in ºC and S in psu).

Model results at the end of one year were treated as preconditioning spin-up and were then used to re-initialize the model (Khangaonkar et al., 2012a,b). The simulation for year 2008 was then repeated. Therefore the influence of the assumed initial conditions for the model spin-up year is minimized, and the difference between Eqn 1 versus Eqn 3 and 4 is considered to have a negligible effect on the simulation for the year 2008.

For the rivers, observations of pH and TA from U.S. and Canadian gauged rivers were used to derive regressions as a function of river flow; then, DIC was calculated using both TA and pH values. In the case of the other freshwater point sources, we used mean monthly time series of pH and median values of TA based on data from U.S. and Canadian point sources and then calculated the corresponding time series for DIC.

An estimated regional value of 400 μatm was used to represent average conditions over the Salish Sea during 2008.[2]

Calibration Approach

Model calibration involves systematic adjustment of model reaction rates and coefficients to best match observations. In a comprehensive biogeochemical model such as the FVCOM-ICM model of the Salish Sea, there are over 200 parameters that control various biogeochemical reactions and the concentrations of 16-20 simulated variables. A comprehensive re-calibration was beyond the scope of this study. Our focus was on adjusting the parameters associated with the new sediment diagenesis (Pelletier et al., 2017) and carbonate chemistry modules. The expectation was that following completion of calibration for these two modules (pH, alkalinity and sediment fluxes), error statistics for all other variables (DO, algal biomass, and nutrients), would be re-examined to ensure that overall model error statistics for all variables continued to remain at the same level of accuracy as reported in Khangaonkar et al. (2012a,b).

To understand how well the model represents the observations, we used both qualitative and quantitative analyses. For the latter, we calculated statistical metrics that allow measuring model performance in terms of correlation (Pearson's coefficient of determination, R^2), accuracy (root mean squared error RMSE), and bias with respect to observed values. In order to conclude that the model is able to represent the observations, the R^2 should be high (a perfect match of model and observations would provide $R^2=1$) and RMSE and bias should be low (these metrics would be zero for a perfect match). In addition, we overlapped observations to simulated time series

[2] PSEMP (2016) reported atmospheric pCO_2 off the Washington coast at Cape Elizabeth and Chá Bă of 390 uatm in 2008 and 399 uatm in 2015, and atmospheric pCO_2 is rising at the rate of about 16 uatm over the 10-year period from 2006 to 2015 (PSEMP, 2016). The annual average atmospheric pCO_2 during 2009 at Twanoh on Hood Canal was 400 uatm (PSEMP, 2016). NOAA's Pacific Marine Environmental Laboratory has installed a CO_2 sensor on the top of the Space Needle to examine the variability in atmospheric pCO2 over Seattle (https://www.pmel.noaa.gov/co2/story/Space+Needle). Average atmospheric pCO_2 over the Salish Sea is likely somewhat higher than at Cape Elizabeth and Chá Bă due to urban emissions of CO_2 into the atmosphere, but lower than the values in the urban environment at the Space Needle. Daily values of atmospheric pCO_2 at the Space Needle tend to be about 20 to 50 uatm higher than off the Washington coast, and occasionally are greater than 450 uatm. We assumed that a value of 400 uatm was a reasonable mid-range estimate for the average conditions over the entire Salish Sea during 2008. We also tested the sensitivity to atmospheric pCO_2 by running a scenario with atmospheric pCO_2 set to 450 uatm.

and vertical profiles of different variables and at different locations to assess the ability of the model to simulate the observations both temporally and spatially. The selected stations were located in four regions of Puget Sound: South Sound (station near Gordon Point), main basin (station near West Point), Hood Canal, and Saratoga Passage (see Figure 3b).

The observations used to evaluate the model's performance came from different sources. As mentioned above, the TA and DIC observations belong to two PRISM cruises in February and August (Feely et al., 2010; Reum et al., 2014; Figure 3a, *pink diamonds*). These cruises also provided other data, such as T, S, DO, NO3, NH4, pH, and saturation state of aragonite, Ω_A (the last two were derived from the TA and DIC observations using CO2SYS). Furthermore, (sometimes monthly) monitoring efforts by Ecology's Marine Monitoring Unit (ECY-MMU; Bos et al., 2017), the King County's Marine and Sediment Assessment Group (King County, 2003), and the Padilla Bay NOAA National Estuarine Research Reserve System (NOAA, 2017) provided observations of T, S, DO, NO_3, and NH_4 (Figure 3a), *green squares, red circles, and black hexagons*, respectively).

Quality control (QC) screening procedures, data quality, and representativeness objectives are found in the Quality Assurance Project Plan or quality assurance/quality control (QAQC) document of each organization as cited above, with the exception of the PRISM cruises which rely on various separate reports (Alin et al., 2016; Feely et al., 2015; Feely et al., 2013.) After checking data qualifiers, we discarded data that did not meet quality objectives.

Application to Scenarios

The model was used to simulate water quality for the following two scenarios:

1. Realistic historical conditions during 2008[3]
2. Reference conditions that are the same as the historical 2008 conditions, except with estimated regional anthropogenic nutrient sources excluded. The regional anthropogenic nutrient loads that were excluded from the reference condition scenario include anthropogenic inorganic N (nitrate and ammonium), anthropogenic organic N (dissolved and particulate), and anthropogenic organic carbon (dissolved and particulate).

The effect of regional anthropogenic nutrient sources on water quality was evaluated by analyzing the difference in results between the historical conditions and the reference conditions. Regional anthropogenic nutrient sources that were excluded in the reference conditions include the anthropogenic component of loading in the wastewater treatment plants and all freshwater sources within Washington State.

The method of estimating the nutrient loading from all existing sources and reference conditions (with estimated regional anthropogenic sources excluded) are presented in Mohamedali et al. (2011) and described in Appendix B.

[3] Feely et al. (2010) used data collected in 2008 to calculate the change in carbonate system variables due to combined global and regional anthropogenic influences. Our use of 2008 to calculate the changes due to regional anthropogenic nutrient sources supports our comparisons with their estimates. The average residence time, salinity, nitrate, and DO deficit in 2008 were slightly higher, but near the median of conditions over the 10-year period from 2005-2015 (PSEMP, 2016). Water temperatures and chlorophyll-a were somewhat lower than normal.

Results

Model Performance

We compared observations from Puget Sound and the Strait of Juan de Fuca from 2008 against model results in several ways. First, we compared all observational data against the corresponding model values in scatter plots (Figure 8). The statistical metrics resulting from this comparison indicated a good overall performance of the model (Table 2). The R^2 values ranged from about 0.3 to 0.8, and they were all significant at more than 99% confidence ($p<0.01$), even though some variables may not be normally distributed, and therefore the R^2 may underestimate the relationship between predicted and observed values. The lowest correlations were for salinity (S) and chlorophyll-a (Chl-a) with $R^2 = 0.37$ and 0.25, respectively ($p<0.01$).

One of the reasons that led to the low R^2 for S was the still-insufficient model resolution in near-shore regions affected by rivers; sometimes a station belongs to the river plume in the observations but not in the model and vice versa. Similarly, Chl-a is patchy and highly variable, making it difficult for the model to accurately represent the spatial and temporal variability. The RMSE values indicate that on average the model was within 1.5 ^{o}C (T), 1.3 psu (S), 2.78 µgl/L (Chl-a), 1.8 mg/L (DO), 0.08 mg/L (NO3-N), 70.3 µmol/kg (DIC), 60.9 µmol/kg (TA), and 0.14 (pH) compared with the observations. The biases were slightly negative (i.e., the mean of model predictions underestimated the mean of observations), except for T, which presented a bias toward warm temperatures.

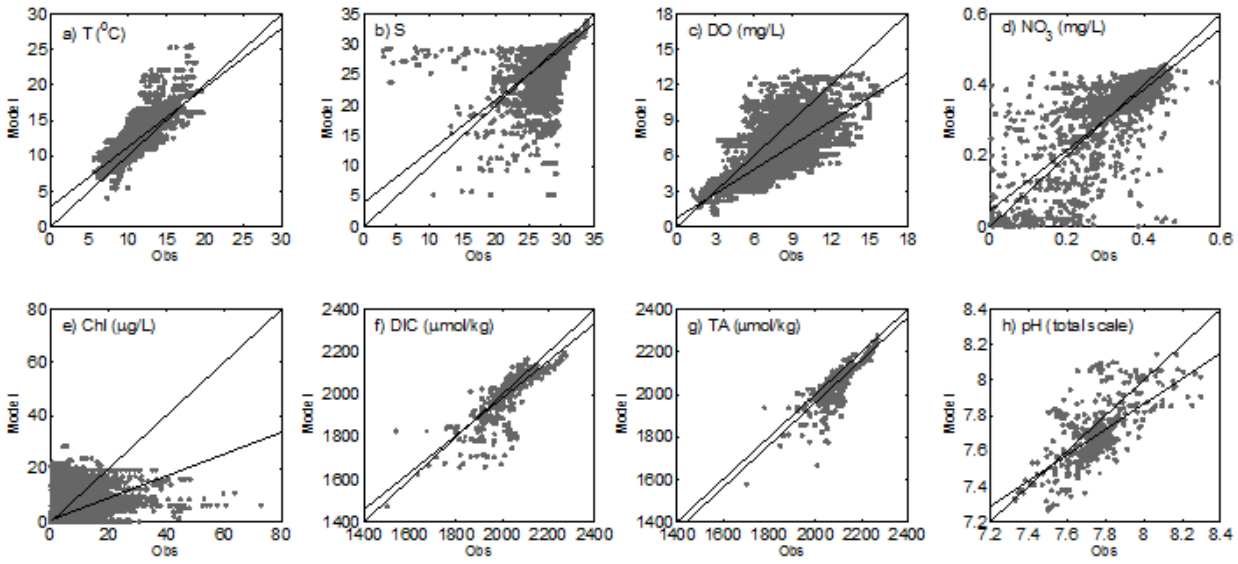

Figure 8. Model vs. observations for the whole Salish Sea Model domain for 2008.

Table 2. Statistical metrics of model global performance for year 2008[a]

	R^2 [b]	RMSE	Bias	N
T (°C)	0.81	1.48	1.28	67858
S (psu)	0.37	1.33	-0.68	66934
Chl (µg/L)	0.25	2.78	-0.30	66041
DO (mg/L)	0.64	1.80	-1.56	66538
NO_3 (mg/L)	0.64	0.08	-0.001	1902
DIC (µmol/kg)	0.59	70.33	-20.13	593
TA (µmol/kg)	0.66	60.89	-38.75	589
pH (total scale)	0.41	0.14	-0.07	584
pCO_2 (uatm)	0.42	330.33	183.4	589
Ω_{arag}	0.47	0.32	-0.12	589

[a] While R^2 is dimensionless, RMSE and bias have the units shown in the first column.
N is the total number of matches between observations and the model.
[b] All the correlations are significant beyond the 1% level.

Overall, while the differences between model and observations (particularly in S and Chl) suggest that there is room for model improvements (e.g., increase resolution in narrow inlets, intertidal regions, and around islands), the statistical metrics are significant and within reasonable values. Our ability to assess model skill is limited to the locations where data were collected.

In this report we use the model to calculate differences in carbonate system variables, between the model run that represents existing conditions in 2008, compared with the model run under reference conditions, to determine change that is caused by regional anthropogenic nutrient sources. Because the predicted carbonate system variables in both of the model runs are highly correlated, the RMSE of the difference between model scenarios ($RMSE_{diff}$) is much less than the RMSE of either the existing or reference condition. Table 3 presents the estimated RMSE of the difference.

Table 3. Estimated RMSE of the difference between the existing condition and the reference condition for the carbonate system variables.

Variable	RMSE of existing and reference conditions	Correlation coefficient between existing and reference conditions	RMSE of difference between existing and reference conditions
DIC ($mmol/m^3$)	70.33	0.999942	0.76
TA ($mmol/m^3$)	60.89	0.999993	0.23
pH (total)	0.14	0.999061	0.0061
pCO_2 (uatm)	330.33	0.996852	26.2
Ω_{arag}	0.32	0.996318	0.027

The following equations (Snedecor and Cochran, 1989) were used to estimate the variance of the difference between existing conditions and reference conditions (Var_{diff} and $RMSE_{diff}$) using the variance of the existing condition as an estimate of the variance of the reference condition (R is Pearson's correlation coefficient between existing and reference conditions):

$Var_{existing} = RMSE_{existing}^2$
$Var_{reference} = RMSE_{reference}^2 = RMSE_{existing}^2$
$Var_{diff} = Var_{existing} + Var_{reference} - 2 * R * RMSE_{existing} * RMSE_{reference}$
$RMSE_{diff} = Var_{diff}^{0.5}$

We selected four stations (see previous section and Figure 3b) to compare the modeled time series at the surface and the bottom layers of the water column against the observations (Figures 9 and 10). The model successfully represented the seasonal cycle of the observations. The model also predicted features related to high frequency variability (e.g., tidal mixing, storm systems, and variability in freshwater discharge), although observed high-frequency data were not available in 2008 for comparison with predictions. In particular, both model and observations showed larger temporal variability at the surface (Figure 9) than at the bottom (Figure 10). This is due to the higher frequency of surface forcing (e.g., air-sea exchange, storms, runoff, photosynthetic processes) compared with that of bottom forcing (incoming waters from the open ocean, sediment fluxes, remineralization processes).

For the carbonate system variables, observations for 2008 were only available in February and August, so observations for other years were added to the time series plots (gray symbols). While we do not expect a perfect match between our 2008 model and observations belonging to other years, the good agreement indicates that both the seasonal cycle and the magnitudes of the 2008 simulation are reasonable.

Vertical profiles for the same four stations (Figure 11) for February (circles) and August (triangles) 2008 showed an overall agreement between model and observations for the carbonate variables. The model reproduced the observed DIC vertical stratification at all stations and both months, while modeled TA tended to have slightly more vertical structure than the observations at Gordon Point and in the main basin.

The errors in both DIC and TA propagate into the calculations of pH and Ω_{arag}, resulting in larger deviations between observed and modeled pH and Ω_A. Nevertheless, in most cases these modeled variables showed a good representation of the observed vertical structure. The largest relative errors between modeled and observation-based pH and Ω_{arag} were found in summer at Gordon Point, due to the combination of errors in TA (model higher than observations) and DIC (model lower than observations).

The model predictions for Ω_{arag} during 2008 are compared with observations measured during 2014-15 in Figure 12. A very close match of predicted and observed values is not expected because the predictions are from 2008 and the observations are from 2014-15. For example, in 2015, water temperatures were warmer than the historic record throughout all Puget Sound basins and depths for nearly the entire year (PSEMP, 2016). Figure 12 demonstrates that modeled seasonal variation is comparable to available monthly observational data.

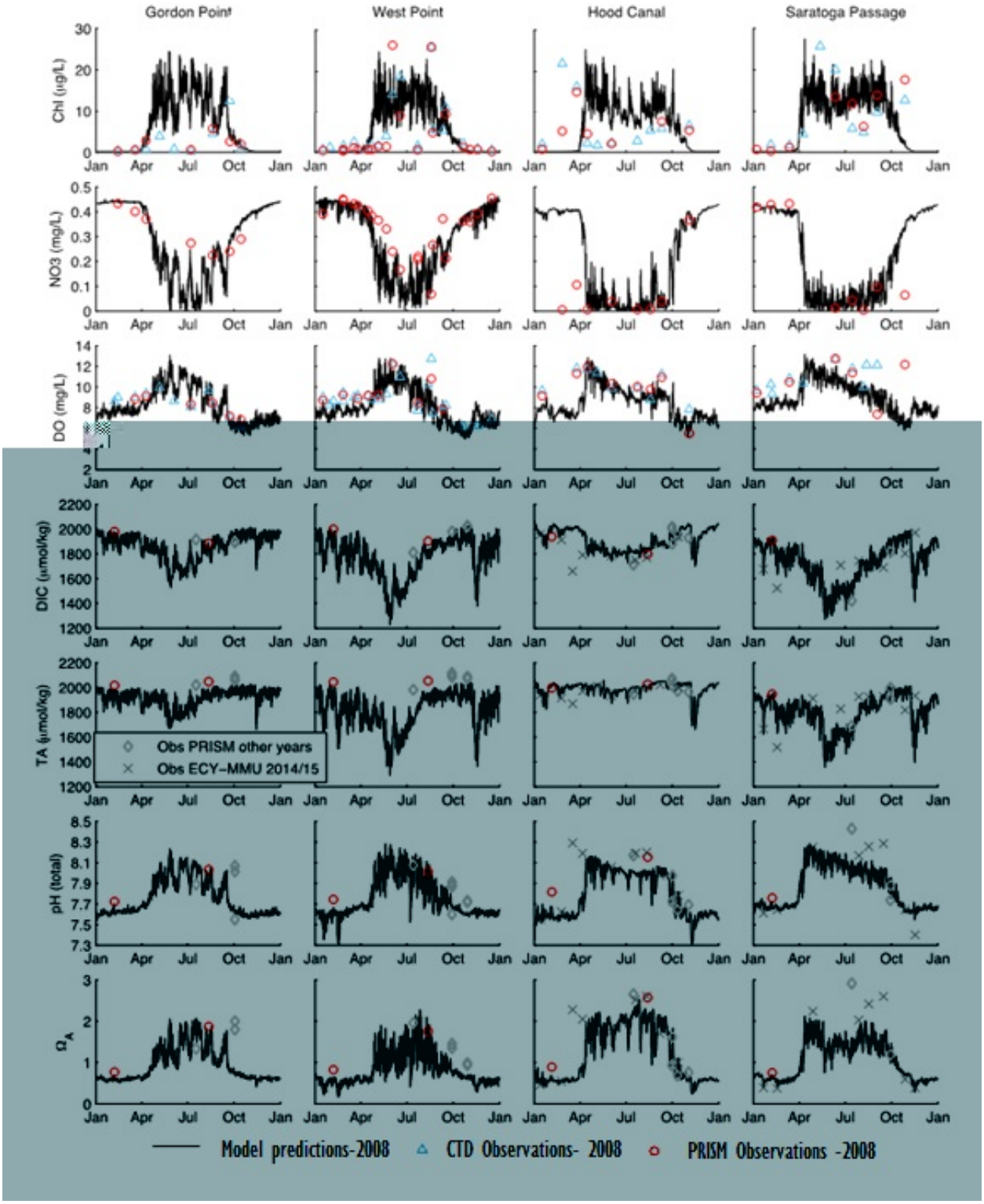

Figure 9. Time series of modeled and observed values at four stations (surface).

Baseline indicates model predictions.

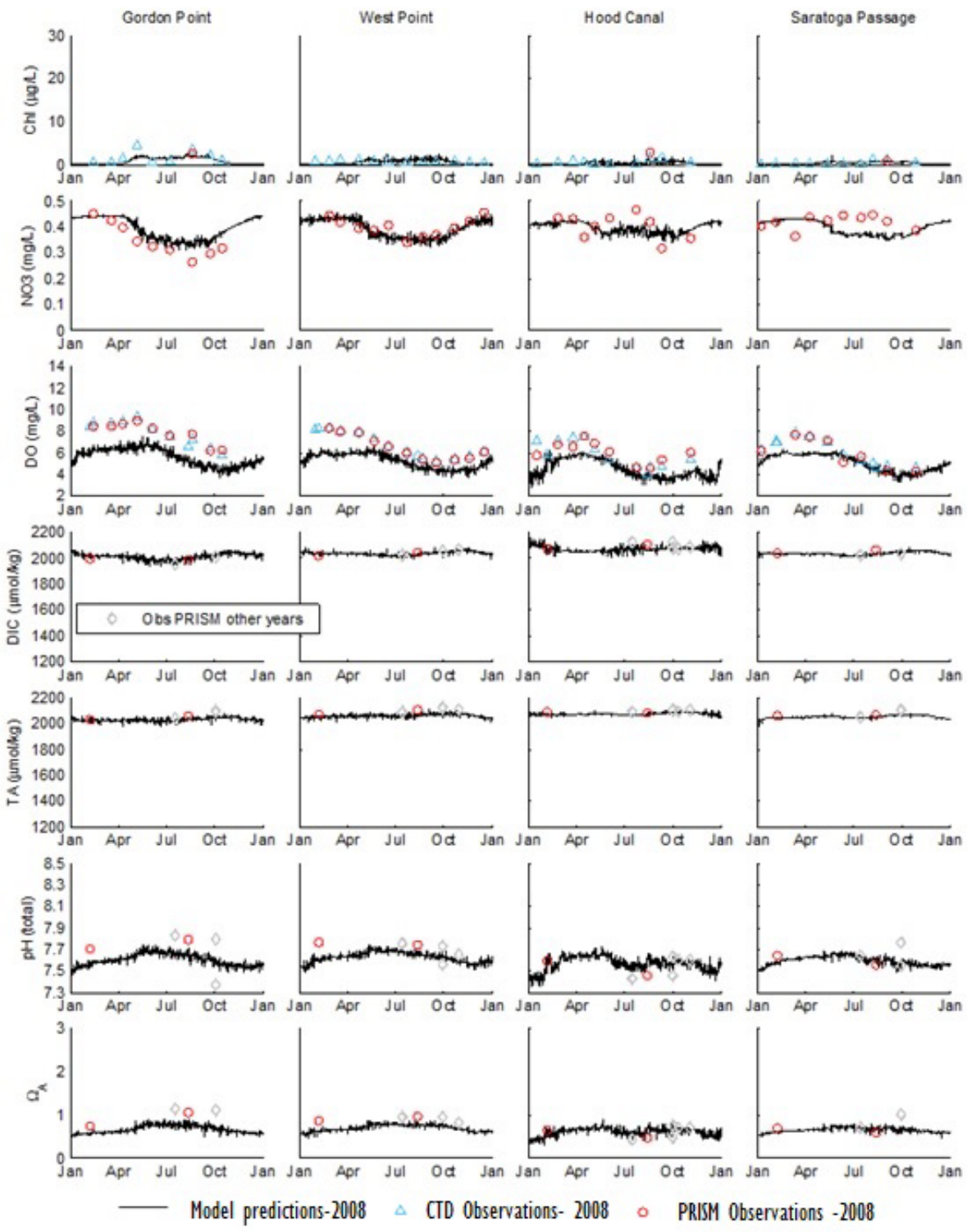

Figure 10. Time series of modeled and observed values at four stations (bottom).

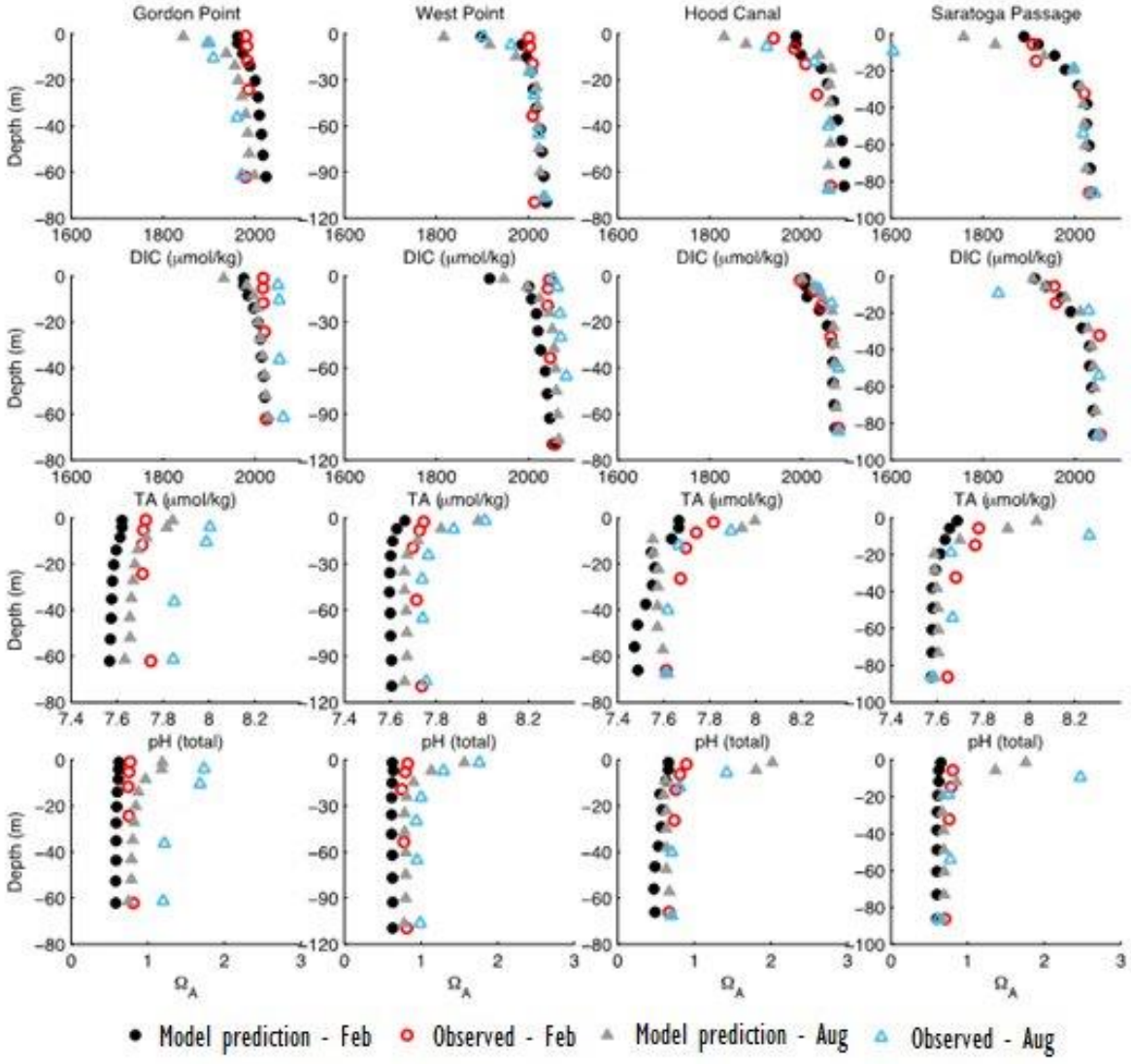

Figure 11. Profiles of model and observed data at four stations.

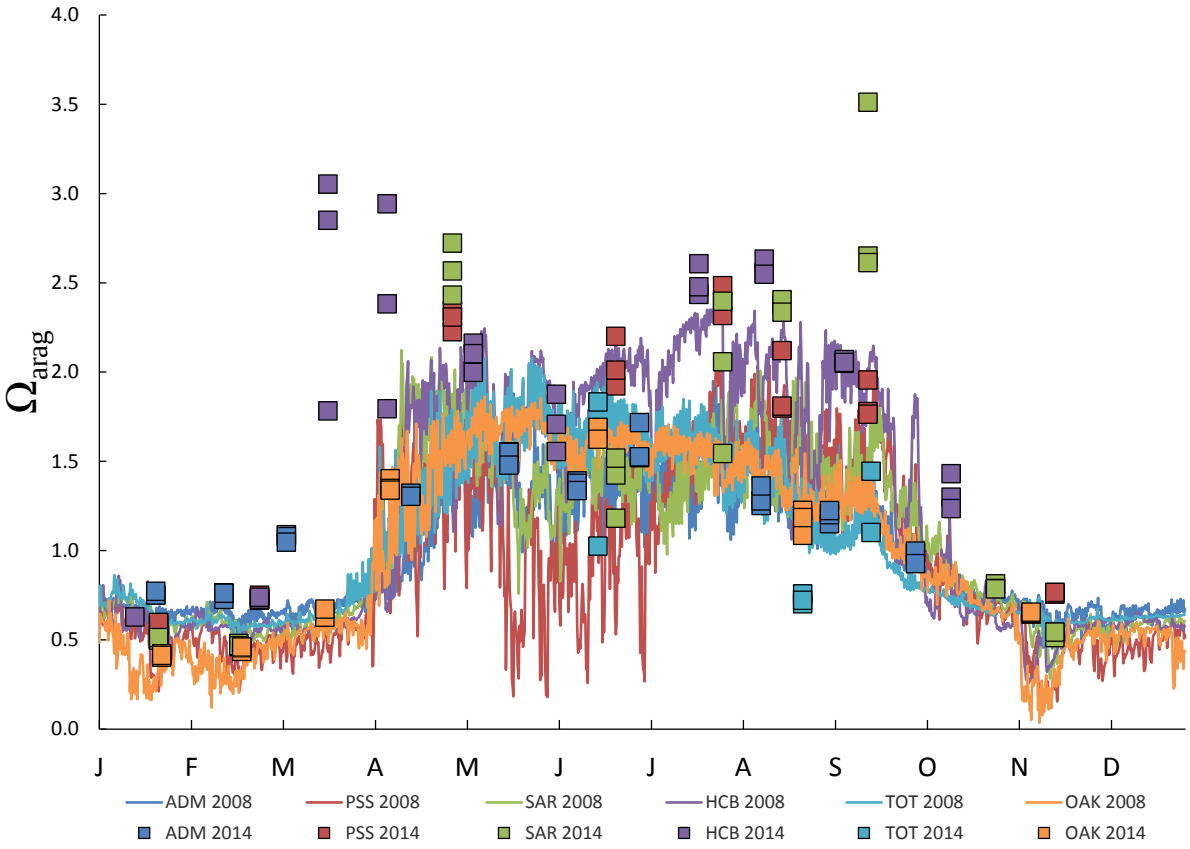

Figure 12. Predictions of Ω_{arag} during 2008 compared with data from 2014-15.
Predicted values are plotted as lines and observed values are plotted as squares.

Model Scenarios[4]

Historical simulated conditions during 2008

pH

The minimum pH during 2008 ranged from about 6.3 to 7.6 in the surface 20 meters (Figure 13a) and 6.0 to 7.8 in the bottom layer (Figure 13b). The lowest minimum pH tended to occur in the surface layer in the vicinity of freshwater influences.

The annual average pH during 2008 ranged from about 7.1 to 7.9 in the surface 20 meters (Figure 14a) and 7.2 to 7.9 in the bottom layer (Figure 14b).

Monthly average pH in the surface and bottom layers ranged from about 6.9 to 8.3 (Appendix C).

[4] All ranges reported are based on the 1st and 99th percentiles of the simulated values unless noted otherwise. Color bars in figures may have ranges that are less than the total range to accentuate spatial variability.

The cumulative time with pH less than 7 in the surface 20 meters was generally less than a few days and was limited to a fairly small area near the Skagit River channel and innermost Skagit Bay during high runoff (Figure 15a). The cumulative time with pH less than 7.5 in the surface 20 meters was up to several months in Lynch Cove and South Hood Canal (Figure 15b). Lynch Cove also had relatively low average pH in the surface 20 meters (Figure 14a) and bottom layer (Figure 14b).

Thalweg transects were selected at two locations to show vertical and longitudinal variations in carbonate system variables, nutrients, and Chl-a: South Hood Canal from Dabob Bay to Lynch Cove, and from Carr Inlet to Edmonds (Figure 16).

The thalweg transect from Carr Inlet to Edmonds of average conditions during May-September reveals that pH remains generally uniform at depth in the main basin (between 7.6 to 7.8) during the growing season, except for the top 5 to 10 meters, where it increases above 8 (Figure 17). The range is lower in the South Hood Canal transect (7.3 to 7.5) throughout the water column, and shows a similar pattern of increasing towards a pH of about 8 in the top 10 meters (Figure 17).

May-September 2008 averages along thalweg transects for DIN, Chl-a, and non-algal organic carbon are presented in Figure 18. Throughout most of the water column below a depth of 20 meters, DIN is fairly uniform in both transects (around 0.4 to 0.5 mg/L). Chl-a concentrations are highest in the euphotic zone above a depth of 20 meters, and higher in the main basin of Puget Sound (Carr Inlet to Edmonds) than in South Hood Canal.

Non-algal organic carbon represents the pool of organic carbon that is subject to release of CO_2 by heterotrophic metabolism, including detrital particulate organic carbon and dissolved organic carbon. Higher average concentrations of non-algal carbon are predicted in the transect from Carr Inlet to Edmonds, of nearly 1 mg/L at the surface and bottom, whereas the averages in the Hood Canal transect ranged from around 0.8 to 0.9 mg/L at the surface and about 0.6 to 0.7 mg/L at the bottom (Figure 18).

Dissolved inorganic carbon (DIC)

The annual average DIC during 2008 ranged from about 530 to 2100 umol/kg in the surface 20 meters (Figure 19a) and 710 to 2200 umol/kg in the bottom layer (Figure 19b). The lowest average DIC tended to occur in the surface layer near freshwater influences and in areas of relatively high primary production.

Monthly average DIC in the surface and bottom layers ranged from about 250 to 2200 umol/kg (Appendix D).

During the warmer, productive months (May-September), DIC concentrations were generally higher throughout most of the water column in South Hood Canal, when compared to the water column in the main basin (Figure 17).

Total alkalinity (TA)

The annual average TA during 2008 ranged from about 470 to 2200 umol/kg in the surface 20 meters (Figure 20a) and 660 to 2300 umol/kg in the bottom layer (Figure 20b). The lowest average TA tended to occur in the surface layer near freshwater influences.
Estuarine TA is lower than TA in the open ocean due to the dilution with freshwater which has lower TA.

Monthly average TA in the surface and bottom layers ranged from about 210 to 2300 umol/kg (Appendix E).

Aragonite saturation state (Ω_{arag})

The minimum Ω_{arag} during 2008 was generally less than 1 everywhere in the surface 20 meters (Figure 21a) and bottom layer (Figure 21b). The lowest Ω_{arag} in the surface 20 meters is predicted in the Whidbey Basin (Skagit Bay, Port Susan, and Penn Cove), South Hood Canal/Lynch Cove, the nearshore areas around the San Juan Islands, and scattered areas of Puget Sound including areas closest to freshwater influences (Figure 21a).

The annual average Ω_{arag} during 2008 ranged from about 0.03 to 1.2 in the surface 20 meters (Figure 22a) and 0.08 to 1.1 in the bottom layer (Figure 22b). The highest average Ω_{arag} in the surface 20 meters occurred in the finger inlets of South Puget Sound (Totten, Eld, Henderson, and inner Carr Inlets), Sinclair and Dyes Inlets, Liberty Bay, Samish Bay, and Sequim Bay. The lowest average Ω_{arag} in the bottom layer occurred in Lynch Cove and Hood Canal, Port Susan, Penn Cove, Bellingham Bay, Samish Bay, and in the Skagit River channels.

The cumulative period of time with Ω_{arag} less than 1 in the surface 20 meters ranged from about six months (from October to March) to the entire year, with the longest durations near largest freshwater inflows (Figure 23a). In most areas the bottom layer Ω_{arag} was less than 1 for the entire year (Figure 23b), with the exception of some shallow areas with bottom layer Ω_{arag} greater than 1 for up to about half the year, including the finger inlets of South Puget Sound (Oakland Bay and Totten, Eld, inner Budd, Case, and Carr Inlets), and Sinclair/Dyes Inlets.

During the warm, productive months (May-September), the average Ω_{arag} in the surface 20 meters remained close to 1, or slightly below 1, in many areas (Figure 24). Refuges with relatively high average Ω_{arag} greater than 1 during May-September are predicted in the finger inlets of South Puget Sound (Oakland Bay and Totten, Eld, Budd, Henderson, innermost Case, and Carr Inlets), in addition to Sinclair/Dyes Inlets, Padilla Bay, Samish Bay, Discovery Bay, and Sequim Bay (Figure 24). The occurrence of Ω_{arag} below 1 is particularly noticeable in the plume of the Fraser River, and to a lesser extent in South Hood Canal/Lynch Cove, the Whidbey Basin (Port Susan, Saratoga Passage, Skagit Bay), Elliott Bay, Commencement Bay, Colvos Passage, the deepest areas of South Puget Sound (Dana Passage through the Nisqually Reach), and the Strait of Juan de Fuca near Admiralty Inlet (Figure 24).

Hood Canal's top 20 meters exhibit low average Ω_{arag} (below 0.8 in the southern portion) during May-September 2008 (Figure 24). The prediction of relatively low Ω_{arag} in Hood Canal in 2008 is consistent with high rates of shellfish larvae die-offs reported by the Hood Canal commercial shellfish growers (Dewey, 2017).

Monthly average Ω_{arag} in the surface and bottom layers ranged from 0 to 2.2 (Appendix F).

pCO_2

The annual average pCO_2 in the surface 20 meters during 2008 ranged from about 590 to 1460 uatm (Figure 25a). Highest average pCO_2 tended to occur in Lynch Cove and Hood Canal. Lowest average pCO_2 occurred in South Puget Sound finger inlets (Oakland Bay and Totten, Eld, Henderson, innermost Case, and Carr Inlets), Sinclair/Dyes Inlets, Skagit Bay, Saratoga Passage, and Sequim Bay.

Monthly average pCO_2 in the surface and bottom layers ranged from about 180 to 2700 uatm (Appendix G).

Atmospheric pCO_2 averages around 400 uatm (the model inputs assume a constant value of 400 uatm). When the pCO_2 in the surface layer of Puget Sound is less than around 400 uatm, the net flux of CO_2 would be from the air to the water. When the surface layer pCO_2 is greater than around 400 uatm, the net flux would be from the water to the air. The cumulative period of time with surface layer pCO_2 less than 400 uatm ranged from about 0 to 170 days (Figure 25b). In other words, the period of time when the net flux of CO_2 is from the water to the air ranges from about half the year to the entire year.

Revelle factor (RF)

The RF is the ratio of instantaneous change in pCO_2 to the change in total DIC and is a measure of the resistance to atmospheric pCO_2 being absorbed by the surface layer (Feely et al., 2010). As the RF increases, the capacity of the water to absorb CO_2 decreases.

The annual average RF in the surface 20 meters ranged from about 8 to 20, with most areas ranging from about 16 to 19 (10^{th} to 90^{th} percentile) (Figure 26). This is very similar to the range of 14-19 reported by Feely et al. (2010), and significantly higher than open-ocean RF values, which range from about 8 to 15 (Sabine et al., 2004). The RF indicates how much change in DIC would be expected with a given change in pCO_2, with high RFs corresponding to smaller changes in DIC. The lowest RF in Puget Sound are predicted in the shallowest areas such as the finger inlets of South Puget Sound, Lynch Cove, Sinclair/Dyes Inlets, Skagit Bay, Samish Bay, Bellingham Bay, and Sequim Bay.

Monthly average RF ranged from about 5 to 23 in the surface and bottom layers (Appendix H).

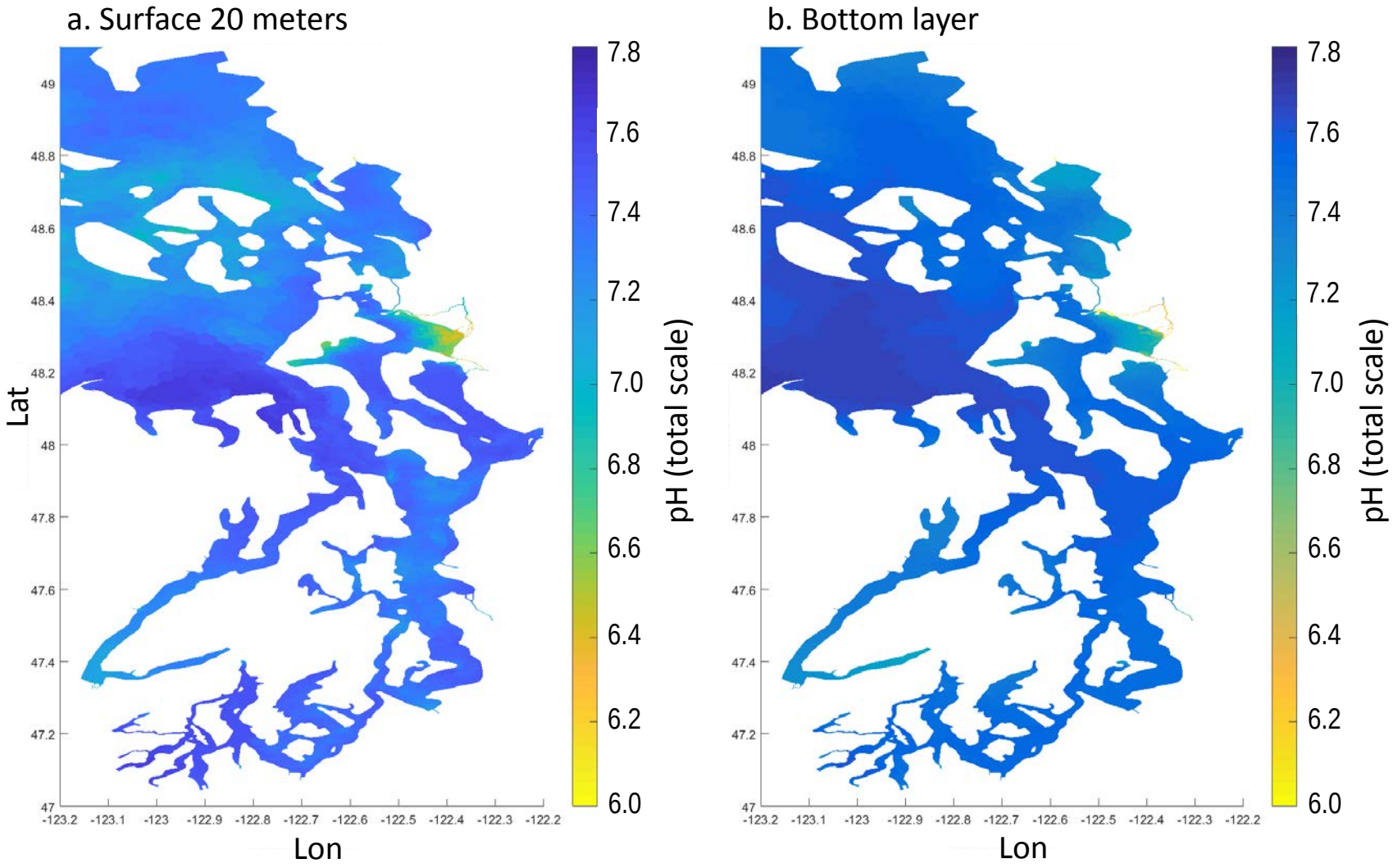

Figure 13. Minimum pH in the surface 20 meters and the bottom layer of Puget Sound in 2008.

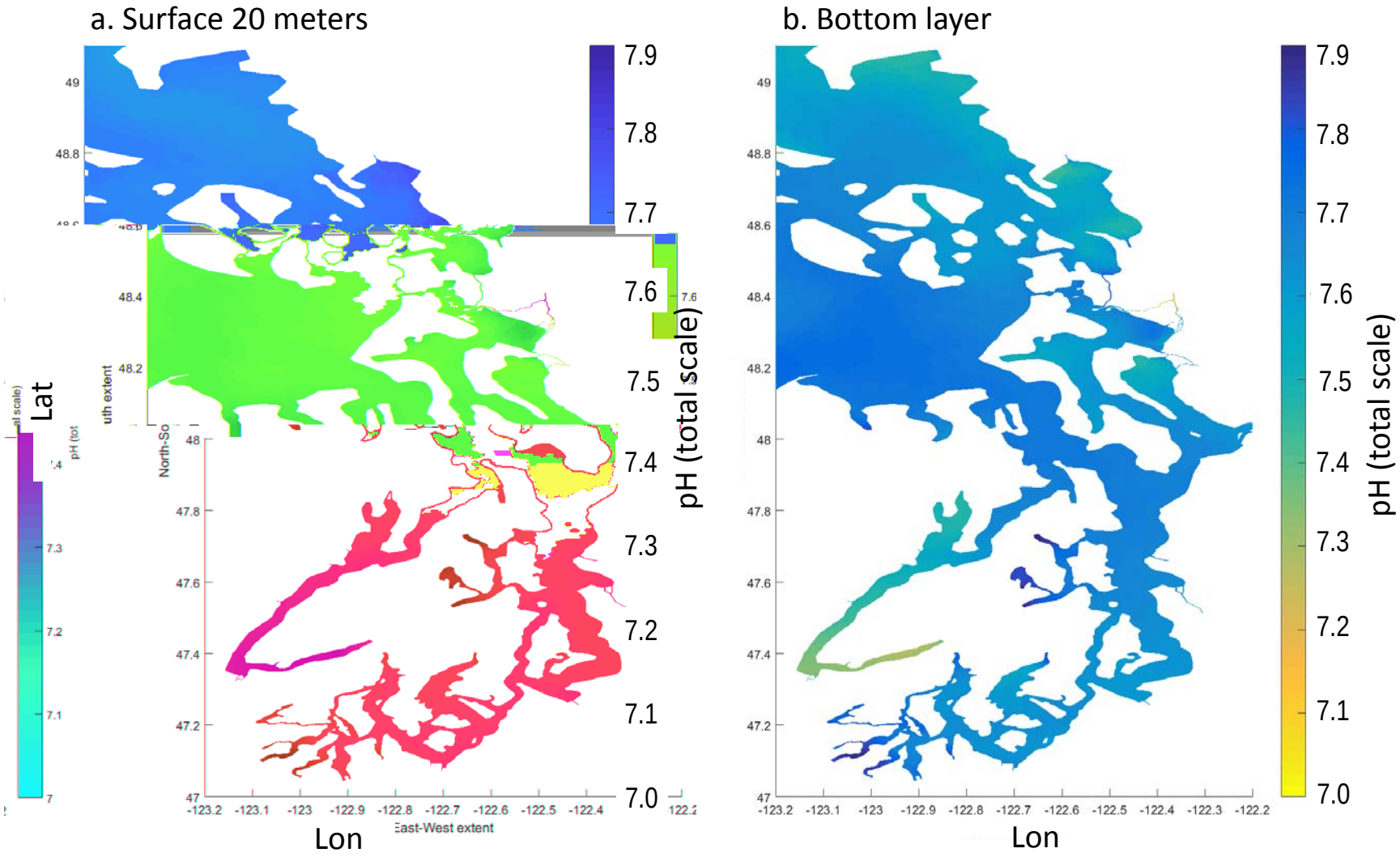

Figure 14. Annual average pH in the surface 20 meters and the bottom layer of Puget Sound in 2008.

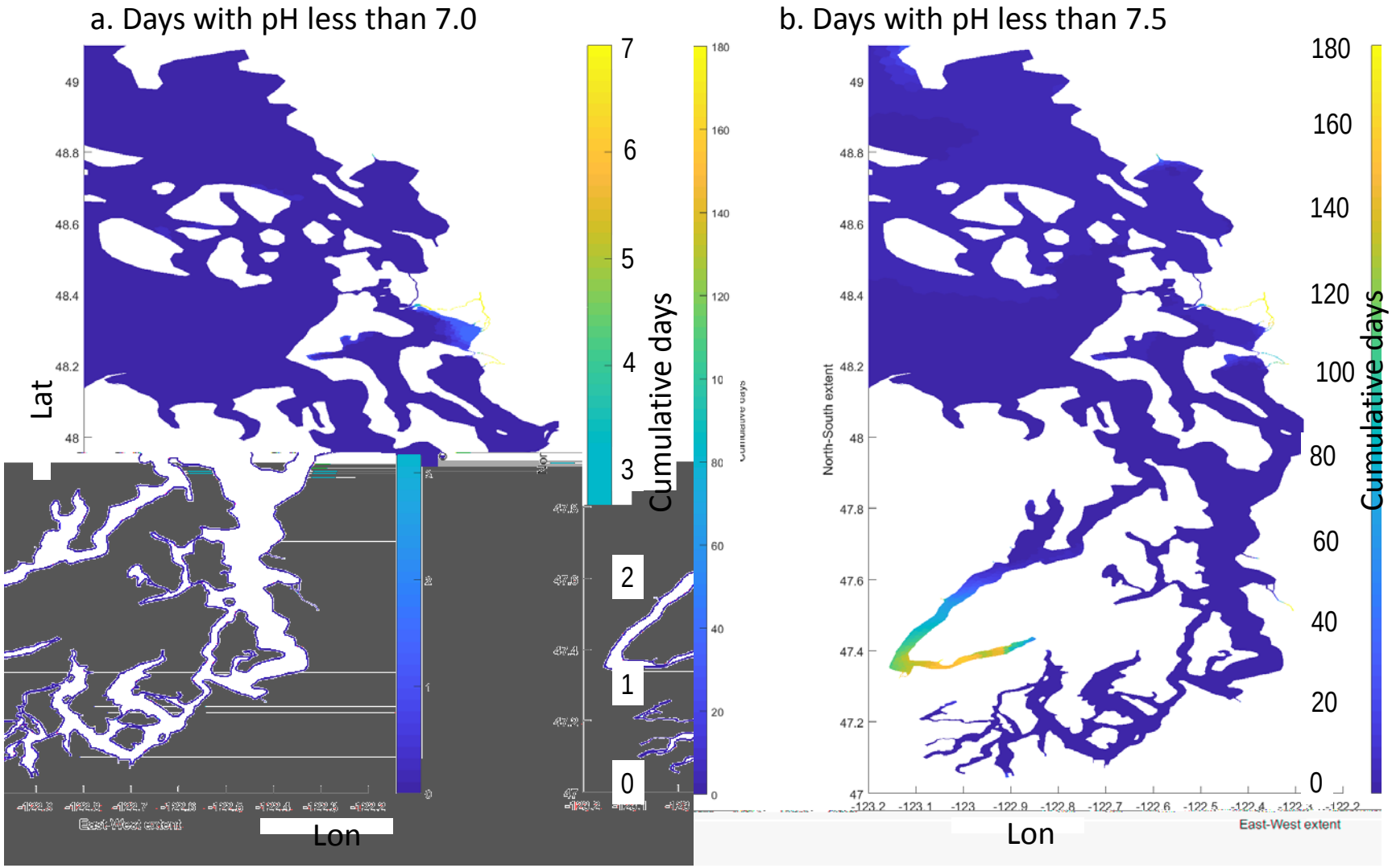

Figure 15. Cumulative number of days with pH less than 7 and 7.5 in the surface 20 meters of Puget Sound from January-December 2008.

Note different scales for a and b.

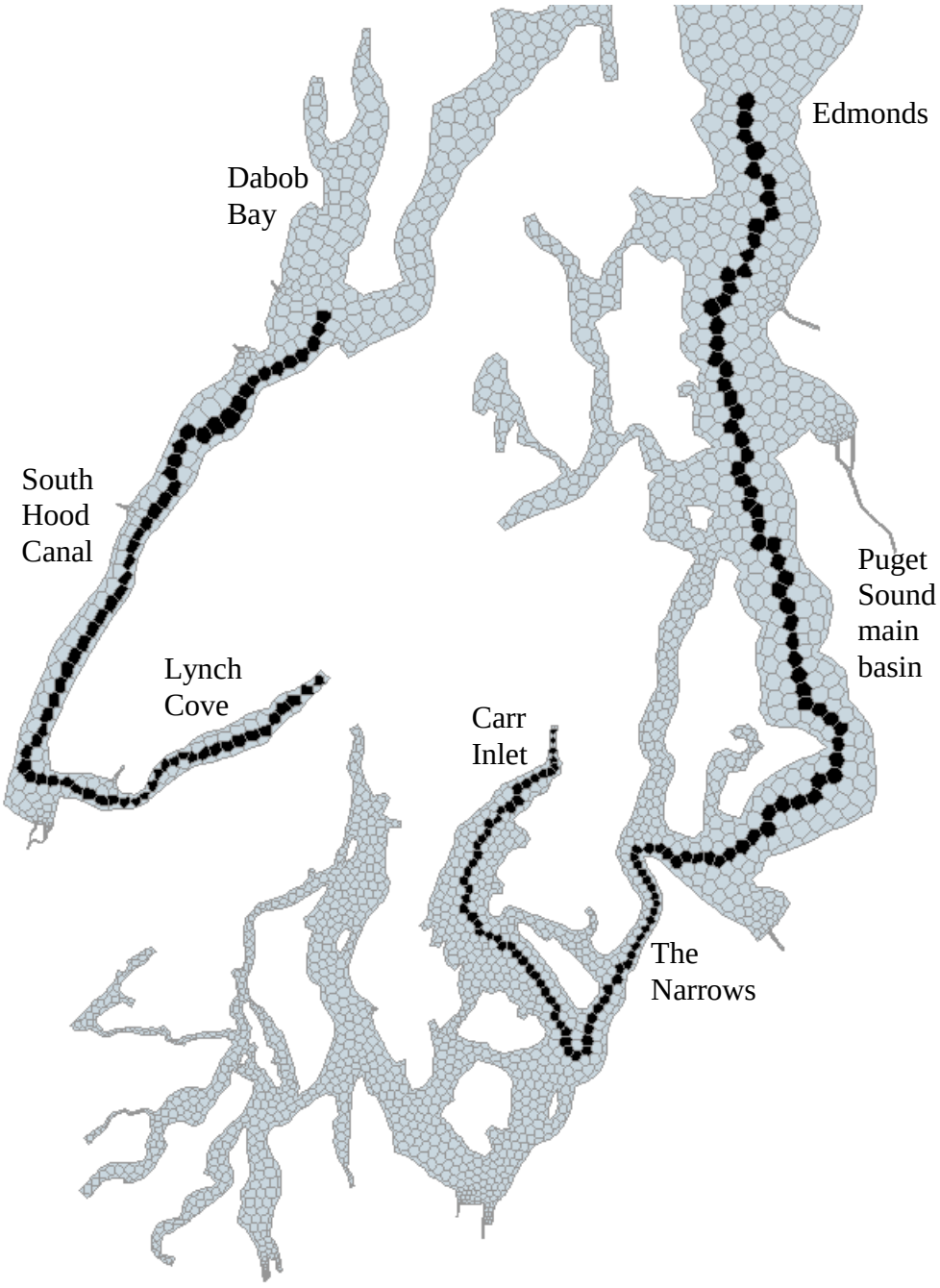

Figure 16. Model grid cells selected along thalweg transects in South Hood Canal and from Carr Inlet to Edmonds.

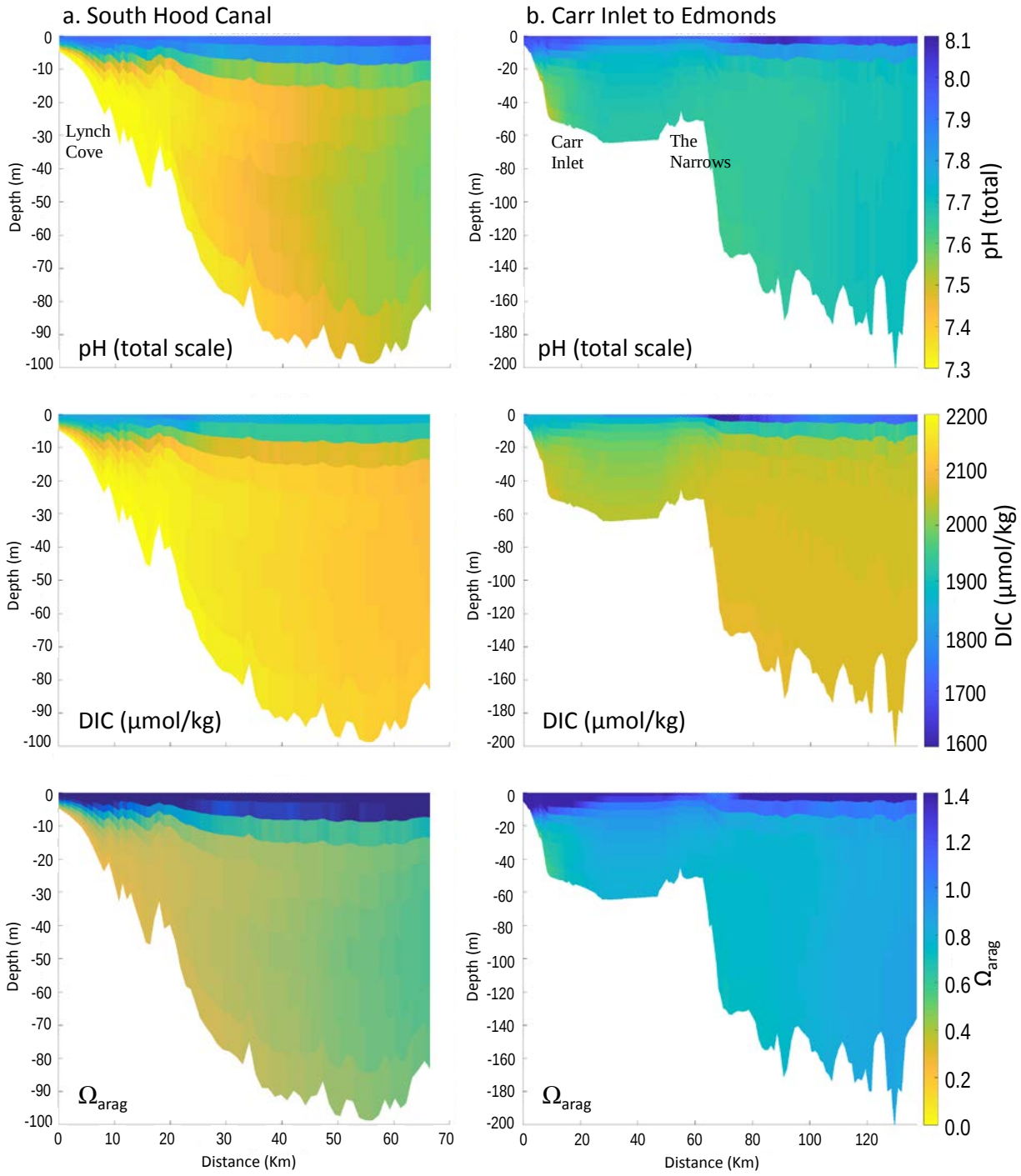

Figure 17. May-September 2008 averages of pH, DIC, and Ω_{arag} along thalweg transects in South Hood Canal and Carr Inlet to Edmonds.

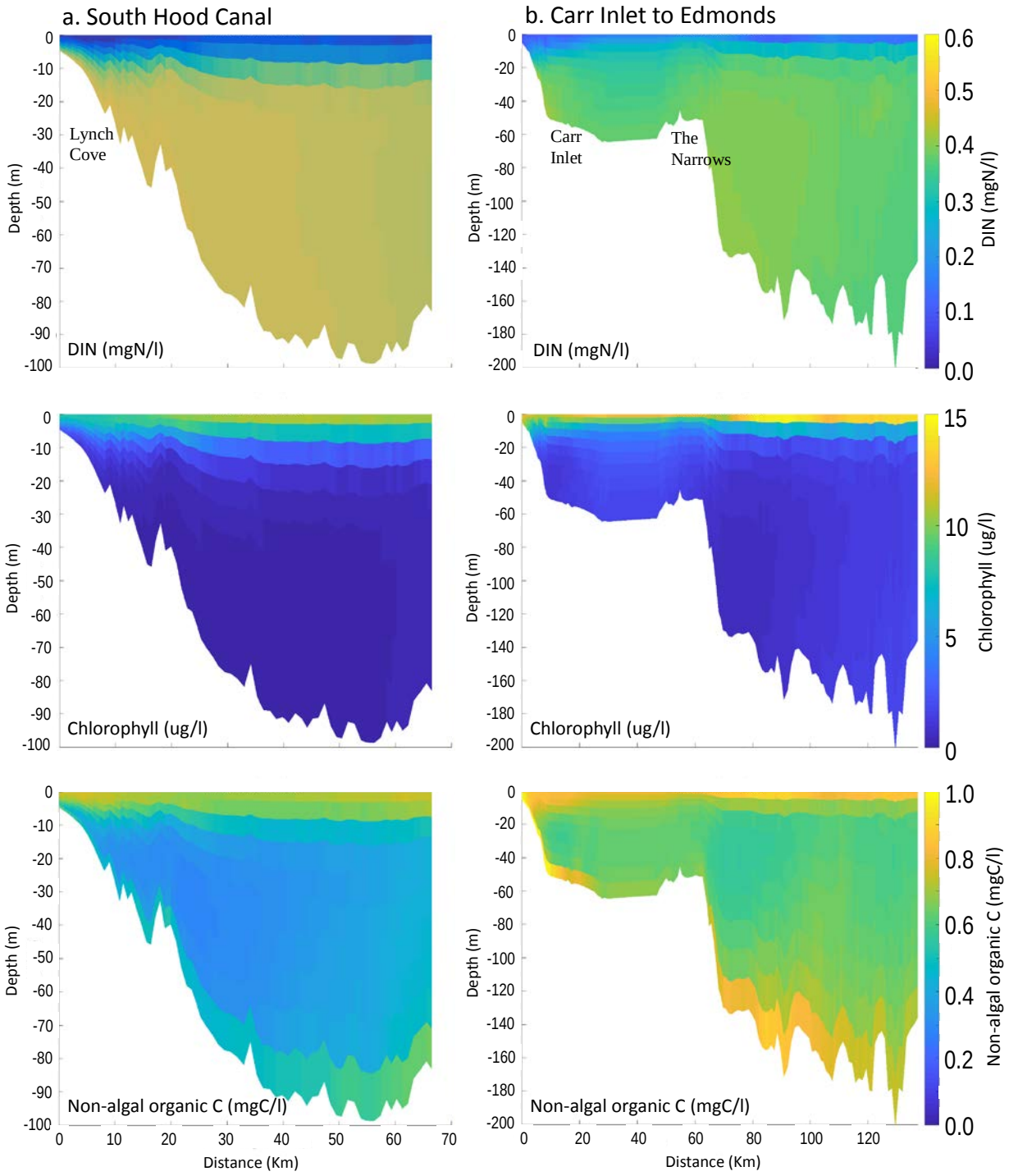

Figure 18. May-September 2008 averages of DIN, Chl-a, and non-algal organic carbon (sum of detrital particulate organic C and dissolved organic C) along thalweg transects in South Hood Canal and Carr Inlet to Edmonds.

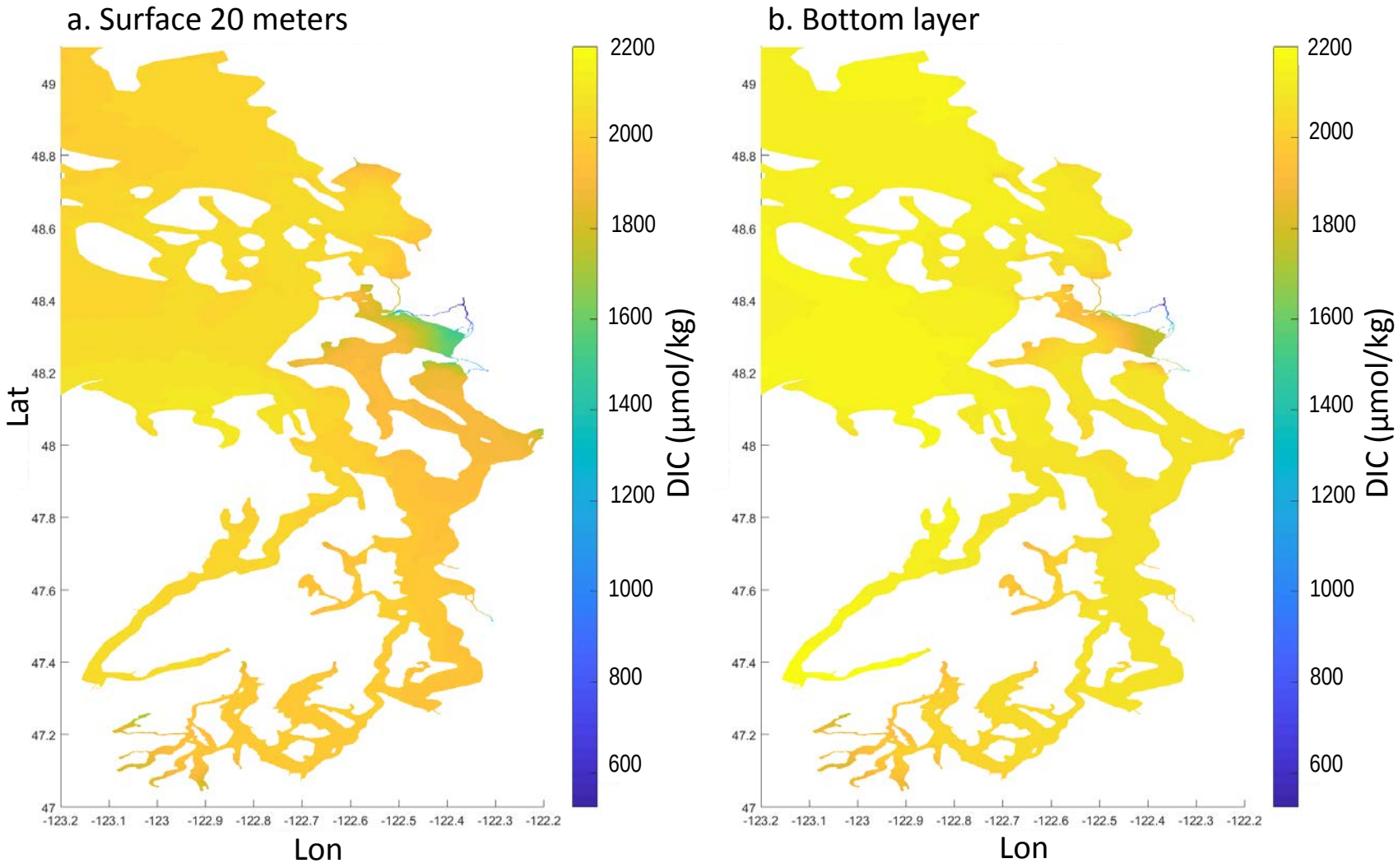

Figure 19. Annual average DIC in the surface 20 meters and the bottom layer of Puget Sound in 2008.

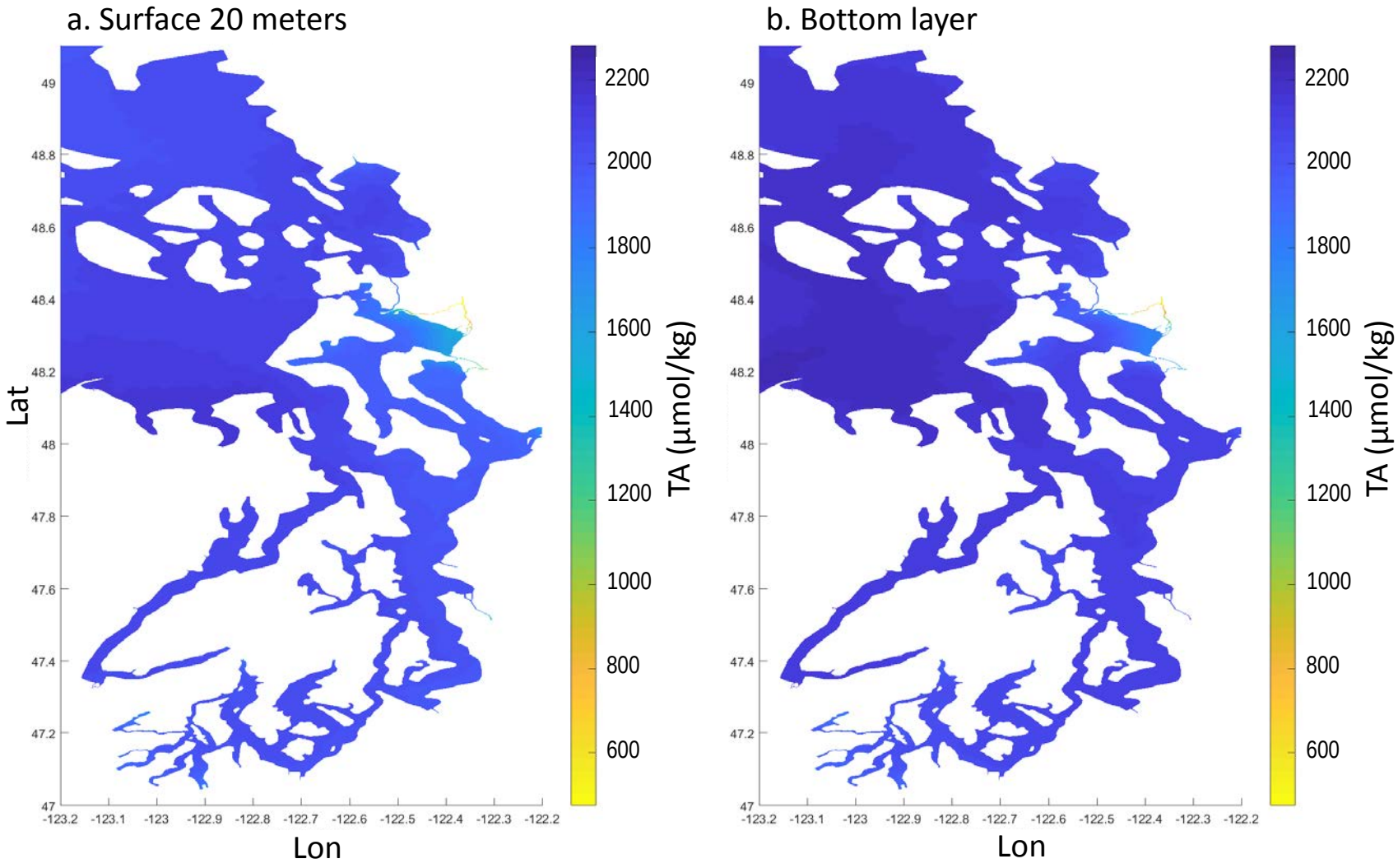

Figure 20. Annual average total alkalinity in the surface 20 meters and the bottom layer of Puget Sound in 2008.

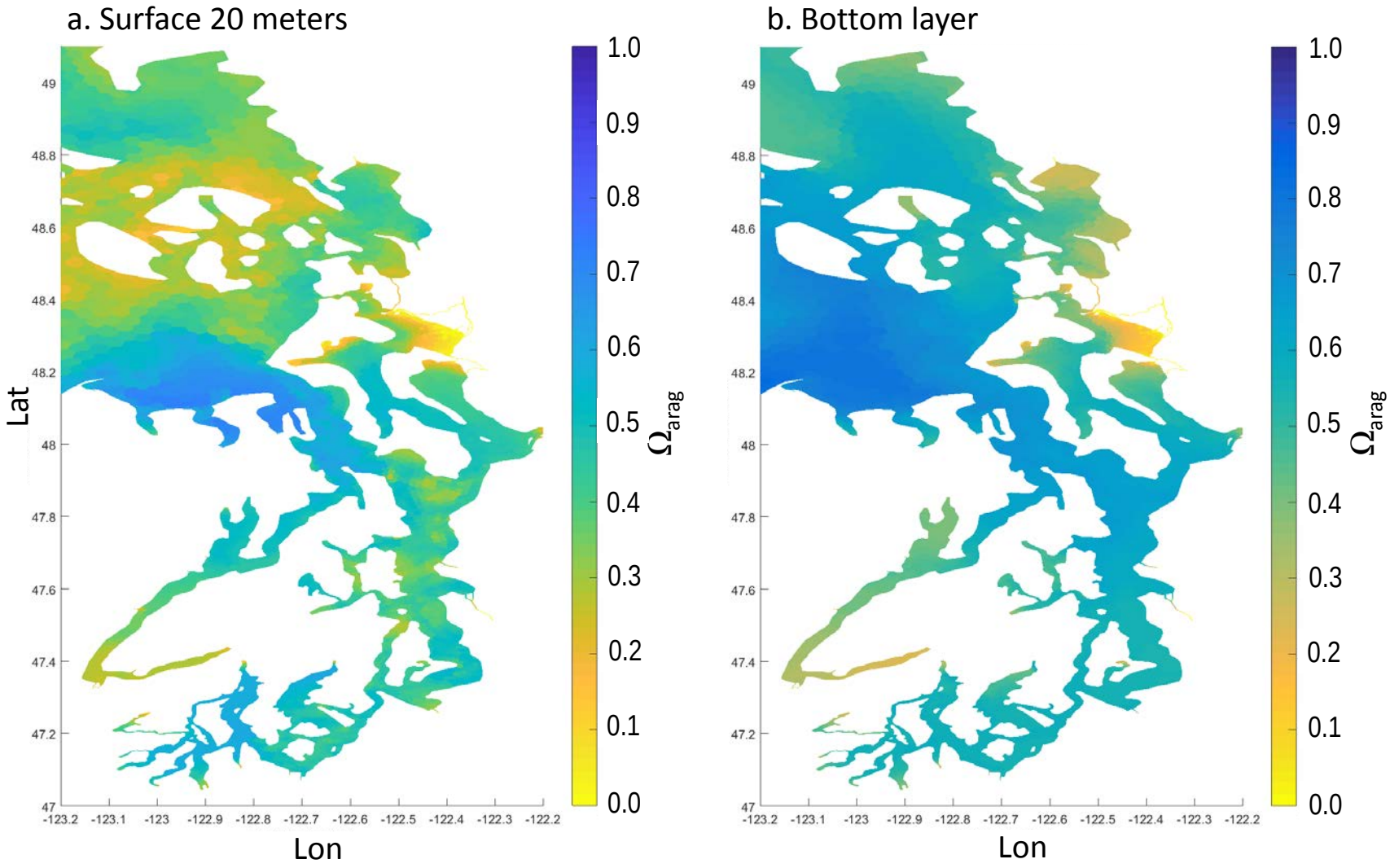

Figure 21. Minimum Ω_{arag} in the surface 20 meters and the bottom layer of Puget Sound in 2008.

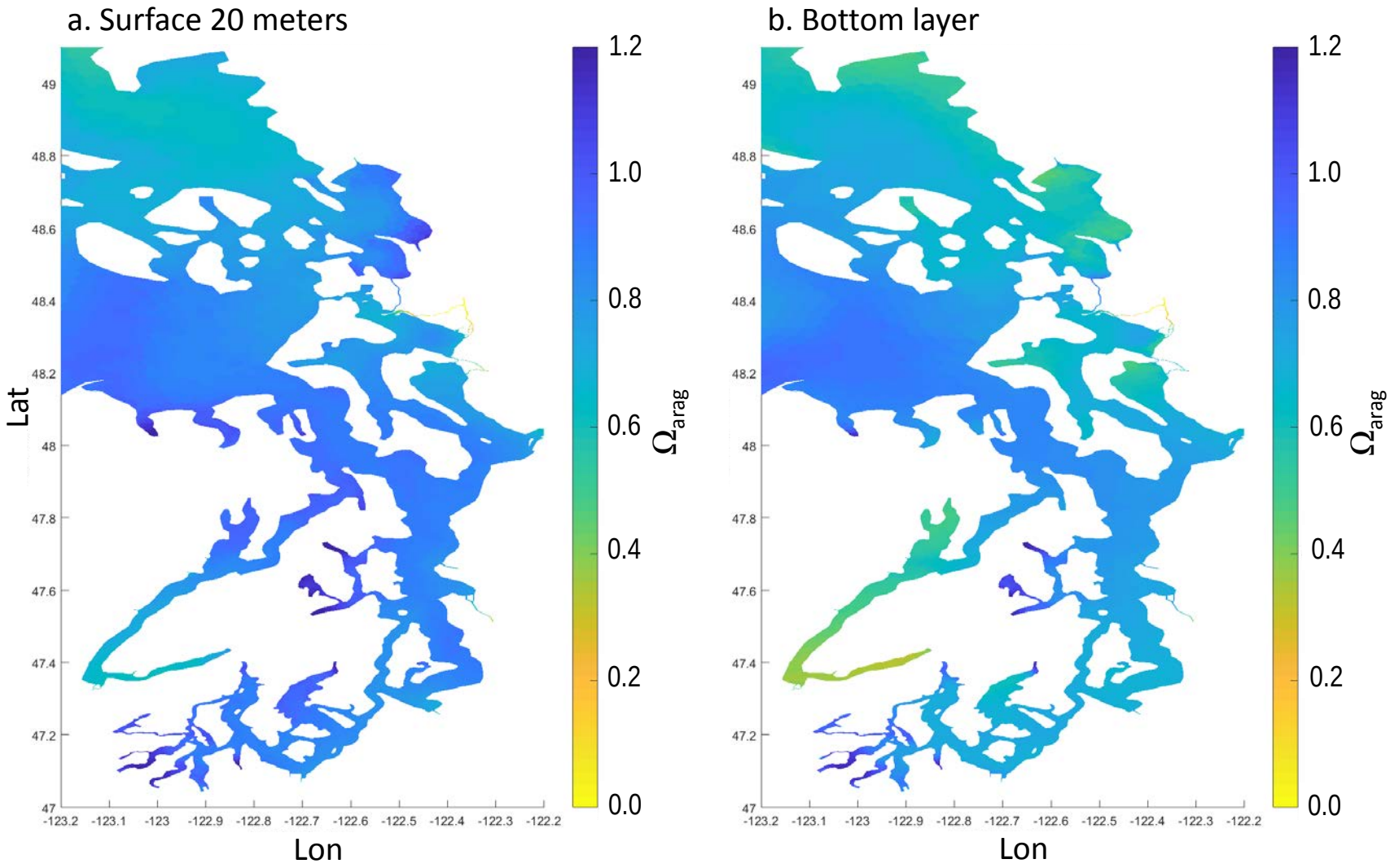

Figure 22. Annual average Ω_{arag} in the surface 20 meters and the bottom layer of Puget Sound in 2008.

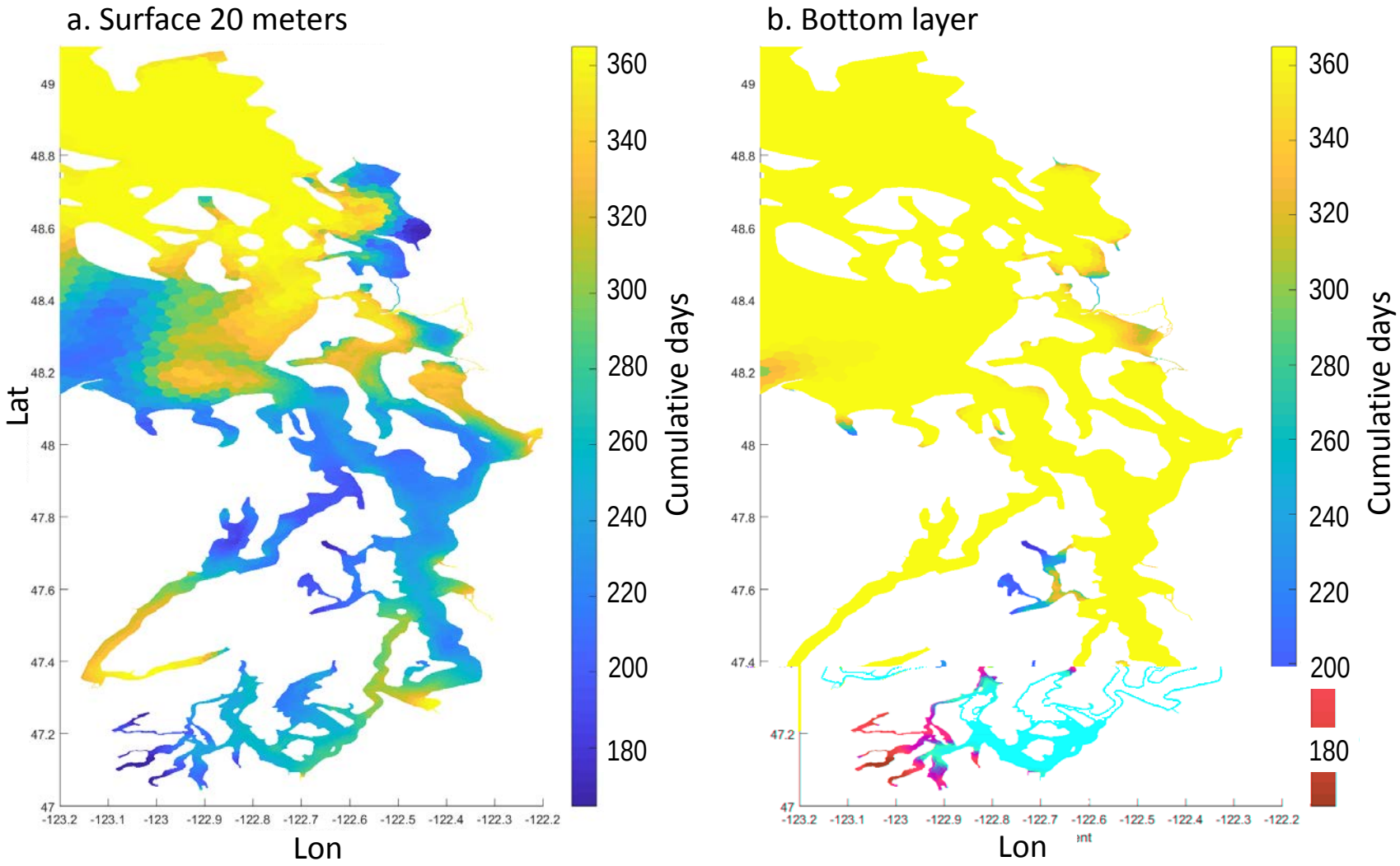

Figure 23. Cumulative days with Ω_{arag} less than 1 in the surface 20 meters and the bottom layer of Puget Sound in 2008.

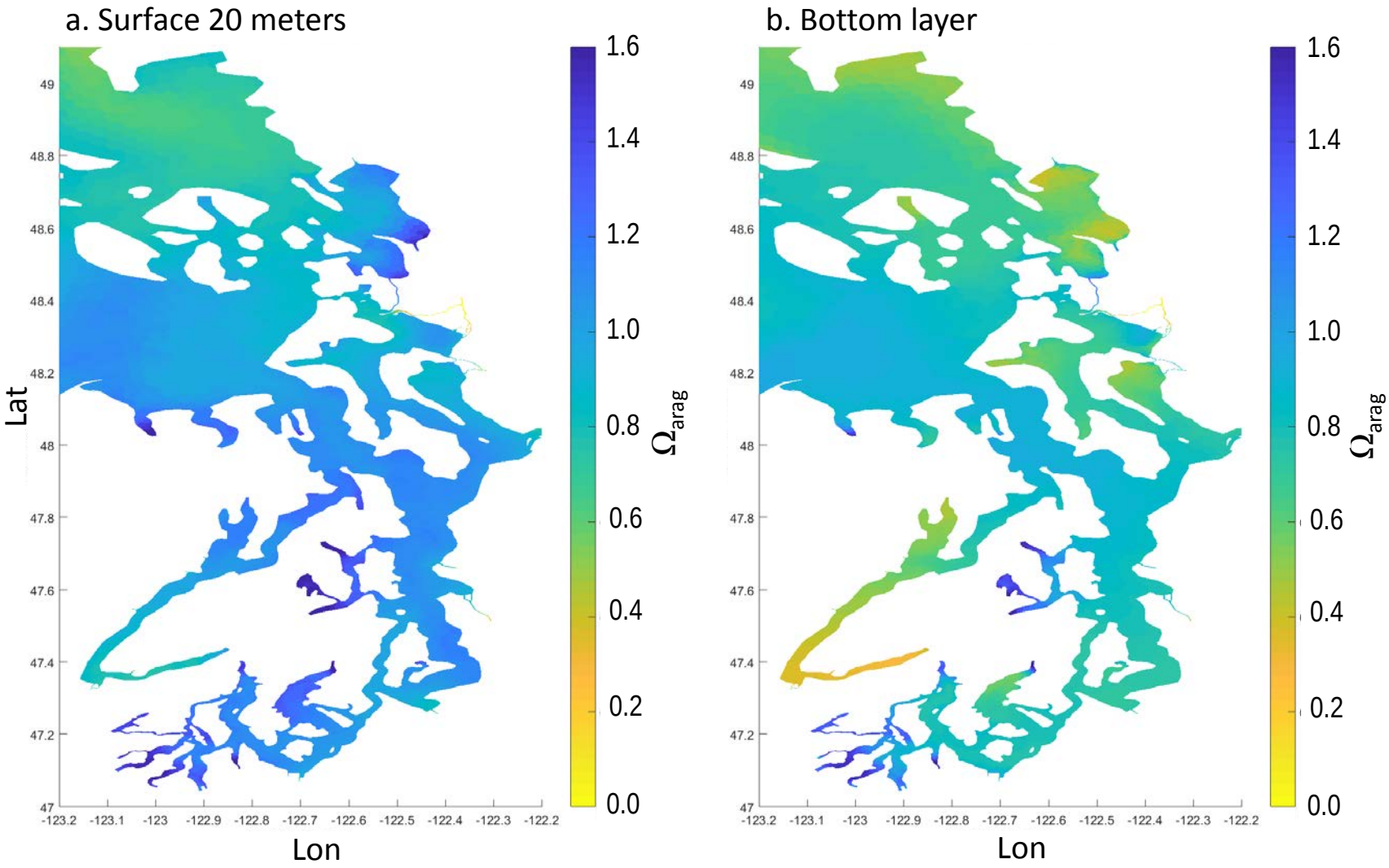

Figure 24. May-September average Ω_{arag} in the surface 20 meters and the bottom layer of Puget Sound in 2008.

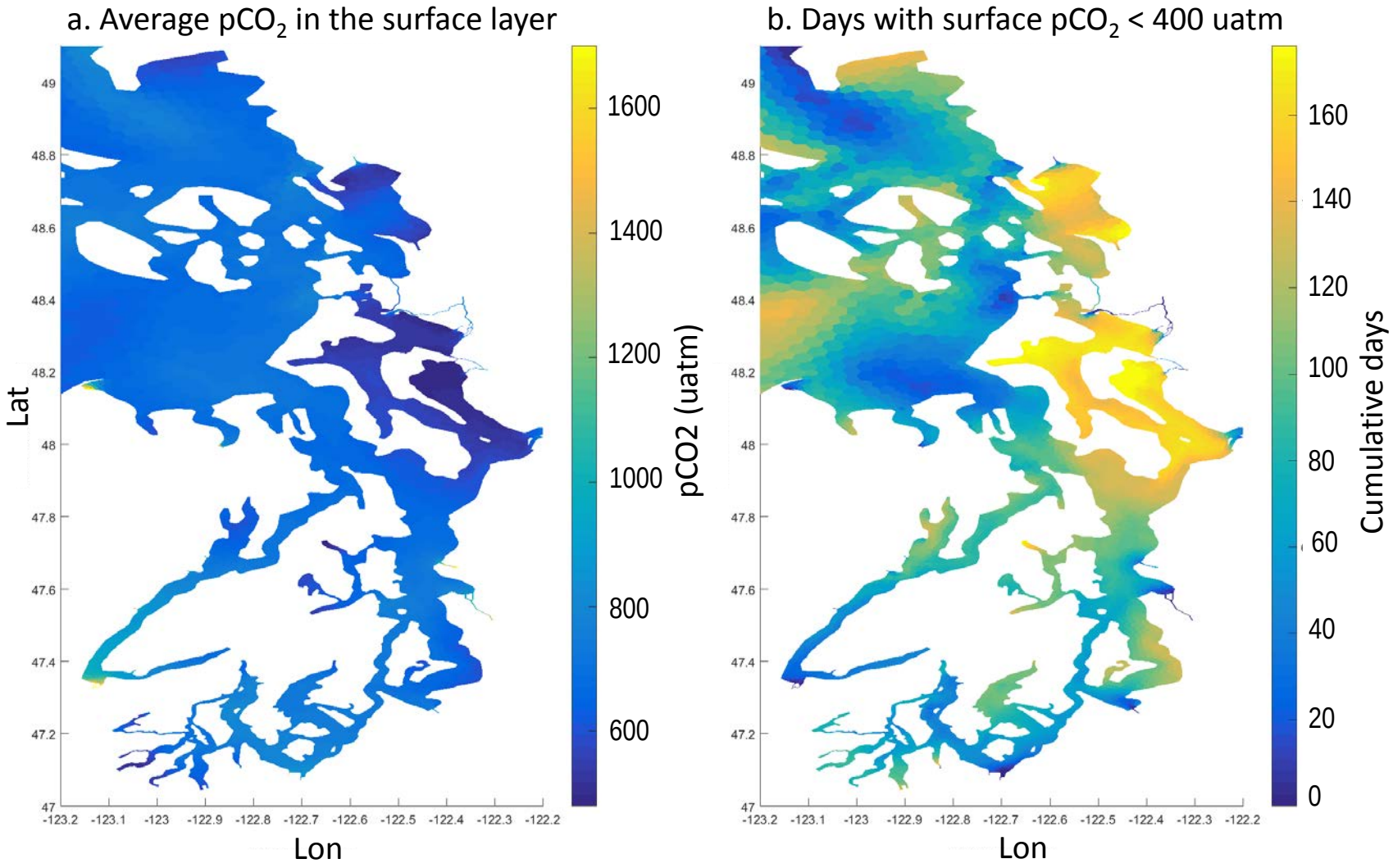

Figure 25. Annual average pCO_2 and cumulative days with pCO_2 less than 400 uatm in the surface layer of Puget Sound from January to December 2008.

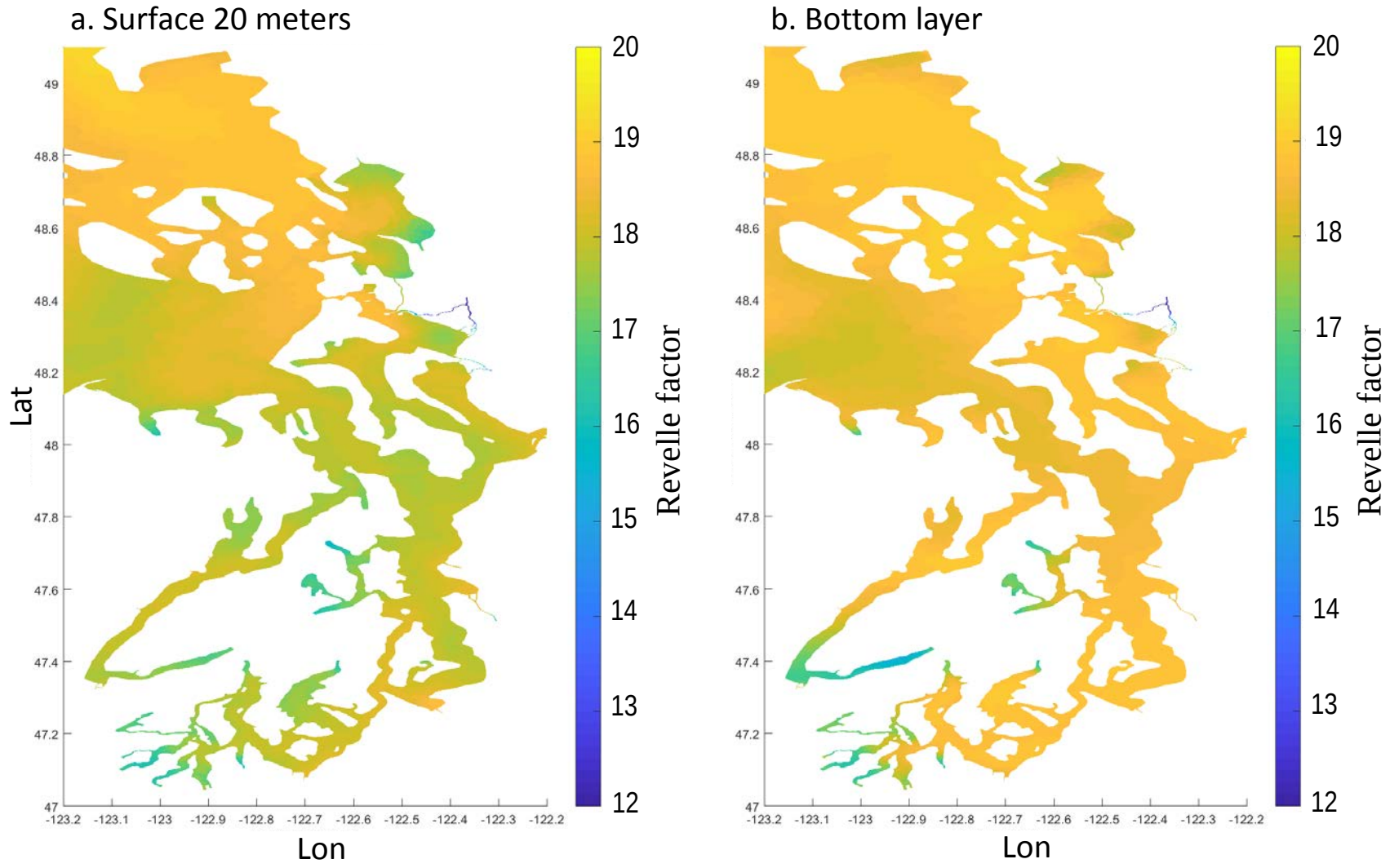

Figure 26. Annual average Revelle factors in the surface 20 meters and the bottom layers of Puget Sound in 2008.

Estimated changes due to regional anthropogenic nutrient sources

The effect of regional anthropogenic nutrient sources was estimated as the difference in predicted concentrations of historical simulated conditions in 2008 versus the reference conditions with estimated regional anthropogenic nutrient sources excluded. Canadian nutrient loads for the reference condition were unchanged and set to 2008 conditions. The estimated regional anthropogenic nutrient loads for the Washington portion of the domain that were excluded from the reference condition scenario include inorganic N (nitrate and ammonium), organic N (dissolved and particulate), and organic carbon (dissolved and particulate) (Appendix B).

Comparison of the loads delivered by the rivers in the reference condition (Appendix B-3), reveals that in rivers flowing into Hood Canal, and for the Skagit River, the background reference condition is close to the existing condition. This is due to relatively low levels of development (in the case of Hood Canal), lack of reference data, and the simplified approach used to determine the reference conditions using fixed monthly concentrations. Appendix B contains further details about the methods that were used to estimate reference conditions. Due to the limitations mentioned above, this analysis represents a first approximation of the impact of regional anthropogenic nutrient sources on the carbonate system.

pH

The annual average change in pH due to regional anthropogenic nutrient sources ranged from about -0.03 to 0.01 in the surface 20 meters (Figure 27a) and from -0.05 to 0.01 in the bottom layer (Figure 27b). Negative values indicate decreases due to regional anthropogenic sources, and positive values indicate increases. The predicted changes due to regional anthropogenic nutrient sources are greater than the uncertainty of the predicted differences (Table 3); therefore, the differences may be considered to be statistically significant.

The largest decreases in pH due to regional anthropogenic sources are predicted in the bottom layer in Case Inlet, Carr Inlet, inner Budd Inlet, Nisqually Reach, Commencement Bay, Colvos Passage, East Passage, Quartermaster Harbor, Port Susan, and Saratoga Passage. The largest increases in pH due to regional anthropogenic sources are predicted in the surface 20 meters in Oakland Bay, Totten Inlet, Eld Inlet, Henderson Inlet, Sinclair/Dyes Inlets, and Samish Bay.

The change in monthly average pH ranged from -0.07 (decrease) to 0.06 (increase) in the surface 20 meters and -0.10 (decrease) to 0.05 (increase) in the bottom layer due to regional anthropogenic nutrient sources (Appendix I). The largest decreases in monthly average pH are predicted in the deepest areas.

Dissolved inorganic carbon (DIC)

The annual average change in DIC due to regional anthropogenic sources ranged from -6.9 (decrease) to 9.2 (increase) umol/kg in the surface 20 meters (Figure 28a), and from -5.4 (decrease) to 16 (increase) umol/kg in the bottom layer (Figure 28b). DIC in the surface 20 meters is predicted to decrease in some areas due to uptake by primary production and freshwater influences. The predicted changes due to regional anthropogenic nutrient sources are

greater than the uncertainty of the predicted differences (Table 3), therefore the differences may be considered to be statistically significant.

The largest increases in DIC due to regional anthropogenic sources are predicted in the bottom layer in Case Inlet, Carr Inlet, inner Budd Inlet, Nisqually Reach, Commencement Bay, Colvos Passage, East Passage, Quartermaster Harbor, Port Susan, Saratoga Passage, and Bellingham Bay. The largest decreases in DIC due to regional anthropogenic sources are predicted in the surface 20 meters in Oakland Bay, Totten Inlet, Eld Inlet, Henderson Inlet, and Sinclair/Dyes Inlets.

Monthly average change in DIC ranges from -20 (decrease) to 16 (increase) umol/kg in the surface 20 meters and -18 (decrease) to 29 (increase) umol/kg in the bottom layer due to regional anthropogenic nutrient sources (Appendix J). The largest increases in monthly average DIC are predicted in the deepest areas.

Aragonite saturation state (Ω_{arag})

The annual average change in Ω_{arag} due to regional anthropogenic nutrient sources ranged from -0.03 (decrease) to 0.05 (increase) in the surface 20 meters (Figure 29a) and from -0.05 (decrease) to 0.04 (increase) in the bottom layer (Figure 29b). The predicted changes due to regional anthropogenic nutrient sources are greater than the uncertainty of the predicted differences (Table 3).

The largest decreases in Ω_{arag} due to regional anthropogenic sources are predicted in the bottom layer in Case Inlet, Carr Inlet, inner Budd Inlet, Dana Passage, Nisqually Reach, Commencement Bay, Colvos Passage, East Passage, Quartermaster Harbor, Port Susan, and Saratoga Passage. The largest increases in Ω_{arag} due to regional anthropogenic sources are predicted in the surface 20 meters in Oakland Bay, Totten Inlet, Eld Inlet, Henderson Inlet, and Sinclair/Dyes Inlets.

The duration of change in Ω_{arag} of less than -0.03 units (decrease of more than 0.03 units) was typically several months in the surface 20 meters (Figure 30a) and up to a year in the bottom layer (Figure 30b). This is predicted mainly in South Puget Sound (Budd, Case, and Carr Inlets, Dana Passage, Nisqually Reach), Commencement Bay, East Passage, Colvos Passage, Sinclair/Dyes Inlets, Port Susan, Saratoga Passage, and Skagit Bay.

Most of the main basin, South Sound, Port Susan, Skagit Bay, and Whidbey Basin display sensitivity to reductions in aragonite saturation levels in the surface 20 meters. Regional anthropogenic nutrient sources are predicted to increase the cumulative number of days with Ω_{arag} less than 1 in the surface 20 meters by about six days in most of South Sound and the main basin, and decrease the number of days with Ω_{arag} less than 1 by up to about eight days in Admiralty Inlet and portions of Whidbey Basin, Bellingham Bay, and Hood Canal (Figure 31).

Monthly average change in Ω_{arag} due to regional anthropogenic nutrient sources ranges from -0.06 (decrease) to 0.19 (increase) in the surface 20 meters and -0.12 (decrease) to 0.17 (increase) in the bottom layer of Puget Sound (Appendix K). The largest decreases in monthly average Ω_{arag} are predicted in the deepest areas.

Dissolved inorganic nitrogen (DIN)

Regional anthropogenic nutrient sources account for up to about 35% of the May-September average DIN in the surface 20 meters (Figure 32a). The greatest fraction of anthropogenic DIN occurs in the vicinity of freshwater influences, with fractions in the range of 10% to 15% over fairly wide areas throughout most of Puget Sound, and around 5% to 10% through most of the Whidbey Basin and inner Bellingham Bay. Monthly DIN concentrations and fractions due to regional anthropogenic nutrient sources are presented in Appendix L.

Chlorophyll-a (Chl-a)

Regional anthropogenic nutrient sources account for up to about 17% of the May-September average Chl-a biomass in the surface 20 meters (Figure 32b). Highest fractions occur in the finger inlets of South Puget Sound. Fractions around 5% to 10% occur over fairly wide areas throughout Puget Sound and the Whidbey Basin. Regional anthropogenic sources account for less than 5% of the Chl-a in Hood Canal. Monthly average concentrations of Chl-a and fractions due to regional anthropogenic nutrient sources are presented in Appendix M.

Non-algal organic carbon

Regional anthropogenic sources account for up to around 35% of the May-September average non-algal organic carbon in the surface 20 meters, with fractions of 20% to 25% fairly widespread through most of the main basin of Puget Sound, inner Budd Inlet, and Port Susan/Possession Sound (Figure 32c). Around 10% to 15% of the non-algal organic carbon in Saratoga Passage and Admiralty Inlet is due to regional anthropogenic sources. Regional anthropogenic sources account for about 5% to 10% of the non-algal organic carbon in Hood Canal. Monthly average concentrations of non-algal organic carbon and fractions due to regional anthropogenic nutrient sources are presented in Appendix N.

A portion of the non-algal organic carbon that is attributed to regional anthropogenic sources is derived from an increase in detritus resulting from increased primary production (autochthonous), and part is from direct loading of watershed sources from rivers and wastewater treatment plants (allochthonous). Additional studies would be needed to quantify the amount from each source and to distinguish between the various allochthonous sources.

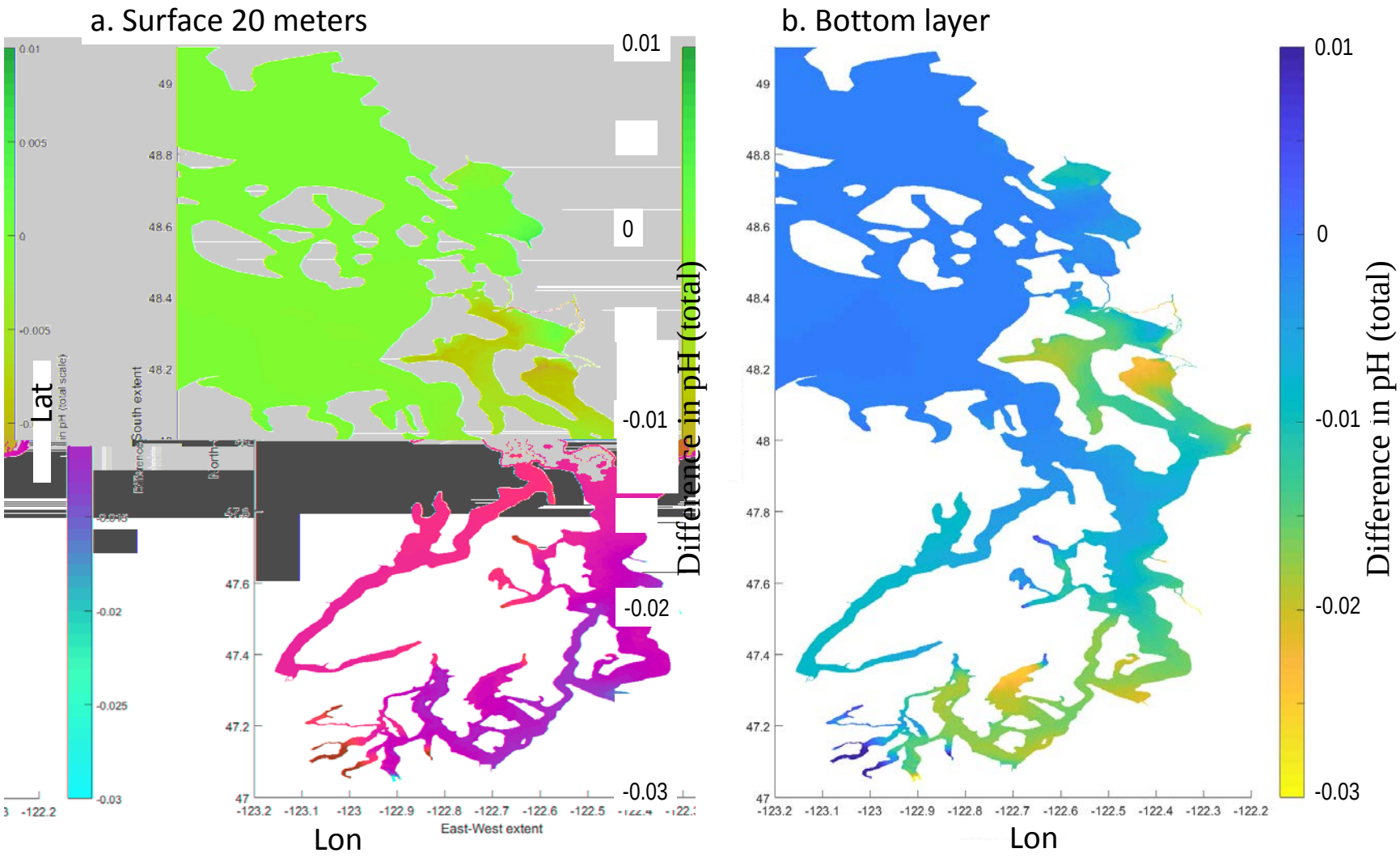

Figure 27. Annual average change in pH due to regional anthropogenic nutrient sources in the surface 20 meters and bottom layer of Puget Sound in 2008.

Negative values indicate decrease in pH due to regional anthropogenic sources.

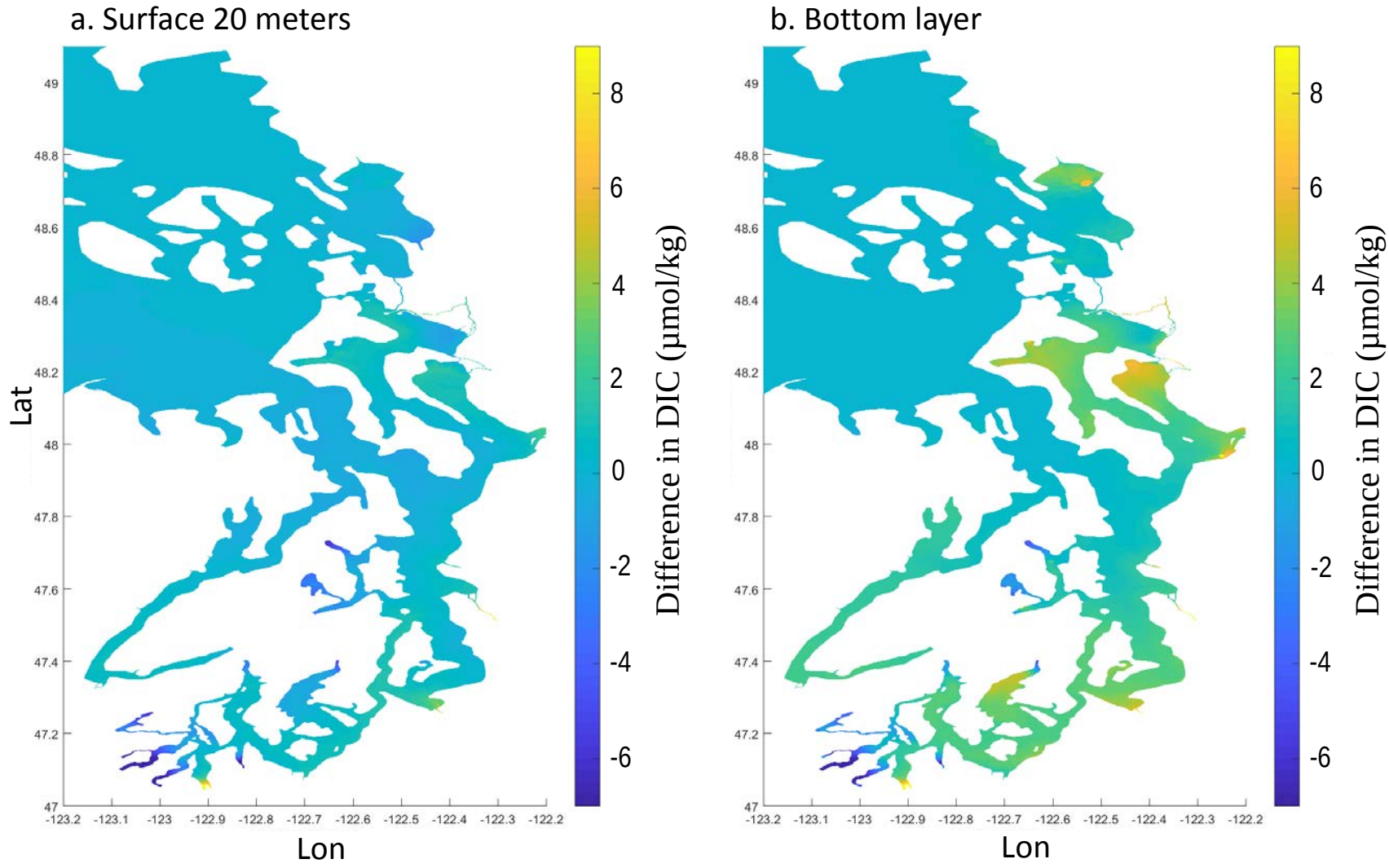

Figure 28. Annual average change in DIC due to regional anthropogenic nutrient sources in the surface 20 meters and bottom layer of Puget Sound in 2008.

Positive values indicate increase in DIC due to regional anthropogenic sources.

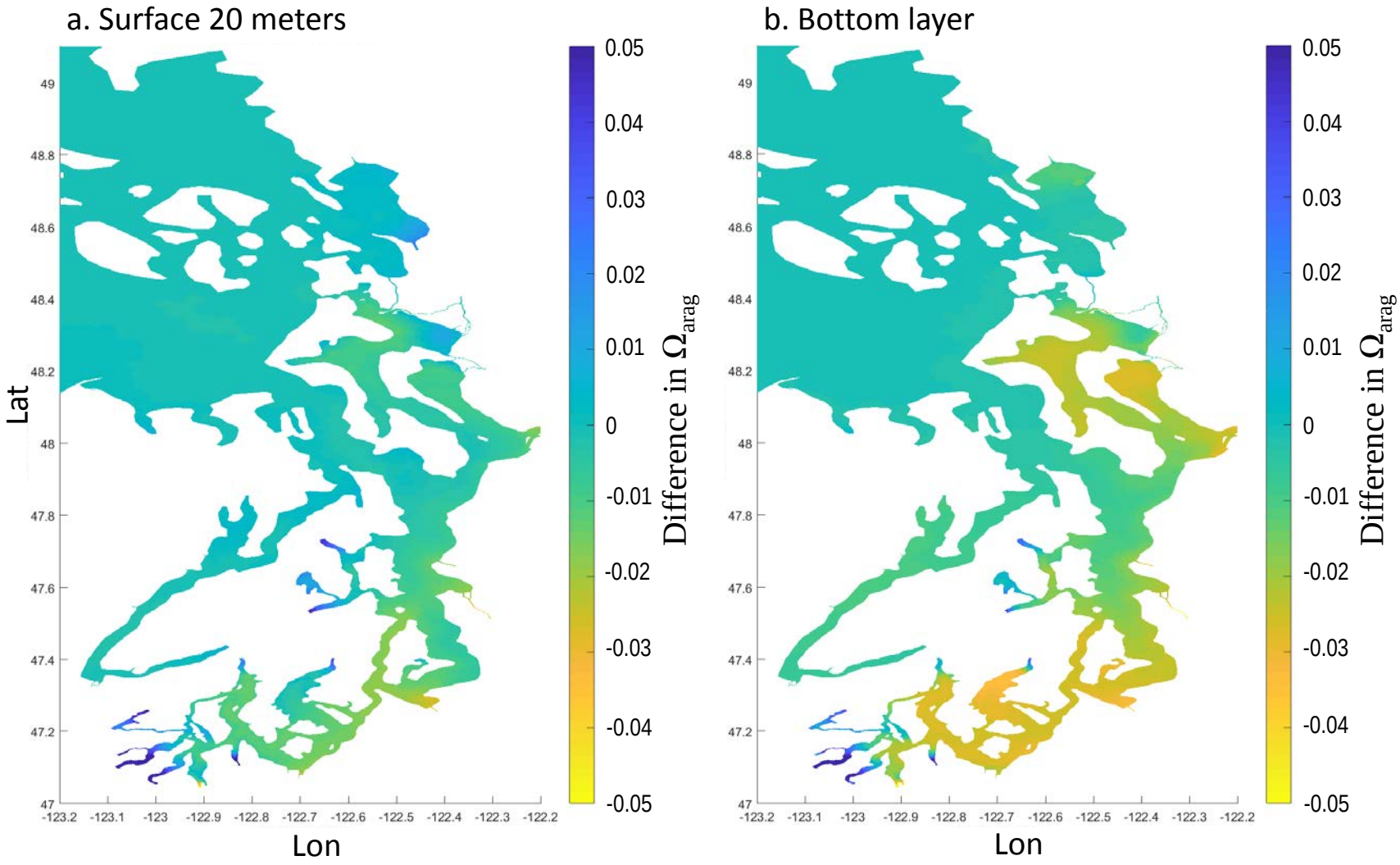

Figure 29. Annual average change in Ω_{arag} due to regional anthropogenic nutrient sources in the surface 20 meters and bottom layer of Puget Sound in 2008.

Negative values indicate decrease in Ω_{arag} due to regional anthropogenic sources.

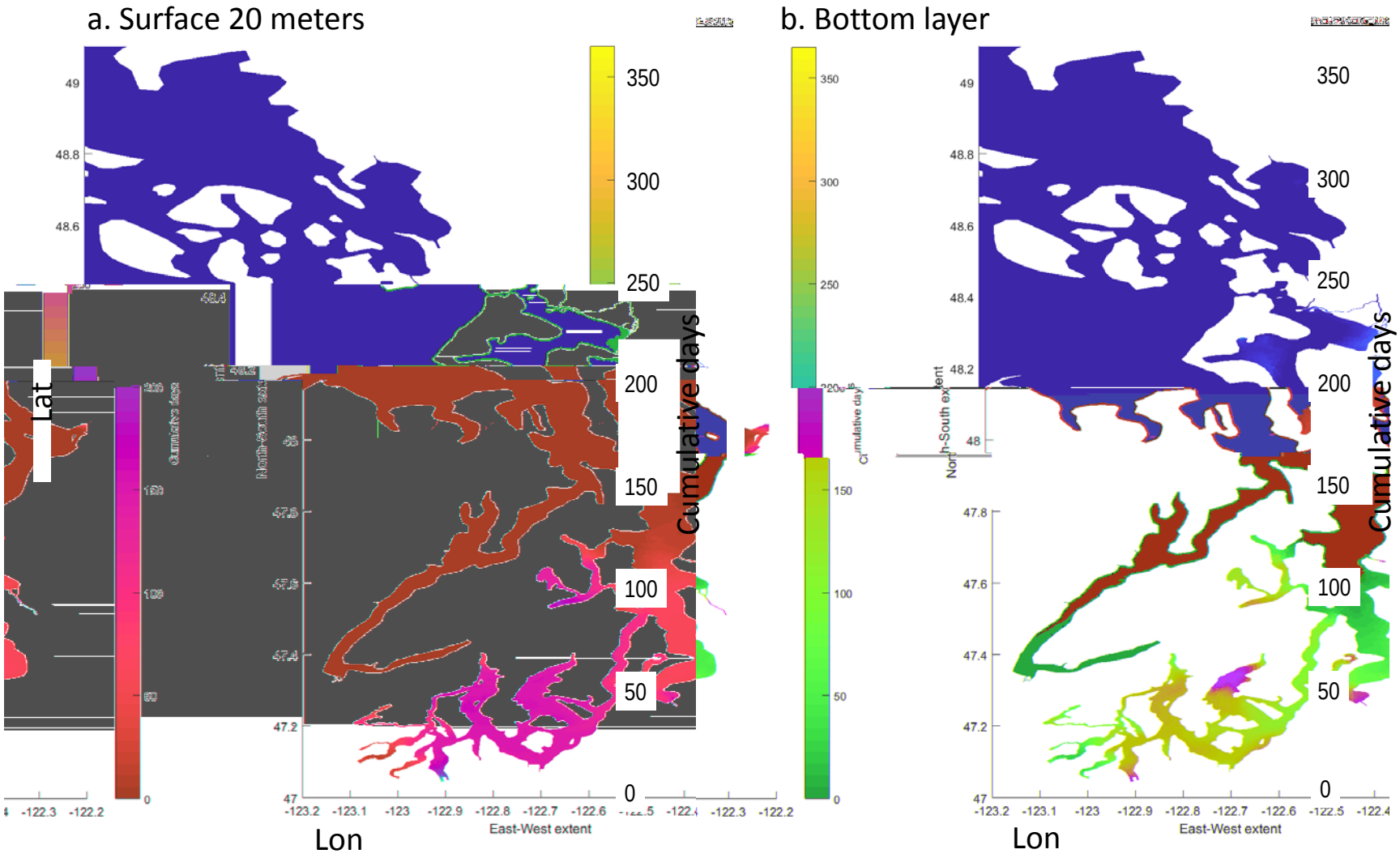

Figure 30. Cumulative days with decrease in Ω_{arag} greater than 0.03 due to regional anthropogenic nutrient sources in the surface 20 meters and bottom layer of Puget Sound in 2008.

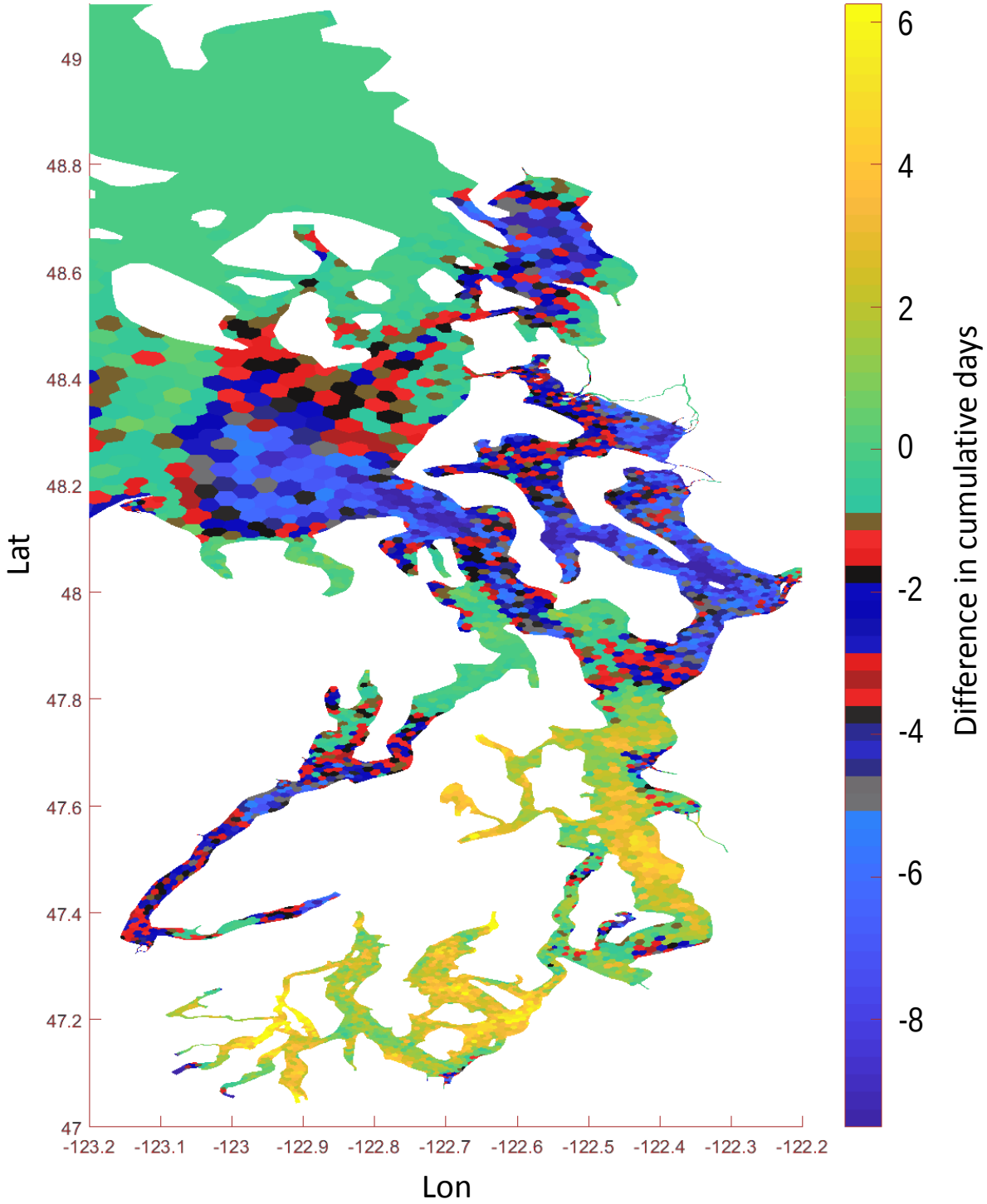

Figure 31. Change in the number of days per year with Ω_{arag} less than 1 in the surface 20 meters of Puget Sound due to regional anthropogenic nutrient sources.

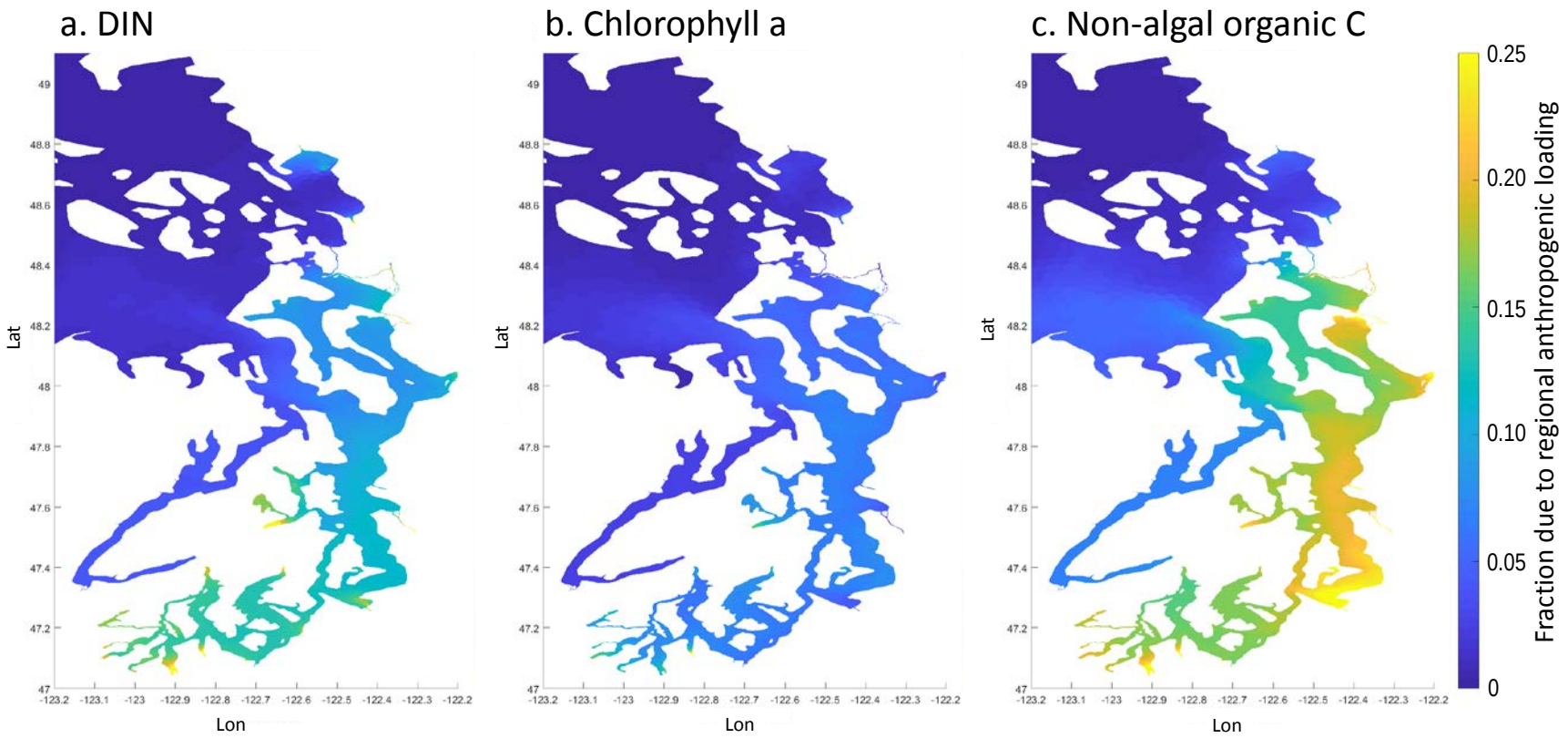

Figure 32. Fraction of DIN, Chl-a, and non-algal organic carbon due to regional anthropogenic sources (average May-September 2008, surface 20 meters).

Estimated sensitivity to increased regional atmospheric pCO_2

The effect of increasing regional atmospheric pCO_2 on the carbonate system variables in the water was estimated by calculating the difference between the following two model runs:

1. Historical conditions for 2008 except with regional atmospheric pCO_2 assumed to be a hypothetical high value of 450 uatm.
2. Historical 2008 conditions with regional atmospheric pCO_2 at 400 uatm (same as the baseline historical conditions used for evaluating the effect of regional anthropogenic nutrient sources).

The assumed hypothetical high value of 450 uatm represents an extreme high daily value for current conditions close to urban areas. The daily average atmospheric pCO_2 at the Space Needle in Seattle occasionally exceeded 450 uatm between 2013 and 2017. Annual average atmospheric pCO_2 off the Washington coast increased by 16 uatm over the 10-year period from 2006 to 2015 (PSEMP, 2016). Therefore, an increase in annual average pCO_2 from 400 to 450 uatm could occur over about the next 30 years.

pH

The annual average change in pH due to hypothetical increased regional atmospheric pCO_2 of 450 uatm ranged from about -0.02 (decrease) to 0 (no change) in the surface 20 meters (Figure 33a) and in the bottom layer (Figure 33b). Negative values for change in pH indicate a decrease in pH due to increased atmospheric pCO_2. The predicted changes due to increased regional atmospheric pCO_2 are greater than the uncertainty of the predicted differences (Table 3); therefore, the differences may be considered to be statistically significant.

Dissolved inorganic carbon (DIC)

The annual average change in DIC due to hypothetical increased regional atmospheric pCO_2 of 450 uatm ranged from 0.25 to 5.2 umol/kg (increase) in the surface 20 meters (Figure 34a) and from 0.14 to 5.1 umol/kg (increase) in the bottom layer (Figure 34b). The predicted changes due to increased regional atmospheric pCO_2 are greater than the uncertainty of the predicted differences (Table 3); therefore, the differences may be considered to be statistically significant.

Aragonite saturation state (Ω_{arag})

The annual average change in Ω_{arag} due to hypothetical increased regional atmospheric pCO_2 of 450 uatm ranged from -0.04 (decrease) to 0 (no change) in the surface 20 meters (Figure 35a) and in the bottom layer (Figure 35b). The predicted changes due to increased regional atmospheric pCO_2 are greater than the uncertainty of the predicted differences (Table 3).

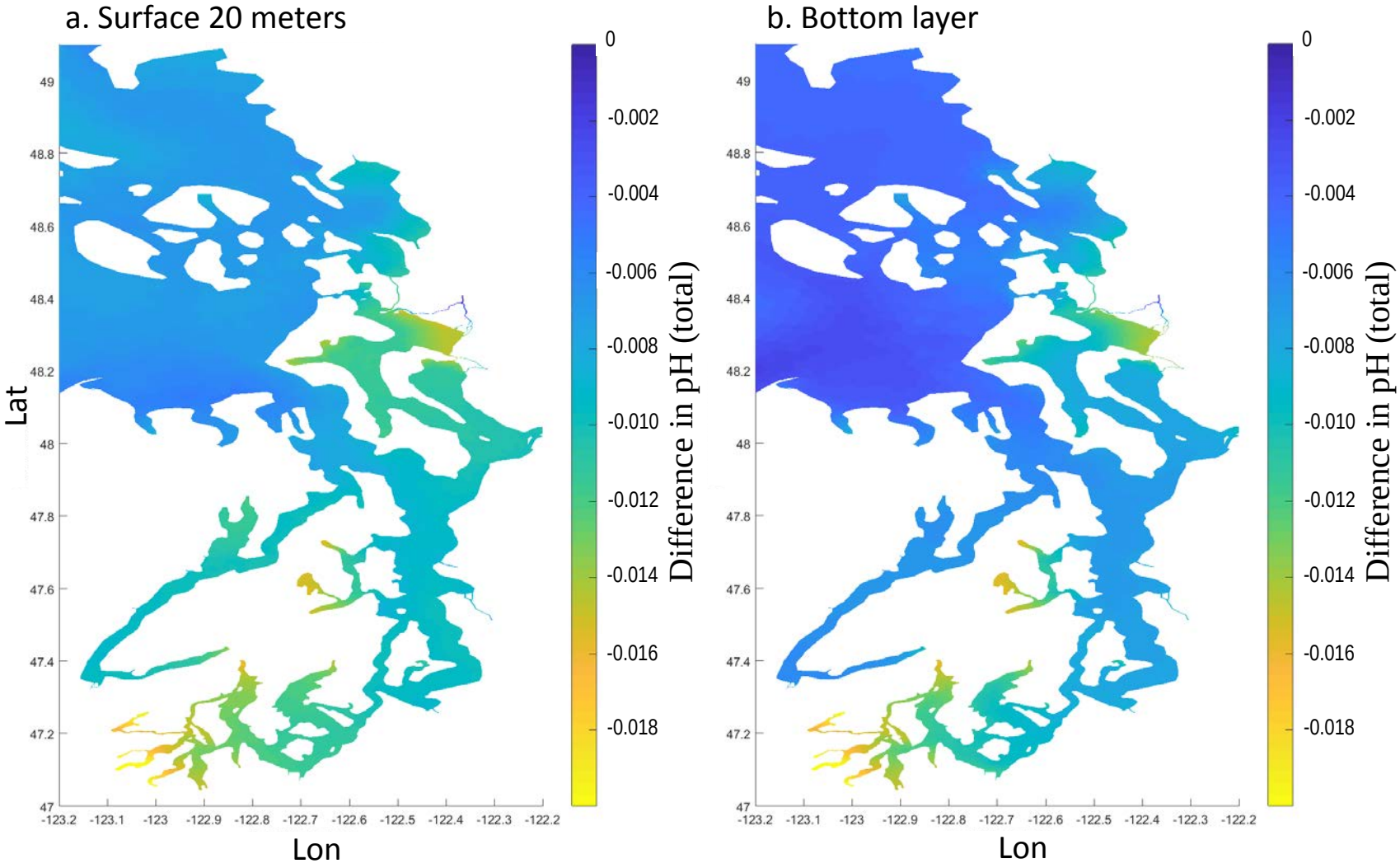

Figure 33. Annual average change in pH due to hypothetical regional atmospheric pCO_2 of 450 uatm in the surface 20 meters and the bottom layer of Puget Sound in 2008. *Negative values indicate decrease in pH.*

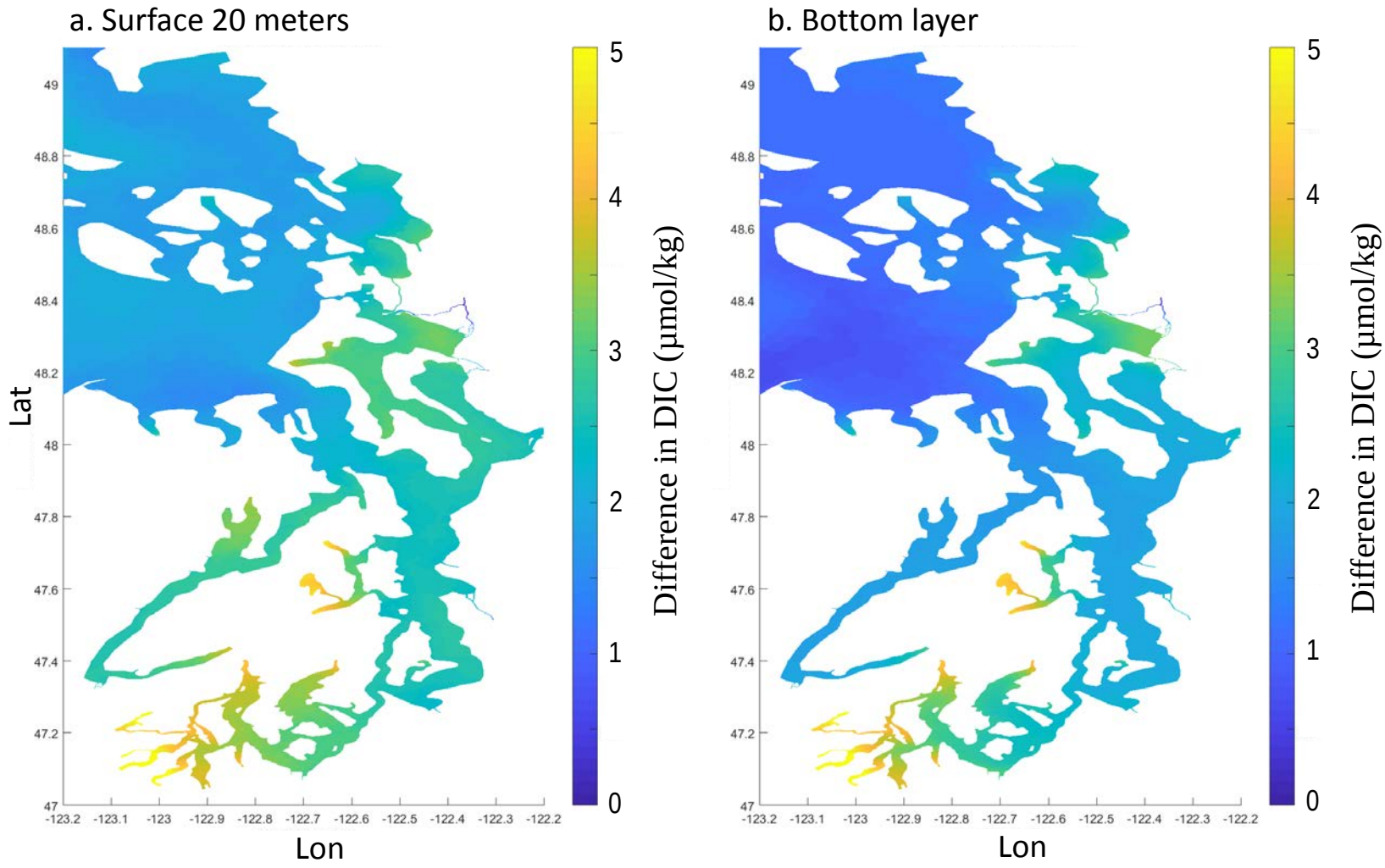

Figure 34. Annual average change in DIC due to hypothetical regional atmospheric pCO_2 of 450 uatm in the surface 20 meters and the bottom layer of Puget Sound in 2008. *Positive values indicate increase in DIC.*

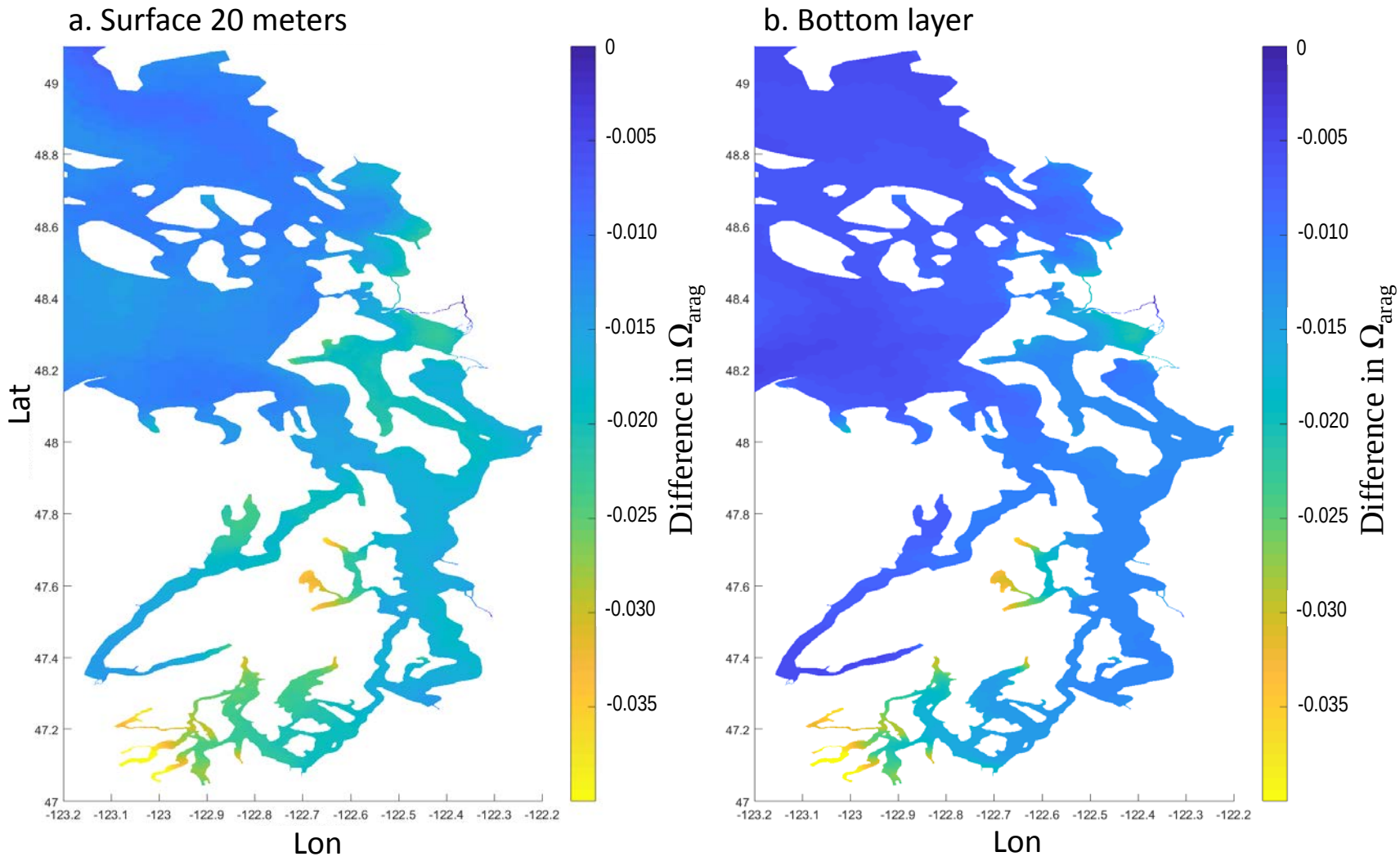

Figure 35. Annual average change in Ω_{arag} due to hypothetical regional atmospheric pCO_2 of 450 uatm in the surface 20 meters and the bottom layer of Puget Sound in 2008. *Negative values indicate decrease in* Ω_{arag}.

Discussion

Data published on the carbonate system in the Pacific Northwest is confined to limited locations or coastal conditions and may not provide the full context for acidification levels in the Salish Sea: Puget Sound, Strait of Georgia, and Strait of Juan de Fuca (e.g., Feely et al., 2010; Ianson et al., 2016). The results of this modeling study provide additional information about spatial and temporal variability of acidification in the surface waters of Puget Sound and provide insight about major processes.

The Pacific Ocean strongly influences conditions in Puget Sound. The deep waters originate in the Pacific Ocean and represent a mix of subtropical and subarctic water masses. Upwelling varies in strength and duration, with short-term intrusions over the sill at Admiralty Inlet (Khangaonkar et al., 2017; Deppe et al., 2013) bringing water low in aragonite saturation state (Ω_{arag}) and pH into Puget Sound.

The surface layer is influenced by vertical mixing with deep waters enhanced by circulation around the sills. Inputs of freshwater and primary productivity within the euphotic zone also influence the carbonate system. Winter conditions produce the most biologically challenging environments in terms of low Ω_{arag} and low pH. However, early life stages generally occur during early spring-fall, and comprise the greatest biological sensitivity for calcifiers, which are one of the most disadvantaged groups of organisms under increasing ocean acidification scenarios (Browman et al., 2013).

Primary production in Puget Sound is highest in the spring and summer with optimum sunlight and intermediate water column stability (Strickland, 1983). Uptake of CO_2 by phytoplankton for photosynthesis decreases the surface water pCO_2, which generally increases the Ω_{arag} above corrosive conditions. Yet, although Ω_{arag} generally reaches levels above the threshold for bivalve biomineralization during the growing season, two sites (Totten Inlet and Admiralty Inlet) show Ω_{arag} at, or below, 1 during portions of the growing season (Figure 12). May-September average Ω_{arag} ranges up to 1.6 in the surface 20 meters, with average decrease of up to 0.03 due to regional anthropogenic sources. Decrease of Ω_{arag} greater than 0.03 due to regional anthropogenic sources is predicted to persist up to several months in most of South Puget Sound.

Uptake of CO_2 to support primary production increases Ω_{arag} in the euphotic zone, but settling of phytoplankton and decomposition of detritus releases CO_2 into the deeper water and decreases Ω_{arag} below the euphotic zone. Species that exploit different depth habitats are likely to experience very different conditions.

Regional versus Global Anthropogenic Influence

The relative importance of regional versus global anthropogenic influences on the carbonate chemistry in the Salish Sea constitutes a fundamental question. In this report we focus on the Salish Sea's carbonate system sensitivity to regional anthropogenic nutrient loadings that also contribute to eutrophication, which leads to increased release of CO_2 at depth.

Feely et al. (2010) reported estimates of changes in the carbonate system due to global anthropogenic processes with a decrease in the surface 20 meters since the preindustrial era of up to about 0.11 (pH) and 0.09 to 0.33 (Ω_{arag}). Larger decreases occur in the summer and in the main basin. Feely et al. (2010) also reported a decrease in the bottom layer from global pre-industrial to present in pH and Ω_{arag} of about 0.00 to 0.06 and 0.02 to 0.16, respectively, with larger decreases in the main basin, and surface increases in DIC of about 13 to 36 umol/kg.

A comparison of predicted changes due to regional anthropogenic nutrient sources estimated in this study, compared with the effect of global anthropogenic sources reported by Feely et al. (2010), is presented in Table 4. The predicted changes due to regional anthropogenic nutrient sources are greater than the uncertainty of the predicted differences (Table 3); therefore, the differences may be considered to be statistically significant.

Table 4. Comparison of estimated regional and global anthropogenic impacts on Salish Sea carbonate chemistry for 2008.

	Regional anthropogenic nutrient sources (this study)	Global anthropogenic sources (Feely et al., 2010)
	Range of monthly average differences between 2008 conditions and an estimated reference condition with regional anthropogenic nutrient sources excluded	Difference between cruise observations (February and August, 2008) and estimated pre-industrial values
pH (surface 0 to 20 m)	-0.07 to 0.06	-0.11 to 0.03
pH (bottom)	-0.10 to 0.05	-0.06 to 0.00
DIC (surface 0 to 20 m) (umol/kg)	-20 to 16	13 to 36
DIC (bottom) (umol/kg)	-18 to 29	7 to 18
Ω_{arag} (surface 0 to 20 m)	-0.06 to 0.19	-0.33 to -0.09
Ω_{arag} (bottom)	-0.12 to 0.17	-0.16 to -0.02

In some areas, the regional anthropogenic nutrient inputs reduce acidification because increased productivity leads to increased uptake of CO_2. In other areas, acidification is increased by regional anthropogenic nutrient sources because the increase in primary production and organic carbon loading leads to increased respiration and release of CO_2 because of increased decay of organic matter. The effect of regional anthropogenic nutrient sources on DIC and pH at the surface and bottom is comparable in magnitude to the published effect of global anthropogenic sources.

Aragonite saturation state (Ω_{arag}) decreased, on average, due to regional anthropogenic nutrient sources. The impact is predicted to be greatest at the bottom in terms of the average magnitude of the change. Regional anthropogenic nutrient sources account for up to about 43% of the depletion of Ω_{arag} compared with the depletion caused by the combined global and regional anthropogenic sources (up to 0.12 depletion of Ω_{arag} from regional anthropogenic nutrient sources compared with up to 0.16 + 0.12 depletion of Ω_{arag} from combined global and regional

anthropogenic sources; Table 4). At the surface, regional anthropogenic nutrient sources account for up to about 15% of the decrease in Ω_{arag} compared with published estimates of changes caused by the combined effect of global and regional anthropogenic sources (up to 0.06 depletion of Ω_{arag} from regional anthropogenic nutrient sources compared with up to 0.33 + 0.06 depletion of Ω_{arag} from combined global and regional anthropogenic sources, Table 4). The relatively smaller depletion of Ω_{arag} by regional anthropogenic sources at the surface could be due to the increases in primary production in the euphotic zone, with corresponding increased uptake of CO_2 by phytoplankton.

Regional anthropogenic nutrient loadings can increase pH and aragonite saturation levels in some areas, particularly in several South Puget Sound shallow inlets and bays. Portions of the main basin, South Puget Sound, Port Susan, Skagit Bay, and Whidbey Basin have higher sensitivity to reductions in aragonite saturation levels due to anthropogenic nutrient loadings. Hood Canal appears to be generally decoupled from the rest of the Salish Sea in terms of regional anthropogenic land-based nutrient influences. This may be due to the nature of the circulatory pattern in the region and the lower level of human development.

Sensitivity to Regional Atmospheric pCO_2

Washington State leaders recognize the dominant influence of global atmospheric pCO_2 levels in the acidification of the Pacific Ocean (Washington State Blue Ribbon Panel on Ocean Acidification, 2012). The surface layer of Puget Sound appears to be outgassing to the local atmosphere between October and March, since surface water pCO_2 levels are above 400 uatm throughout Puget Sound during these wet-season months.

Regional atmospheric pCO_2 values are higher in the winter than at a global marine reference location (e.g., NOAA Earth System Research Laboratory, Mauna Loa, Hawaii) but can decline below the Hawaiian record during the growing season. During the summer months, phytoplankton productivity likely decreases pCO_2 to the point where local atmospheric pCO_2 represents a source of carbon to most of Puget Sound. A hypothetical increase in atmospheric pCO2 from 400 to 450 uatm was predicted to result in significant decreases in pH and Ω_{arag}, and increases in DIC.

Spatial Variation in Predicted Changes in Carbonate System Variables

The occurrence of the highest Ω_{arag} during the phytoplankton growing season suggests that uptake of dissolved CO_2 due to primary production is a very important process to explain seasonal variations in Ω_{arag}. The uptake of CO_2 by primary production could provide a benefit by increasing Ω_{arag} (e.g., Jutterstrom et al., 2014). The release of dissolved CO_2 due to decay of the organic carbon, in addition to ocean inputs of waters rich in dissolved CO_2, contributes to the observed decreases in Ω_{arag} during the winter months, and could also decrease Ω_{arag} in the deeper waters below the euphotic zone during the growing season.

Future Directions

Though limited, these model results illustrate important seasonal patterns in the surface waters of Puget Sound. Applying the model for additional years to examine inter-annual variations is necessary to better understand total variability and possible trends, as are additional observational data, such as TA and DIC, to provide information to assess model skill. Ecology's distributed monitoring station network design covers broad spatial areas and provides context for other parameters on a monthly basis, yet carbonate system data both in the middle of the channels and nearshore are needed. More information will be needed to constrain the carbonate system in Puget Sound and must include a combination of high temporal resolution data, a distributed network able to capture broad spatial patterns, as well as numerical models to explore continuous variations in space and time.

Conclusions

Results of this study support the following conclusions.

- A numerical model has been developed to provide predictions of carbonate system variables in the Salish Sea. The model predictions provide information about spatial and temporal variations in the carbonate system variables. Available data sources, including the Department of Ecology's pilot study of measurement of dissolved inorganic carbon (DIC) and alkalinity at six stations during 2014-2015, provided very useful data for model confirmation. The model predictions compare reasonably well with observed data.

- Increased dissolved inorganic nitrogen (DIN), phytoplankton biomass, and non-algal organic carbon caused by regional anthropogenic nutrient sources can significantly contribute to acidification in the Salish Sea.

- Regional anthropogenic nutrient sources are predicted to cause changes in pH and DIC in both bottom and surface waters, and are comparable in magnitude to the changes caused by global anthropogenic sources. The greatest increases in DIC and decreases in pH and Ω_{arag} due to regional anthropogenic nutrient sources tend to occur either near freshwater influences or at depth where bottom depths are below the euphotic zone.

- Aragonite saturation state (Ω_{arag}) decreased, on average, due to regional anthropogenic nutrient sources. The impact is predicted to be greatest at the bottom of the water column in terms of the average magnitude of the change. Compared with published estimates of changes caused by increasing global CO_2, regional anthropogenic nutrient sources account for up to about 43% of the total anthropogenic depletion of Ω_{arag} at the bottom, and up to about 15% of the total anthropogenic depletion of Ω_{arag} at the surface. More observational data is needed to evaluate these findings.

- The Ω_{arag} in certain regions appears to be more sensitive to anthropogenic nutrient loadings. Specifically, portions of the main basin, South Sound, Port Susan, Skagit Bay, and Whidbey Basin all present higher sensitivity of aragonite saturation levels in response to anthropogenic nutrient loadings. Hood Canal appears to be generally decoupled from the rest of the Salish Sea in terms of the magnitude of anthropogenic, land-derived nutrient influence. This is likely due in part to circulation and the lower level of development in Hood Canal.

- Regional anthropogenic nutrient loadings can increase pH and aragonite saturation levels in some areas, particularly in several South Sound shallow inlets and bays during the growing season. More observational data are needed to evaluate these findings.

- During 2008, Puget Sound pH levels generally were within the water quality standard range of 7 to 8.5. Some areas in Skagit Bay may have experienced excursions of pH below 7 for up to about a few days. The cumulative period of time with Ω_{arag} less than 1 in the surface 20 meters ranged from about six months (October to March) to the entire year, with the longest durations near largest freshwater inflows. In most areas, the bottom layer Ω_{arag} was less than 1 for the entire year, with the exception of some shallow areas with bottom layer Ω_{arag} greater than 1 for up to about half the year, including the finger inlets of South Puget Sound. During the warm, productive months (May-September), the average Ω_{arag} in the surface 20 meters remained close to 1, or slightly below 1, in many areas. Refuges with relatively high average

Ω_{arag} greater than 1 during May-September are predicted in the finger inlets of South Puget Sound (Oakland Bay and Totten, Eld, Budd, Henderson, innermost Case, and Carr Inlets), in addition to Sinclair/Dyes Inlets, Padilla Bay, Samish Bay, Discovery Bay, and Sequim Bay. The occurrence of Ω_{arag} below 1 is particularly noticeable in the plume of the Fraser River and in South Hood Canal/Lynch Cove, the Whidbey Basin (Port Susan, Saratoga Passage, Skagit Bay), and to a lesser extent in Elliott Bay, Commencement Bay, Colvos Passage, the deepest areas of South Puget Sound (Dana Passage through the Nisqually Reach), and the Strait of Juan de Fuca near Admiralty Inlet.

- Predictions for 2008 reveal that surface layer pCO_2 was generally higher than atmospheric pCO_2 for at least half of the year in all areas, and up to the entire year in some areas. Therefore, the net flux of CO_2 is from the water to the air most of the time in most areas. Surface pCO_2 is less than atmospheric pCO_2; therefore, the net flux of CO_2 is from the air to the water for less than half of the year in some areas, typically in the most productive regions during the phytoplankton growing season.

Recommendations

Results of this study support the following recommendations.

- Additional modeling scenarios should be conducted to evaluate the following:
  - The effect of climate change on acidification within the Salish Sea.
  - The effect of various individual sources or types of sources (e.g., point sources, nonpoint sources, local atmospheric pCO_2).
- Additional model simulations should be performed for different years to estimate inter-annual variability. We recommend applying the acidification model for simulation of every year since 2006 to the present to develop a 10-year simulation period.
- Additional model sensitivity and uncertainty analyses should be conducted to determine which processes contribute most to model uncertainty and to gain information to improve model skill.
- The Department of Ecology's network of both marine and freshwater ambient monitoring stations should be supplemented with routine collection of monthly carbonate system samples at selected locations to provide data for model calibration and confirmation. Dissolved and particulate organic carbon monitoring is needed in freshwater stations to evaluate nutrient loads. In addition, nearshore measurement stations are necessary and should be established when resources allow. More information is needed to constrain the carbonate system in Puget Sound and must include a combination of high temporal resolution continuous data, in addition to a distributed network able to capture broad spatial patterns.
- Reference conditions need to be reviewed and improved, if data are available. For those watersheds that appear to have significant anthropogenic influence on specific areas of the Salish Sea, we recommend performing additional watershed-specific analysis to track, identify, and estimate nutrient contributions from different upstream sources. Future work should investigate a more site-specific approach to estimate reference inorganic nitrogen and organic carbon concentrations, especially in rivers that are large in terms of flow, have known watershed anthropogenic nutrient sources that do not seem to be reflected in our current estimates of reference conditions, and/or where model results show that marine water quality dynamics are sensitive to nutrient inputs from these rivers.
- Existing nutrient loading inventories need to be continually reviewed and improved, as data become available. We recommend comparing regression estimates developed by Mohamedali et al. (2011) for point and nonpoint source boundary conditions with observed data from 2008 and future years for which the model might be run.
- Explore changes to the Salish Sea Model, including improvements to the vertical discretization scheme and finer horizontal resolution, to enhance model performance.
- During periods when the oceanic forcing results in low aragonite saturation levels throughout much of the Salish Sea, as it was in 2008, further depression of aragonite saturation levels due to anthropogenic loadings, as described above, may be of biological relevance to certain species during critical biomineralization periods. More research aimed at determining the

biological relevance of fractional changes to already low aragonite saturation levels and other carbonate system parameters, and the impact of the temporal resolution of such changes, is needed.

- Targets or criteria for acceptable change in carbonate system variables should be established to allow the model to be used to evaluate alternative management scenarios of nutrient loading.

References

Alin, Simone R.; Newton, Jan; Sutton, Adrienne J.; Mickett, John (2016). Dissolved inorganic carbon, total alkalinity, phosphate, silicate, and other variables collected from profile and discrete sample observations using CTD, Niskin bottle and other instruments in the northwest coast of the United States near the Cha Ba mooring off La Push, Washington from 2011-05-22 to 2014-10-24 (NCEI Accession 0145160). Version 1.1. NOAA National Centers for Environmental Information. Dataset.

Artioli, Y., J.C. Blackford, M. Butenschön, J.T. Holt, S.L. Wakelin, H. Thomas, A. Boges, J.I. Acllen. 2012. The carbonate system in the North Sea: Sensitivity and model validation. Journal of Marine Systems 102-104: 1-13. http://www.CO2.ulg.ac.be/pub/artioli_et_al_2012.pdf.

Artioli, Y., J.C. Blackford, G. Nondal, R.G.J. Bellerby, S.L. Wakelin, J.T. Holt, M. Butenschön, J.I. Allen. 2013. Heterogeneity of impacts of high CO2 on the North Western European Shelf. Biogeosciences 11:601-612. Doi: 10.5194/bg-11-601-2014. https://www.researchgate.net/publication/258758267_Heterogeneity_of_impacts_of_high_CO2_on_the_North_Western_European_Shelf.

Barton, A., B. Hales, G.G. Waldbusser, C. Langdon, and R.A. Feely. 2012. The Pacific oyster, *Crassostrea gigas*, shows negative correlation to naturally elevated carbon dioxide levels: Implications for near-term ocean acidification effects. Limnology and Oceanography 57: 698-710. doi: 10.4319/lo.2012.57.3.0698.

Bednaršek, N., G. A. Tarling, D. C. E. Bakker, S. Fielding, E. M. Jones, H. J. Venables, P. Ward, A. Kuzirian, B. Lézé, R. A. Feely, & E. J. Murphy. 2012. Extensive dissolution of live pteropods in the southern ocean. Nature Geoscience 5, 881-885 (2012). DOI:10.1038/ngeo1635

Bianucci, L., W. Long, T. Khangaonkar, G. Pelletier, A. Ahmed, T. Mohamedali, M. Roberts, and C. Figueroa-Kaminsky. 2017. Elementa: Science of the Anthropocene. Special Feature: Advances in ocean acidification. (in review).

Bos, J. C. Krembs, and S. Albertson. 2016. Quality assurance for long-term marine water column pH data. Washington State Department of Ecology, Olympia, WA. Publication No. 16-03-042. https://fortress.wa.gov/ecy/publications/SummaryPages/1603042.html

Bos, J., M. Keyzers, L. Hermanson, C. Krembs, and S. Albertson. 2015. Quality Assurance Monitoring Plan: Long-Term Marine Waters Monitoring, Water Column Program. Washington State Department of Ecology, Olympia, WA. Publication No. 15-03-101. https://fortress.wa.gov/ecy/publications/SummaryPages/1503101.html

Browman, H., Dupont, S., Havenhand, J., Robbins L, 2013. Biological Responses to Ocean Acidification, Chapter 3 in AMAP Assessment 2013: Arctic Ocean Acidification. Arctic Monitoring and Assessment Programme (AMAP), Oslo, Norway. viii + 99 pp. ISBN – 978-82-7971-082-0

Busch D.S., M. Maher, P. Thibodeau, and P. McElhany. (2014) Shell Condition and Survival of Puget Sound Pteropods Are Impaired by Ocean Acidification Conditions. PLoS ONE 9(8): e105884. DOI:10.1371/journal.pone.0105884

Cerco CF, Cole T. 1993. Three-dimensional eutrophication model of Chesapeake Bay. Journal of Environmental Engineering 119(6): 1006-1025.

Cerco CF, Cole TM. 1994. Three-Dimensional Eutrophication Model of Chesapeake Bay. Volume 1: Main Report. DTIC Document.

Chan, F., Boehm, A.B., Barth, J.A., Chornesky, E.A., Dickson, A.G., Feely, R.A., Hales, B., Hill, T.M., Hofmann, G., Ianson, D., Klinger, T., Largier, J., Newton, J., Pedersen, T.F., Somero, G.N., Sutula, M., Wakefield, W.W., Waldbusser, G.G., Weisberg, S.B., and Whiteman, E.A. The West Coast Ocean Acidification and Hypoxia Science Panel: Major Findings, Recommendations, and Actions. California Ocean Science Trust, Oakland, California, USA. April 2016. http://westcoastoah.org/wp-content/uploads/2016/04/OAH-Panel-Key-Findings-Recommendations-and-Actions-4.4.16-FINAL.pdf

Chen C, Liu H, and Beardsley RC. 2003. An unstructured grid, finite-volume, three-dimensional, primitive equations ocean model: application to coastal ocean and estuaries. Journal of atmospheric and oceanic technology 20(1): 159-186.

Department of Fisheries and Oceans. 2015. Line P Program, URL: http://www.pac.dfo-mpo.gc.ca/science/oceans/data-donnees/line-p/index-eng.html.

Deppe, R.W., J. Thomson, C. Krembs, and B. Polagye, Hypoxic intrusions to Puget Sound from the Ocean, Oceans. 2013 .MTS/IEEE, San Diego, CA (2013). https://depts.washington.edu/nnmrec/docs/20130430_DeppeW_pres_Hypoxia.pdf

Dewey, Bill, Taylor Shellfish Farms, personal communication, March 17, 2017.

Dickson, A.G. 1990. Thermodynamics of the dissociation of boric acid in synthetic seawater from 273.15 to 318.15 K, Deep-Sea Res., 37, 755–766.

Di Toro DM. 2001. Sediment flux modeling. Wiley-Interscience New York.

Fassbender, A.J., S.R. Alin, R.A. Feely, A.J. Sutton, J.A. Newton, and R.H. Byrne. 2016. Estimating total alkalinity in the Washington State coastal zone: complexities and surprising utility for ocean acidification research. Estuaries and Coasts. DOI: 10.1007/s12237-016-0168-z

Feely, R. A., S. R. Alin, B. Hales, G. C. Johnson, R. H. Byrne, W. T. Peterson, X. Liu, and D. Greeley. 2015. Chemical and hydrographic profile measurements during the West Coast Ocean Acidification Cruise WCOA2013 (August 3-29, 2013), Carbon Dioxide Inf. Anal. Center, Oak Ridge Natl. Lab. US Dep. Energy, Oak Ridge, Tennessee, doi:10.3334/CDIAC/OTG.COAST_WCOA2013.

Feely, Richard A.; Alin, Simone R.; Hales, Burke; Johnson, Gregory C.; Byrne, Robert; Peterson, William; Liu, Xuewu; and Greeley, Dana. 2015. Dissolved inorganic carbon, total alkalinity, pH and other variables collected from profile and discrete sample observations using CTD, Niskin bottle, and other instruments from R/V Fairweather and R/V Point Sur in the U.S. West Coast California Current System during the 2013 West Coast Ocean Acidification Cruise (WCOA2013) from 2013-08-05 to 2013-08-28 (NCEI Accession 0132082). Version 2.2. NOAA National Centers for Environmental Information. Dataset.

Feely R.A., Alin S.R., Newton J., Sabine C.L., and Warner M. et al. 2010. The combined effects of ocean acidification, mixing, and respiration on pH and carbonate saturation in an urbanized estuary. Estuarine, Coastal and Shelf Science 88(4): 442-449. doi:10.1016/j.ecss.2010.05.004.

Feely, R.A., T. Klinger, J.A. Newton, and M. Chadsey. 2012. Scientific Summary of Ocean Acidification in Washington State Marine Waters. NOAA OAR Special Report.

Feely, R.A. S.R. Alin, B. Carter, N. Bednarsek, B. Hales, F. Chan, T.M. Hill, B. Gaylord, E. Sanford, R.H. Byrne, C.L. Sabine, D. Greeley, and L. Juranek. 2016. Chemical and biological impacts of ocean acidification along the west coast of North America. Estuarine, Coastal and Shelf Science (2016). DOI: 10.1016/j.ecss.2016.08.043

Fennel, K., J. Wilkin, M. Previdid, and R. Najjar. 2008. Denitrification effects on air-sea CO2 flux in the coastal ocean: Simulations for the northwest North Atlantic. Geophysical Research Letters L24608, doi:10.1029/2008GL036147. https://www.researchgate.net/publication/228697840_Denitrification_effects_on_air-sea_CO2_flux_in_the_coastal_ocean_Simulations_for_the_northwest_North_Atlantic

Hauri, C., N. Gruber, M. Vogt, S.C. Doney, R.A. Feely, Z. Lachkar, A. Leinweber, A.M.P. McDonnel, M. Munnich, and G.-K. Plattner. 2013. Spatiotemporal variability and long-term trends of ocean acidification in the California Current System. Biogeosciences 10:193-216 doi: 10.5194/BG-10-193-2013. http://www.biogeosciences.net/10/193/2013/bg-10-193-2013.pdf

Hettinger, A., E. Sanford, T.M. Hill, A.D. Russell, K.N.S. Sato, J. Hoey, M. Forsch, H.N. Page, and B. Gaylord. 2012. Persistent carry-over effects of planktonic exposure to ocean acidification in the Olympia oyster. Ecology 93:2758-2768.

Ho D.T., Law C.S., Smith M.J., Schlosser P., Harvey M., et al. 2006. Measurements of air-sea gas exchange at high wind speeds in the Southern Ocean: Implications for global parameterizations. Geophysical Research Letters 33(16). doi:10.1029/2006gl026817.

Ianson, D., S.E. Allen, B.L. Moore-Maley, S.C. Johannessen, and R.W. Macdonald (2016). Vulnerability of a semi-enclosed estuarine sea to ocean acidification in contrast with hypoxia, Geophys.Res.Lett. 43, 5793–5801, DOI:10.1002/2016GL068996.

Jutterstrom, S., H.C. Andersson, A. Omstedt, and J.M. Malmaeus. 2014. Multiple stressors threatening the future of the Baltic Sea-Kattegat marine ecosystem: implications for policy and management actions. Marine Pollution Bulletin 86 (2014) 468-480. DOI: 10.1016/j.marpolbul. 2014.06.027

Khangaonkar, T., B. Sackmann, W. Long, T. Mohamedali, and M. Roberts. 2012a. Simulation of annual biogeochemical cycles of nutrient balance, phytoplankton bloom(s), and DO in Puget Sound using an unstructured grid model. Ocean Dynamics. (2012) 62:1353–1379. DOI 10.1007/s10236-012-0562-4.

Khangaonkar T., W. Long, B. Sackmann, T. Mohamedali, and M. Roberts. 2012b. Puget Sound Dissolved Oxygen Modeling Study: Development of an Intermediate Scale Water Quality Model. PNNL-20384 Rev 1, prepared for the Washington State Department of Ecology by Pacific Northwest National Laboratory, Richland, WA. Ecology Publication No. 12-03-049. https://fortress.wa.gov/ecy/publications/SummaryPages/1203049.html

Khangaonkar T., Yang Z., Kim T., and Roberts M. 2011. Tidally averaged circulation in Puget Sound sub-basins: Comparison of historical data, analytical model, and numerical model. Estuarine, Coastal and Shelf Science 93(4): 305-319.

Khangaonkar, T., W. Long, and W. Xu. 2017. Assessment of circulation and inter-basin transport in the Salish Sea including Johnstone Strait and Discover Islands pathways. Ocean Modelling 109 (2017) 11-32. DOI: 10.1016/j.ocemod.2016.11.004

Kim, T. and T. Khangaonkar. 2011. An Offline Unstructured Biogeochemical Model (UBM) for Complex Estuarine and Coastal Environments. Environmental Modelling Software 31 (2012) Pages 47-63.

King County, Marine and Sediment Assessment Group. 2016. Offshore Water Monitoring Program discrete data from 2008. K. Stark, W. Eash-Loucks, and S. Jaeger (Eds). Retrieved from: http://green2.kingcounty.gov/marine/Monitoring/Offshore

King County, 2003. Marine Ambient and Outfall Monitoring Program – 2003. Sampling and Analysis Plan. Prepared by Daniel Smith, Marine Monitoring Group, King County Department of Natural Resources and Parks, Water and Land Resources Division, Seattle, WA. http://green2.kingcounty.gov/ScienceLibrary/Document.aspx?ArticleID=224

Krause, D., D.P. Boyle, and F. Base. 2005. Comparison of different deficiency criteria for hydrological model assessment. Advances in Geoscience 5:89-97.

Krembs, C. 2015. Personal communication with Mindy Roberts by email January 27, 2015. Washington State Department of Ecology, Olympia, WA.

Lewis, E. and D.W.R. Wallace. 1998. Program Developed for CO2 System Calculations, ORNL/CDIAC-105, Carbon Dioxide Information Analysis Center, Oak Ridge National Laboratory.

Lombard, S. and C. Kirchmer, 2004. Guidelines for Preparing Quality Assurance Project Plans for Environmental Studies. Washington State Department of Ecology, Olympia, WA. Publication No. 04-03-030. https://fortress.wa.gov/ecy/publications/SummaryPages/0403030.html

Long, W., T. Khangaonkar, M. Roberts, and G. Pelletier. 2014. Approach for Simulating Acidification and the Carbon Cycle in the Salish Sea to Distinguish Regional Source Impacts. Washington State Department of Ecology Publication No. 14-03-002. https://fortress.wa.gov/ecy/publications/SummaryPages/1403002.html.

Lueker, T.J., Dickson, A.G., and Keeling, C.D. 2000. Ocean pCO2 calculated from dissolved inorganic carbon, alkalinity, and equations for K1 and K2: validation based on laboratory measurements of CO2 in gas and seawater at equilibrium, Mar. Chem., 70, 105–119.

MacCready, P., N. Banas, and S. Siedlecki. 2013. Proposal for the Development of an Ocean Acidification Forecast Model. Submitted to the Washington Ocean Acidification Center.

Mackas, D.L. and M.D. Galbraith. 2010. Pteropod time-series from the NE Pacific. ICES Journal of Marine Science (2010) 69(3), 448-459. DOI:10.1093/icesjms/fsr163

Mathieu, N., 2006. Replicate Precision for Twelve Total Maximum Daily Load (TMDL) Studies and Recommendations for Precision Measurement Quality Objectives for Water Quality Parameters. Washington State Department of Ecology, Olympia, WA. Publication No. 06-03-044. https://fortress.wa.gov/ecy/publications/SummaryPages/0603044.html

Miller, L.A., Christian, M. Davelaar, W.K. Johnson, and J. Linguanti. 2010. Carbon Dioxide, Hydrographic and Chemical Data Obtained During the Time Series Line P Cruises in the North-East Pacific Ocean from 1985-2010. http://cdiac.ornl.gov/ftp/oceans/CLIVAR/Line_P.data/. Carbon Dioxide Information Analysis Center, Oak Ridge National Laboratory, US Department of Energy, Oak Ridge, Tennessee. doi: 10.3334/CDIAC/otg.CLIVAR_Line_P_2009.

Mohamedali, T. M. Roberts, B. Sackmann, and A. Kolosseus. 2011. Puget Sound dissolved oxygen model nutrient load summary for 1999-2008. Washington Department of Ecology. Olympia, WA. Publication No. 11-03-057. https://fortress.wa.gov/ecy/publications/SummaryPages/1103057.html

Murray, J.W., E. Roberts, E. Howard, M. O'Donnell, C. Bantam, E. Carrington, M. Foy, B. Paul, and A. Fay. 2015. An inland sea high nitrate-low chlorophyll (HNLC) region with naturally high pCO2. Limnology and Oceanography. doi: 10.1002/lno.10062.

Newton, J. and A. Devol. 2012. Quality Assurance Project Plan. Long-term, High Resolution Marine Water Quality Monitoring in Puget Sound using Profiling Buoys, 2012-2013 Activities (the same procedures were followed for 2008 data). University of Washington, Seattle, WA. http://orca.ocean.washington.edu/ORCA_QAPP.pdf

Nightingale P.D, Malin G., Law C.S., Watson A.J., Liss P.S., et al. 2000. In situ evaluation of air-sea gas exchange parameterizations using novel conservative and volatile tracers. Global Biogeochemical Cycles 14(1): 373-387.

NOAA, Padilla Bay National Estuarine Research Reserve System, 2017. Quality Assurance and Quality Control (QAQC), http://cdmo.baruch.sc.edu/data/qaqc.cfm

NOAA National Estuarine Research Reserve System (NERRS). System-wide Monitoring Program. Data accessed from the NOAA NERRS Centralized Data Management Office website: http://www.nerrsdata.org/; *accessed* 13 October 2016.

Orr J.C., Fabry V.J., Aumont O., Bopp L., Doney S.C., et al. 2005. Anthropogenic ocean acidification over the twenty-first century and its impact on calcifying organisms. Nature 437(7059): 681-6. doi:10.1038/nature04095.

Orr, J.C., J.-M. Epitalon, and J.-P. Gattuso. 2015. Comparison of ten packages that compute ocean carbonate chemistry. Biogeosciences 12:1483-1510. doi: 10.5194/bg-12-1483-2015.

Pelletier, G., E. Lewis, and D. Wallace. 2013. CO2SYS.XLS: A calculator for the CO2 system in seawater for Microsoft Excel/VBA. Washington State Department of Ecology, Olympia, WA and Brookhaven National Laboratories, Upton, NY. www.ecy.wa.gov/programs/eap/models.html.

Pelletier, G.J., L. Bianucci, W. Long, T. Khangaonkar, T. Mohamedali, A. Ahmed, and C. Figueroa-Kaminsky. 2017. Salish Sea Model, Sediment Diagenesis Module. Washington State Department of Ecology, Olympia, WA. Publication No. 17-03-010. https://fortress.wa.gov/ecy/publications/SummaryPages/1703010.html

PSEMP Marine Waters Workgroup. 2016. Puget Sound marine waters: 2015 overview. S. K. Moore, R. Wold, K. Stark, J. Bos, P. Williams, K. Dzinbal, C. Krembs and J. Newton (Eds). URL: www.psp.wa.gov/PSEMP/PSmarinewatersoverview.php.

Reum J.C., Alin S.R., Feely R.A., Newton J., Warner M., et al. 2014. Seasonal carbonate chemistry covariation with temperature, oxygen, and salinity in a fjord estuary: implications for the design of ocean acidification experiments. PloS one 9(2): e89619. doi:10.1371/journal.pone.0089619.

Roberts, M., G. Pelletier, T. Khangaonkar, and W. Long. 2015a. Quality Assurance Project Plan: Salish Sea Dissolved Oxygen Modeling Approach: Sediment-Water Interactions. Washington State Department of Ecology Publication No. 15-03-103. https://fortress.wa.gov/ecy/publications/SummaryPages/1503103.html.

Roberts, M., G. Pelletier, T. Khangaonkar, W. Long, and L. Bianucci. 2015b. Quality Assurance Project Plan: Salish Sea Acidification Model Development. Washington State Department of Ecology Publication No. 15-03-109. https://fortress.wa.gov/ecy/publications/SummaryPages/1503109.html

Roberts, M., T. Mohamedali, B. Sackmann, T. Khangaonkar, and W. Long. 2014. Dissolved Oxygen Assessment for Puget Sound and the Straits: Impacts of Current and Future Human Nitrogen Sources and Climate Change through 2070. Washington State Department of Ecology Publication No. 14-03-007. https://fortress.wa.gov/ecy/publications/SummaryPages/1403007.html

Sabine, C.L., Feely, R.A., Gruber, N., Key, R.M., Lee, K., Bullister, J.L., Wanninkhof, R., Wong, C.S., Wallace, D.W.R., Tilbrook, B., Millero, F.J., Peng, T.H., Kozyr, A., Ono, T., and Rios, A.F., 2004. The oceanic sink for anthropogenic CO2. Science 305, 367e371.

Sackmann, B. 2009. Quality Assurance Project Plan: Puget Sound Dissolved Oxygen Modeling Study: Intermediate-scale Model Development. Washington State Department of Ecology Publication No. 09-03-110.
https://fortress.wa.gov/ecy/publications/summarypages/0903110.html.

Snedecor, G.W. and W.G. Cochran. 1989. Statistical methods. Eighth edition. Iowa State University Press.

Strickland, R.M. 1983. The fertile fjord. Washington Sea Grant Program, University of Washington Press.

Thomsen, J., Haynert, K., Wegner, K. M., and Melzner, F., 2015. Impact of seawater carbonate chemistry on the calcification of marine bivalves, Biogeosciences, 12, 4209-4220, doi:10.5194/bg-12-4209-2015,

Uppström, L. R. 1974. The Boron/Chlorinity Ratio of Deep-Sea Water from the Pacific Ocean, in: Deep-Sea Research and Oceanographic Abstracts, 21, 161–162, Elsevier, 1974.

WAC 173-201A. Water Quality Standards for Surface Waters in the State of Washington Washington State Department of Ecology, Olympia, WA.
www.ecy.wa.gov/laws-rules/ecywac.html

Waldbusser, G., B. Hales, C.J. Langdon, B.A. Haley, P. Schrader, E.L. Brunner, M.W. Gray, C.A. Miller, and I. Gimenez. 2014. Saturation-state sensitivity of marine bivalve larvae to ocean acidification. Nature Climate Change 15 December 2014, doi: 10.1038/NCLIMATE2479.

Waldbusser G.G., Hales B., Langdon C.J., Haley B.A., Schrader P., Brunner E.L., et al. 2015. Ocean Acidification Has Multiple Modes of Action on Bivalve Larvae. PLoS ONE 10(6): e0128376. doi:10.1371/journal.pone.0128376

Wanninkhof, R. 1992. Relationship between wind speed and gas exchange over the ocean. Journal of Geophysical Research 97(C5): 7373. doi:10.1029/92jc00188.

Wanninkhof, R. 2014. Relationship between wind speed and gas exchange over the ocean revisited. Limnol Oceanogr Methods 12(6): 351-362.

Washington Sea Grant. 2014. Ocean Acidification in the Pacific Northwest. May 2014 fact sheet. http://wsg.washington.edu/admin/pdfs/ocean-acidification/OAFAQ-PacNW.pdf.

Washington State Blue Ribbon Panel on Ocean Acidification. 2012. Ocean Acidification: From Knowledge to Action. Adelsman, H., L. Whitely Binder, M. Chadsey (editors). Washington State Department of Ecology Publication No. 12-01-015.

Washington State Blue Ribbon Panel on Ocean Acidification. 2012. Ocean Acidification: From Knowledge to Action, Washington State's Strategic Response. H. Adelsman and L. Whitely Binder (eds). Washington Department of Ecology, Olympia, Washington. Publication No. 12-01-015. https://fortress.wa.gov/ecy/publications/publications/1201015.pdf.

Washington State Department of Ecology, 2015. Marine Water Quality Monitoring web site, Environmental Assessment Program. Long-Term Marine Monitoring Data for Puget Sound and Coastal Bays. http://www.ecy.wa.gov/programs/eap/mar_wat/index.html. Data retrieved September 2016.

Wootton, J.T. and C.A. Pfister. 2012. Carbon system measurements and potential climatic drivers at a site of rapidly declining ocean pH. PLOS One 7(12): e53396. doi:10.1371/journal.pone.0053396.

Yang Z, Khangaonkar T, Labiosa R, and Kim T. 2010. Puget Sound Dissolved Oxygen Modeling Study: Development of an Intermediate-Scale Hydrodynamic Model. Richland, Washington: Pacific Northwest National Laboratory.

Appendices

Appendix A. Model equations

A.1 TA equations

TA increases (decreases) due to processes that produce (consume) NH4 or consume (produce) NO3. Therefore, TA in the model increases due to new primary production, remineralization of LDON and RDON, water column denitrification, and sediment fluxes of NH4; it decreases due to regenerated primary production, water column nitrification, and sediment fluxes of NO3. The equation for TA follows (note that the factor 14 represents the conversion of grams of nitrogen to moles of nitrogen, i.e., 14 gN = 1 molN):

$$\frac{\partial TA}{\partial t} = PP_{new} - PP_{reg} - Nitr_{TA} + R_{LDON} + R_{RDON} + Den_{TA} + P_{predTA} + P_{lossTA} + Sed_{TA}$$

where each term represents the following:

$$PP_{new} = New\ primary\ production = \sum_{i=1}^{2} (1 - PNi) * Pi * ANCi * Bi/14$$

$$PP_{reg} = Regenerated\ primary\ production = \sum_{i=1}^{2} PNi * Pi * ANCi * Bi/14$$

where the subscripts i=1,2 represent diatoms and dinoflagellates, respectively. The preferential uptake of NH4 is $PNi = NH4\left(\frac{NO3}{(KhNi+NH4)*(KhNi+NO3)} + \frac{KhNi}{(NO3+NH4)*(KhNi+NO3)}\right)$ as in Thomann and Fitzpatrick (1982). *Bi* is the algal biomass in gC/m^3 and the coefficient *ANCi* is the nitrogen-to-carbon ratio for each type of phytoplankton. *Pi* is the total phytoplankton growth, given by $Pi = PMi * FTi * FIi * min(NLi, PLi) / CCHLi$, where the temperature dependence term *FTi* is $e^{-KTg1i*(T-TMPi)^2}$ if temperature < *TMPi* and $e^{-KTg2i*(T-TMPi)^2}$ otherwise. The light limitation term is $FIi = Iavg/\sqrt{(Pi/\alpha i)^2 + Iavg^2}$ (Jassby and Platt, 1976), where *Iavg* is the average irradiance in each cell (incoming irradiance undergoes an exponential decay with depth).

The nutrient limitation terms for nitrogen and phosphorus are $NLi = \frac{NH4+DIN-PNi*DIN}{KhNi+NH4+DIN-PNi*DIN}$ and $PLi = \frac{PO4}{KhPi+PO4}$, respectively, where DIN=NH4+NO3. The values of the coefficients *PMi* (maximum growth rate in d^{-1}), *CCHLi* (carbon-to-chlorophyll ratio in gC/gChl), *ANCi*, *KhNi* (half saturation concentration for nitrogen uptake in gN/m^3), *KhPi* (half saturation concentration for phosphorus uptake in gP/m^3), *KTg1i*, *KTg2i*, and *αi* (photosynthesis vs. irradiance slope) are inputs to the model and can be found in Table A1.

$$Nitr_{TA} = water\ column\ nitrification = 2 * NT/14$$

where $NT = \frac{DO}{DO+KhOnt} * \frac{NH4}{KhNnt+NH4} * FT_{nt} * NTM$ is the nitrification rate in gN/m^3/d, with $FT_{nt} = e^{-KTNT1*(TMNT-T(I,K))^2}$ if temperature < *TMNT* and $FT_{nt} = e^{-KTNT2*(TMNT-T(I,K))^2}$ otherwise. The factor 2 represents that both the consumption of NH4 and the production of NO3 during nitrification decrease TA (Wolf-Gladrow et al., 2007). The coefficients *KhOnt* (half

saturation concentration for DO uptake during nitrification in gO_2/m^3), *KhNnt* (half saturation concentration of NH4 required for nitrification in gN/m^3), *KTNT1*, *KTNT2*, *TMNT*, and *NTM* (maximum nitrification rate in $gN/m^3/d$) are given in Table A1.

$$R_{LDON} = remineralization\ of\ LDON = \frac{DO + AANOX * KhOdoc}{KhOdoc + DO} * KLDON * FTrm * \frac{LDON}{14}$$

$$R_{RDON} = remineralization\ of\ RDON = \frac{DO + AANOX * KhOdoc}{KhOdoc + DO} * KRDN * FTrm * \frac{RDON}{14}$$

where $= KLDN + KDNALG * (\sum_{i=1}^{2} Bi) * \frac{KhNavg}{KhNavg+DIN}$, with *KhNavg = (KhN1+KhN2)/2*, and $FTrm = e^{KTMNL*(T-TRMNL)}$. The input coefficients *KTMNL*, *TRMNL*, *AANOX* (ratio of denitrification to oxic carbon respiration), *KhOdoc* (half saturation concentration of DO required for oxic respiration), *KLDN* (remineralization rate of LDON in d^{-1}), and *KRDN* (remineralization rate of RDON in d^{-1}) are found in Table A1.

$$Den_{TA} = water\ column\ denitrification$$
$$= ANDC * KLDOC * FTrm * AANOX * \frac{KhOdoc}{KhOdoc + DO} * \frac{NO3}{KhNdn + NO3} * \frac{LDOC}{14}$$

where the input coefficients *ANDC* (mass of nitrate-nitrogen reduced per mass of dissolved organic carbon oxidized in gN/gC) and *KhNdn* (half saturation concentration of NO3 required for denitrification in gN/m^3) are given in Table A1.

$$P_{predTA} = P\ losses\ by\ predation = \frac{1}{14}\sum_{i=1}^{2} FNIP * BPRi * FTpr * ANCi$$

where $FTpr = e^{KTPR(T-TRPR)}$ is the temperature dependence and the input coefficients *KTPR*, *TRPR*, *BPRi* (predation rate at temperature *TRPR*, in d^{-1}), and *FNIP* (fraction of inorganic nitrogen produced by predation), are provided in Table A1.

$$P_{lossTA} = P\ losses\ by\ basal\ mentabolism\ and\ photorespiration$$
$$= \frac{1}{14}\sum_{i=1}^{2} FNIi * ANCi * (Pi * PRSPi + BMi) * Bi$$

where $BMi = BMRi * e^{KTBi(T-TRi)}$ and the input coefficients *KTBi*, *TRi*, *BMRi* (metabolic rate at temperature *TRi*, in d^{-1}), *FNIi* (fraction of inorganic nitrogen produced by basal metabolism and photorespiration), and *PRSPi* (fraction of photosynthesis lost to photorespiration) can be found in Table A1.

$$Sed_{TA} = sediment\ flux\ of\ TA\ to\ water = \frac{(BenthicFlux_{NH4} - BenthicFlux_{NO3})}{14} * \frac{1000}{dz_{bott}}$$

where dz_{bott} is the thickness of the bottom layer of the water column and $BenthicFlux_{NH4}$ and $BenthicFlux_{NO3}$ are the fluxes of NH4 and NO3 from the top sediment layer to the water column (units are $gN/m^2/d$, such that the factor 1000/14 converts them to $mmolN/m^2/d$). They are calculated as $BenthicFlux_C = S * (C_{TopSediment} - C_{BottomSeawater})$, where C stands for the concentrations of either NH4 or NO3 and S represents the surface diffusion velocity (in m/d): $S = SOD/DO_{BottomSeawater}$, where SOD stands for Sediment Oxygen Demand ($gO_2/m^2/d$) and is divided by the DO concentration in the bottom layer of the water column (gO_2/m^3). The calculation of SOD, S, and the benthic fluxes follows an iterative approach described in Roberts et al. (2015a) and Di Toro (2001). Sed_{TA} is only added to the bottom layer of water column.

A.2 DIC equations

The processes that consume DIC are primary production and water column nitrification, while production of DIC occurs through remineralization of LDOC and RDOC, water column denitrification, phytoplankton losses by predation, basal metabolism and photorespiration, and sediment fluxes. Air-sea CO_2 fluxes can either increase or decrease DIC depending on whether the atmospheric pCO_2 is higher or lower than the seawater's. The equation for the temporal rate of change in DIC is represented by

$$\frac{\partial DIC}{\partial t} = -PP - Nitr_{DIC} + R_{LDOC} + R_{RDOC} + Den_{DIC} + P_{predDIC} + P_{lossDIC} + GasEx + Sed_{DIC}$$

where each term represents the following (please refer to Appendix A.1 for indices, functions, and parameters that were already defined there)

$$PP = primary\ production = \sum_{i=1}^{2} Pi * Bi$$

$$Nitr_{DIC} = water\ column\ nitrification = \frac{NT}{14 * 11}$$

where the factor 14 transforms the nitrification rate NT (in $gN/m^3/d$) to $mol/m^3/d$ and the factor 11 is the molN-to-molC ratio (Billen, 1976; Wezernak and Gannon, 1967).

$$R_{LDOC} = remineralization\ of\ LDOC = KLDOC * FTrm * \frac{DO}{KhOdoc + DO} * LDOC$$

$$R_{RDOC} = remineralization\ of\ RDOC = KRDOC * FTrm * \frac{DO}{KhOdoc + DO} * RDOC$$

$$Den_{DIC} = water\ column\ denitrification$$
$$= KLDOC * FTrm * AANOX * \frac{DO}{KhOdoc + DO} * \frac{NO3}{KhNdn + NO3} * LDOC$$

$$P_{predDIC} = P\ losses\ by\ predation = \sum_{i=1}^{2} FDOP * BPRi * FTpr * \frac{DO}{KhRi + DO}$$

where FDOP (fraction of inorganic carbon produced by predation) and $KhRi$ (half saturation concentration for LDOC excretion, in gO_2/m^3) are given in Table A1. The main difference between $P_{predDIC}$ and P_{predTA} is is the oxygen dependence term in $P_{predDIC}$. When DO becomes

scarce (DO close or lower than *KhRi*), the fraction of inorganic carbon produced by predation decreases while the excretion of LDOC increases by a factor $1 - DO/(KhRi + DO)$.

$$P_{lossDIC} = P\ losses\ by\ basal\ metabolism\ and\ photorespiration$$
$$= \sum_{i=1}^{2} FCIi * (Pi * PRSPi * BMi) * \frac{DO}{KhRi + DO} * Bi$$

again, a DO-dependence term means that the generation of inorganic carbon decreases as DO becomes closer or less than *KhRi*. *FCIi* (fraction of inorganic carbon produced by basal metabolism and photorespiration) is not directly given as an input, but calculated as the reminder of all other fractions sourced to LDOC, RDOC, LPOC, and RPOC: $FCLi = 1 - FCLDi - FCRDi - FCLPi - FCRPi$ (where all of the fractions other than *FCLi* are given as inputs, shown in Table A1).

$$GasEx = air - sea\ CO_2\ exchange = 0.251 * WMS^2 * \sqrt{\frac{600}{Sc}} * \frac{24}{100} * \frac{CO^*_{2sat} - CO^*_{2surf}}{dz_{surf}}$$

where *WMS* is the wind speed (m/s) provided as input to the model, *Sc* is the Schmidt number for CO_2 (Wanninkhof, 2014), the factor 24/100 converts the units of the term to its left from cm/hr (as in Wanninkhof, 2014) to m/d, and dz_{surf} is the thickness of the surface layer. When gaseous CO_2 from the atmosphere dissolves in seawater, it first gets hydrated into aqueous form (CO_{2aq}) and immediately reacts with water to form carbonic acid (H_2CO_3) with the equilibrium reaction $CO_{2aq} + H_2O \leftrightarrow H_2CO_3$. Since it is difficult to distinguish analytically between CO_{2aq} and H_2CO_3, a hypothetical species called CO_2^* expresses the sum of both concentrations.

Therefore, the exchange of CO_2 between air and sea depends on the difference between the seawater saturation concentration of CO_2^* (CO^*_{2sat}) and the CO_2^* at surface (CO^*_{2surf}). The latter is calculated from CO2SYS equations and CO^*_{2sat} is calculated from the atmospheric pCO_2 (pCO_{2atm}) through Henry's Law: $CO^*_{2sat} = K0 * pCO_{2atm}$, where *K0* is the equilibrium constant of the reaction $CO_{2(gas)} \leftrightarrow CO^*_2$ from Weiss (1974). *GasEx* is only added to the surface layer of water column

$$Sed_{DIC} = sediment\ flux\ of\ DIC\ to\ water = \frac{BenthicFlux_{CO2}}{dz_{bott}} * \frac{1000}{12}$$

where $BenthicFlux_{CO2}$ is the flux of CO2 from the sediment layer to the water column (in $gC/m^2/d$) and the factor 1000/12 converts it to mmolC/m2/d (using a mole-to-gram ratio for carbon of 12 gC/molC). $BenthicFlux_{CO2}$ is calculated as the sum of the CO_2 produced by aerobic oxidation of organic matter in the sediments (*CSOD*) and the CO_2 produced by anoxic oxidation of dissolved organic carbon by denitrification (*CDen*): $BenthicFlux_{CO2} = (CSOD + CDen)/2.667$, where *CSOD* and *CDen* have units of $gO_2/m^2/d$ and the denominator is the oxygen-to-carbon ratio (2.667 gO_2/gC). The calculation of *CSOD* and *CDen* follows an iterative approach described in Roberts et al. (2015a) and Di Toro (2001). Sed_{DIC} is only added to the bottom layer of water column.

Table A1. Biological model parameters from equations in Appendix A[a].

Parameter	Description	Value[b]
AANOX	Ratio of denitrification to oxic carbon respiration	0.5
ANCi	Nitrogen-to-carbon ratio of algae group *i*	0.175, 0.175 gN/gC
ANDC	Mass of nitrate-nitrogen reduced per mass of dissolved organic carbon oxidized	0.933 gN/gC
BMRi	Metabolic rate at temperature *TRi* of algae group *i*	0.1, 0.1 d^{-1}
BPRi	Predation rate on algae group *i* at temperature *TRPR*	1.0, 0.5 d^{-1}
CCHLi	Carbon-to-chlorophyll ratio of algae group *i*	0.027, 0.020 gC/gChl
FCLDi	Fraction of LDOC produced by predation of algae group *i*	0, 0
FCLPi	Fraction of LPOC produced by predation of algae group *i*	0, 0
FCRDi	Fraction of RDOC produced by predation of algae group *i*	0, 0
FCRPi	Fraction of RPOC produced by predation of algae group *i*	0, 0
FDOP	Fraction of inorganic carbon produced by predation	0
FNIi	Fraction of inorganic nitrogen produced by basal metabolism and photorespiration of algae group *i*	0.55, 0.55
FNIP	Fraction of inorganic nitrogen produced by predation	0.4
KhNdn	Half saturation concentration of NO3 required for denitrification	0.1 gN/m^3
KhNi	Half saturation concentration for nitrogen uptake by algae group *i*	0.06, 0.06 gN/m^3
KhNnt	Half saturation concentration of NH4 required for nitrification	0.5 gN/m^3
KhOdoc	Half saturation concentration of DO for oxic respiration	0.5 gO_2/m^3
KhOnt	Half saturation concentration of DO required for nitrification	3.0 gO_2/m^3
KhPi	Half saturation concentration for phosphorus uptake by algae group *i*	0.02, 0.02 gP/m^3
KhRi	Half saturation concentration for LDOC excretion by algae group *i*	0.5, 0.5 gO_2/m^3
KLDN	Minimum remineralization rate of LDON	0.05 d^{-1}
KRDN	Remineralization rate of RDON	0.0025 d^{-1}
KTBi	Effect of temperature on basal metabolism of algae group i	0.032, 0.032 $^oC^{-1}$
KTG1i	Effect of temperature below TMPi on growth of algae group *i*	0.008, 0.2 $^oC^{-1}$
KTg2i	Effect of temperature above TMPi on growth of algae group *i*	0.05, 0.0008 $^oC^{-1}$
KTMNL	Effect of temperature deviations from TRMNL on remineralization	0.092 $^oC^{-1}$
KTNT1,2	Effect of temperature below, above TMNT on nitrification	0.0045, 0.0045 $^oC^{-1}$
KTPR	Effect of temperature in predation	0.069 $^oC^{-1}$
NTM	Maximum nitrification rate at optimal temperature	0.4 $gN/m^3/d$
PMi	Maximum growth rate of algae group *i*	300-525, 357-525 d^{-1} [c]
PRSPi	Fraction of photosynthesis lost to photorespiration by algae group *i*	0.25, 0.25
TMNT	Optimal temperature for nitrification	30.0 ^{o}C
TMPi	Optimal temperature for growth of algae group *i*	12.0, 18.0 ^{o}C
TRi	Reference temperature for metabolism by algae group *i*	20.0, 20.0 ^{o}C
TRMNL	Reference temperature for remineralization	20.0 ^{o}C
TRPR	Reference temperature for predation	20.0 ^{o}C
αi	Photosynthesis vs. irradiance slope for algae group *i*	6, 6 $\frac{gC/gChl/d}{\mu E/m^2/s}$

[a] Coefficients that end with "*i*" represent two algae groups: diatoms (*i*=1) and dinoflagellates (*i*=2)

[b] If two values are provided, the first correspond to diatoms (*i*=1) and the second to dinoflagellates (*i*=2)

[c] There were two values set for each algal group (the smaller one in the Puget Sound main basin)

Appendix B. Estimation of freshwater boundary inputs from existing conditions and a reference condition with estimated regional anthropogenic sources excluded

B.1 Estimation of existing and reference condition loading with estimated regional anthropogenic sources excluded
B.2 Time-series plots of existing (2008) and reference conditions for all point source loads
B.3 Time-series plots of existing (2008) and reference conditions for all nonpoint source loads
B.4 Time-series plots of existing (2008) conditions for all point source flows
B.5 Time-series plots of existing (2008) conditions for all nonpoint source flows

Appendix C. Monthly average pH

C.1 Monthly average pH in the surface layer
C.2 Monthly average pH in the surface 20 meters
C.3 Monthly average pH in the bottom layer

Appendix D. Monthly average DIC

D.1 Monthly average DIC in the surface layer
D.2 Monthly average DIC in the surface 20 meters
D.3 Monthly average DIC in the bottom layer

Appendix E. Monthly average TA

E.1 Monthly average TA in the surface layer
E.2 Monthly average TA in the surface 20 meters
E.3 Monthly average TA in the bottom layer

Appendix F. Monthly average Ω_{arag}

F.1 Monthly average Ω_{arag} in the surface layer
F.2 Monthly average Ω_{arag} in the surface 20 meters
F.3 Monthly average Ω_{arag} in the bottom layer

Appendix G. Monthly average pCO2

G.1 Monthly average pCO2 in the surface layer
G.2 Monthly average pCO2 in the surface 20 meters
G.3 Monthly average pCO2 in the bottom layer

Appendix H. Monthly average Revelle factors

H.1 Monthly average Revelle factors in the surface layer
H.2 Monthly average Revelle factors in the surface 20 meters
H.3 Monthly average Revelle factors in the bottom layer

Appendix I. Monthly average change in pH due to regional anthropogenic nutrient sources

I.1 Monthly average change in pH in the surface layer
I.2 Monthly average change in pH in the surface 20 meters
I.3 Monthly average change in pH in the bottom layer

Appendix J. Monthly average change in DIC due to regional anthropogenic nutrient sources

J.1 Monthly average change in DIC in the surface layer
J.2 Monthly average change in DIC in the surface 20 meters
J.3 Monthly average change in DIC in the bottom layer

Appendix K. Monthly average change in Ω_{arag} due to regional anthropogenic nutrient sources

K.1 Monthly average change in Ω_{arag} in the surface layer
K.2 Monthly average change in Ω_{arag} in the surface 20 meters
K.3 Monthly average change in Ω_{arag} in the bottom layer

Appendix L. Monthly average DIN

L.1 Monthly average DIN in the surface 20 meters
L.2 Monthly average fraction of DIN in the surface 20 meters due to regional anthropogenic sources

Appendix M. Monthly average chlorophyll-a

M.1 Monthly average chlorophyll-a in the surface 20 meters
M.2 Monthly average fraction of chlorophyll-a in the surface 20 meters due to regional anthropogenic sources

Appendix N. Monthly average non-algal organic carbon

N.1 Monthly average non-algal organic C in the surface 20 meters
N.2 Monthly average fraction of non-algal organic C in the surface 20 meters due to regional anthropogenic sources

Appendix O. Glossary, acronyms, and abbreviations

Glossary

Anthropogenic: Human-caused.

Clean Water Act: A federal act passed in 1972 that contains provisions to restore and maintain the quality of the nation's waters. Section 303(d) of the Clean Water Act establishes the TMDL program.

Dissolved oxygen (DO): A measure of the amount of oxygen dissolved in water.

National Pollutant Discharge Elimination System (NPDES): National program for issuing, modifying, revoking and reissuing, terminating, monitoring, and enforcing permits, and imposing and enforcing pretreatment requirements under the Clean Water Act. The NPDES program regulates discharges from wastewater treatment plants, large factories, and other facilities that use, process, and discharge water back into lakes, streams, rivers, bays, and oceans.

Nonpoint source: Pollution that enters any waters of the state from any dispersed land-based or water-based activities, including but not limited to atmospheric deposition, surface-water runoff from agricultural lands, urban areas, or forest lands, subsurface or underground sources, or discharges from boats or marine vessels not otherwise regulated under the NPDES program. Generally, any unconfined and diffuse source of contamination. Legally, any source of water pollution that does not meet the legal definition of "point source" in section 502(14) of the Clean Water Act.

Parameter: Water quality constituent being measured (analyte). A physical, chemical, or biological property whose values determine environmental characteristics or behavior.

pH: A measure of the acidity or alkalinity of water. A low pH value (0 to 7) indicates that an acidic condition is present, while a high pH (7 to 14) indicates a basic or alkaline condition. A pH of 7 is considered to be neutral. Since the pH scale is logarithmic, a water sample with a pH of 8 is ten times more basic than one with a pH of 7.

Point source: Sources of pollution that discharge at a specific location from pipes, outfalls, and conveyance channels to a surface water. Examples of point source discharges include municipal wastewater treatment plants, municipal stormwater systems, industrial waste treatment facilities, and construction sites where more than 5 acres of land have been cleared.

Pollution: Contamination or other alteration of the physical, chemical, or biological properties of any waters of the state. This includes change in temperature, taste, color, turbidity, or odor of the waters. It also includes discharge of any liquid, gaseous, solid, radioactive, or other substance into any waters of the state. This definition assumes that these changes will, or are likely to, create a nuisance or render such waters harmful, detrimental, or injurious to (1) public health, safety, or welfare, or (2) domestic, commercial, industrial, agricultural, recreational, or other legitimate beneficial uses, or (3) livestock, wild animals, birds, fish, or other aquatic life.

Salish Sea: Puget Sound, Strait of Georgia, and Strait of Juan de Fuca.

Stormwater: The portion of precipitation that does not naturally percolate into the ground or evaporate but instead runs off roads, pavement, and roofs during rainfall or snow melt. Stormwater can also come from hard or saturated grass surfaces such as lawns, pastures, playfields, and from gravel roads and parking lots.

Total Maximum Daily Load (TMDL): Water cleanup plan. A distribution of a substance in a waterbody designed to protect it from not meeting (exceeding) water quality standards. A TMDL is equal to the sum of all of the following: (1) individual wasteload allocations for point sources, (2) the load allocations for nonpoint sources, (3) the contribution of natural sources, and (4) a Margin of Safety to allow for uncertainty in the wasteload determination. A reserve for future growth is also generally provided.

Watershed: A drainage area or basin in which all land and water areas drain or flow toward a central collector such as a stream, river, or lake at a lower elevation.

303(d) list: Section 303(d) of the federal Clean Water Act requires Washington State to periodically prepare a list of all surface waters in the state for which beneficial uses of the water – such as for drinking, recreation, aquatic habitat, and industrial use – are impaired by pollutants. These are water quality-limited estuaries, lakes, and streams that fall short of state surface water quality standards and are not expected to improve within the next two years.

Acronyms and Abbreviations

Ω_{arag}	Aragonite saturation state
C	Carbon
Chl-a	Chlorophyll-a
CO_2	Carbon dioxide
CTD	Conductivity, temperature, and depth
DIC	Dissolved inorganic carbon
DIN	Dissolved inorganic nitrogen
DO	Dissolved oxygen
Ecology	Washington State Department of Ecology
EIM	Environmental Information Management database
EPA	U.S. Environmental Protection Agency
et al.	And others
Lat	Latitude
Lon	Longitude
NH_4	Ammonium
NO_3	Nitrate
NOAA	National Oceanic and Atmospheric Administration
pCO_2	Partial pressure of carbon dioxide
PNNL	Pacific Northwest National Laboratory
PO_4	Phosphate
PRISM	Puget Sound Regional Synthesis Model
RMSE	Root mean square error
S	Salinity

SSM	Salish Sea Model
T	Temperature
TA	Total alkalinity
UW	University of Washington
WAC	Washington Administrative Code

Units of Measurement

ft	feet
g	gram, a unit of mass
kg	kilograms, a unit of mass equal to 1,000 grams
kg/d	kilograms per day
km	kilometer, a unit of length equal to 1,000 meters
m	meter
mg	milligram
psu	practical salinity units
s.u.	standard units
uatm	microatmospheres